Spring 2009

An integrated damping and strengthening strategy for performance-based seismic design and retrofit of highway bridges

Kazi Rezaul Karim

Follow this and additional works at: https://scholarsmine.mst.edu/masters_theses

Part of the Civil Engineering Commons

Department:

Recommended Citation

Karim, Kazi Rezaul, "An integrated damping and strengthening strategy for performance-based seismic design and retrofit of highway bridges" (2009). *Masters Theses*. 6782.
https://scholarsmine.mst.edu/masters_theses/6782

AN INTEGRATED DAMPING AND STRENGTHENING STRATEGY FOR

PERFORMANCE-BASED SEISMIC DESIGN AND RETROFIT OF HIGHWAY

BRIDGES

by

KAZI REZAUL KARIM

A THESIS

Presented to the Faculty of the Graduate School of the

MISSOURI UNIVERSITY OF SCIENCE AND TECHNOLOGY

In Partial Fulfillment of the Requirements for the Degree

MASTER OF SCIENCE IN CIVIL ENGINEERING

2009

Approved by

Genda Chen, Advisor
Victor Birman
Oh-Sung Kwon

To my wife, Tania Sultana, for her continued support and encouragement

PUBLICATION THESIS OPTION

Part of this thesis has been prepared in the style utilized by the <u>ASCE Journal of Structural Engineering.</u> Papers 1, 2 and 3 (pages 10-160) will be submitted for publication in that journal. However, other sections of this thesis have been prepared utilizing the general thesis style.

ABSTRACT

In this study, a damping-enhanced strengthening (DES) strategy was introduced to retrofit bridge structures for multiple performance objectives. The main objectives of this study are (1) to numerically demonstrate the effectiveness of the anchoring mechanism of a constrained damping layer in the proposed DES system, and (2) to evaluate the performances of a highway bridge retrofitted with a DES retrofit technique of viscoelastic (VE) damping and carbon-fiber-reinforced-polymer (CFRP) strengthening components that are nearly independent under weak earthquakes but strongly coupled under strong earthquakes.

The effects of various constrained surface damping layers on the responses of simply-supported beams and cantilevered columns were first investigated analytically. An emphasis was then placed on the development of a finite element modeling technique to simulate the effect of a distributed VE damping layer on the responses of columns. Finally, the DES strategy was applied to retrofit the Old St. Francis River Bridge columns. Both operational and safety performance objectives of the bridges were evaluated with pushover analyses under earthquakes of various magnitudes.

An anchored constrained damping layer was found several times more effective than a conventional constrained layer, particularly when covering 20-80% of the column height. To meet the two performance objectives, the Old St. Francis River Bridge columns must be wrapped with three plies of CFRP sheets and one VE layer. The new retrofit strategy is well suited in the context of next-generation performance-based seismic design and retrofit of highway bridges and other structures.

ACKNOWLEDGMENTS

I would like to express my appreciation and gratitude to the members of my advisory committee, Dr. Genda Chen, Dr. Victor Birman and Dr. Oh-Sung Kwon, for their guidance and support throughout this study. I am especially grateful to my advisor, Dr. Genda Chen, for his unending patience as I completed this study under stressful time constraints.

I would also like to thank Suriya Prakash Shanmugam for all of his help during this study. His initial help in providing me transportation and a place to stay with my wife is greatly appreciated. In addition, I would like to thank Dr. Wenjian Wang for his help with the software and programming aspects of this study. Without his help, I would have had much greater difficulties completing this thesis.

Financial support to complete this study was provided by the University Transportation Center at the Missouri University of Science and Technology through its Graduate Research Assistantship Program. This support is greatly appreciated.

Finally, I would like to thank my wife and my closest friends for their continued support and encouragement throughout my journey through graduate school. They have all been extremely patient with me as I have worked to complete this portion of my education.

TABLE OF CONTENTS

Page

LIST OF ILLUSTRATIONS

Figure   Page

PAPER 3

LIST OF TABLES

1. INTRODUCTION

1.1. OVERVIEW

Earthquake hazards have become a matter of increased concern over the last several decades. In recent history, earthquakes have ravaged various countries throughout the world causing great damage. The survival of bridges during earthquakes is often of critical importance, as bridges provide a means for food and supplies to reach those affected in the emergency. Therefore, it is a priority of civil engineers to design bridges along essential transportation routes that will remain functional even after a devastating earthquake event.

In the United States, efforts have been made to increase research in the area of seismic activities. This includes retrofitting of previously erected structures located in seismically vulnerable areas. The development of the Federal Highway Administration's Seismic Retrofitting Manual for Highway Bridges (hence referred to as the FHWA Manual) in 2005 has provided engineers with a solid resource for both evaluating and retrofitting existing bridge structures.

1.2. OBJECTIVES OF THE STUDY

This study addresses several key issues related to the performance-based seismic design and retrofit of reinforced concrete (RC) structures with the recently proposed damping-enhanced strengthening (DES) strategy. Emphases were placed on (1) to quantify the effects of various constraining mechanisms of a viscoelastic (VE) layer in the DES strategy, and (2) to approximately investigate how effective the proposed DES

strategy is at the bridge system level in terms of both operational and safety performance objectives. Specifically, the main objectives of this study are (1) to investigate the effect of a distributed VE layer on the bending vibration of beams, (2) to investigate the VE layer damping effect on the elastic responses of bridge columns, and (3) to evaluate the multiple performances of bridge columns under various earthquakes of different magnitudes.

The surface damping effect plays a significant role in the reduction of seismic responses by the DES strategy, particularly for elastic or near elastic responses. Therefore, it is necessary to apply suitable materials that can induce the damping effect to the system to reduce its responses. VE materials in distributed form were commonly used in mechanical and aerospace engineering to control vibration-induced fatigue in airframes and for general vibration suppression. In this study, VE materials in distributed form were used for obtaining possible damping effects since they are widely used as damping materials. To maximize the damping effect, however, an anchored constrained VE layer configuration was used in this study for both simply supported beams and cantilever columns. Each VE layer is constrained at one end in order to increase its shear deformation and thus dissipate energy. If two VE layers are considered, they are constrained at the two ends, respectively.

Since the intent was to analyze the bridge based on FEM, one significant step towards that goal was to develop a finite element modeling technique for the implementation of the DES methodology in practical application. Specifically, discrete springs were introduced to model the effects of distributed VE damping layers on the response of columns and the structural system at large. The discrete spring model was

validated against the analytical solution. The validated model was then applied to investigate the effect of VE layers on the in-plane and out-of-plane motions of the three-column bent from a three-span steel-girder bridge.

Another component of the DES system is the strengthening of structures. To respond to ever-increasing retrofitting needs, several strengthening techniques, such as fiber-reinforced-polymer (FRP) jacketing, have been used over the past two decades. These techniques can be used to provide an existing reinforced concrete (RC) column with effective confinement so that the column will not collapse during a strong earthquake event. In performance-based seismic design, ductility is considered to be a key factor to meet the seismic demand. This is because most structures behave in-elastically during an earthquake. Because FRP confinement makes a structure more ductile, in this study FRP was applied around the bridge columns to strengthen it against seismic loadings.

Since the proposed DES methodology is intended to evaluate multiple performances of structures, it is desirable to apply the methodology to some structures that have deficiencies in some performance levels. With this objective, the Old St. Francis River Bridge was considered in this study to investigate its multiple performances in the context of DES methodology under different levels of earthquakes. The reason for considering this bridge structure was that it was built in 1977 without seismic considerations, and according to the detailed structural condition evaluation of this bridge based on capacity over demand ratio, it was found that the bridge structure has deficiencies in several areas, viz. bearing failure in shear and insufficient anchorage, poor detailing at the top and bottom of columns, moderate buckling of diaphragm/cross frame,

column shear failure at the operational and safety performance levels. Since the bridge structure has deficiencies in several areas, particularly at both operational and safety levels, application of DES methodology on this bridge structure may give additional insight regarding the proposed new retrofit technique.

Based on the results of the evaluation of the considered bridge, the proposed DES methodology is intended to allow engineers to design and retrofit structures for multiple performance objectives simultaneously so that the designed and retrofitted structures have similar margins of performance under different levels of earthquake hazards. The DES methodology has two components, viz. damping and strengthening components. The damping component ensures the operational level of the structure under a small earthquake and the strengthening component ensures the safety level of the structure under a large earthquake. Therefore, depending upon the deficiency in each level, the engineers may be able to make their decision regarding how the structure should be designed and retrofitted based on the proposed DES methodology.

1.3. SCOPE OF THE STUDY

This study consisted of formulation of analytical solutions for bending vibrations of simply supported beams under different configurations of constrained VE layers; analytical derivation of the distributed VE layers damping effects on the responses of circular columns; modeling of the VE layers with discrete springs in a finite element model; and nonlinear pushover analyses of the bridge columns. This section presents the objectives and background information of this study and Section 2 presents a brief review of the related literature.

Paper 1 deals with the responses of a simply supported beam and a plate-strip with different configurations of constrained VE layers. The equation of bending vibration was formulated and the responses were obtained in the form of acceleration ratio based on steady state analysis. The responses were also obtained for different thicknesses of VE layers as well as different thicknesses of beams and plate-strips.

Paper 2 deals with the responses of circular bridge columns under different thicknesses of VE layers. The equation of motion for circular columns with VE layer was formulated and the responses were obtained in a finite element model in the form of acceleration ratio based on steady state analysis. In the finite element model, VE layers were modeled as discrete springs and the discrete spring model was validated against the analytical solution.

Paper 3 deals with the performance evaluation of the Old St. Francis River Bridge columns based on DES methodology. The bridge columns were retrofitted with FRP and the capacities were evaluated based on nonlinear pushover analysis. The VE layer damping effects were incorporated and the evaluation was done based on demand versus capacity ratios. Finally, Section 3 presents conclusions of the study.

2. REVIEW OF LITERATURE

2.1. OVERVIEW

A literature review of various vibration control publications and research reports was conducted with the goal of gathering information about damping materials and modeling techniques for vibration suppression. A literature review of various earthquake engineering publications and research reports was also conducted with the goal of gathering information about current practices regarding design and retrofit of bridge structures and modeling techniques for performance evaluation.

2.2. DAMPING MATERIALS

Since the middle of the 20th century, sandwich materials have been used more and more in industry. In 1959, Kerwin (1959) established the expression of the bending rigidity of a sandwich beam by adopting a linear longitudinal displacement field in each layer and considering the viscoelastic (VE) layer shearing effects. Mead (1962), while following the same approach as Kerwin (1959), generalized the result to a simply supported sandwich plate. Nowadays, sandwich plates and shells are very widely used in building and industries such as car making, sporting equipment, ship building and aeronautic and spacecrafts. The lightness and reduction of vibrations by energy dissipation contribute to the success and large use of sandwich material.

In fact, the use of VE materials in sandwich structures increases their dissipative character. The energy dissipations generated mainly by shear effect are modeled by a hysteretic structural damping. While a significant amount of literature exists regarding

investigation and modeling of the vibratory behavior of sandwich beams and plates with VE material cores, it has been generally understood that when designing a damping treatment, one has to consider five key points, viz. 1) the thickness of the VE material, 2) the modulus of the VE material, 3) the location of the VE material, 4) the thickness of the constraining layer, and 5) the modulus of the constraining layer, i.e. the type of material (Austin 1998; Inman 2001; Wand 2001; Silva et al. 2005; Hao and Rao 2005; Hammami et al. 2005). The design process consists of finding the combination of the above options that result in the maximum damping for the vibration modes of interest.

VE materials in distributed form were commonly used in mechanical engineering to control vibration-induced fatigue in airframes (Ross et al. 1959) and for general vibration suppression (Morgenthaler 1987: Gehling 1987). In civil engineering, however, VE materials were exclusively applied in VE dampers that can be installed between two adjacent floors in buildings. Most of the early investigations were included in Soong and Dargush (1997), Hanson and Soon (2001), and Soon and Spencer (2002). Original developments on this subject included the damper characterization (Zhang et al. 1989; Zhang and Soong 1992; Shen and Soon 1995), shake table tests of steel frames (Aiken et al. 1993; Bergman and Hanson 1993; Chang et al. 1992, 1995, 1996), laboratory tests on lightly-reinforced concrete frames (Foutch el al. 1993), and damper applications for retrofitting of buildings (Kasai et al. 1993; Chang et al. 1995).

2.3. SEISMIC DESIGN AND RETROFIT

The design concept for multiple performance objectives was introduced in FEMA (1997) and the recommended load and resistance factor design (LRFD) guidelines for the

seismic design of highway bridges (ATC/MCEER 2008). The current practice, however, is to design a structure for one performance level and then to check its adequacy for other levels if necessary. This practice could lead to an uneconomical design with inconsistent margins of compliance to different performance objectives. How to design directly for multiple performance objectives has never before been discussed for both new design and retrofit projects.

Over 50% of the bridges in the NBI database representing the 1970's construction methods which incorporate no seismic design considerations are structurally deficient (Chen et al. 2002). To respond to ever-increasing retrofitting needs, several strengthening techniques, such as fiber reinforced polymer (FRP) jacketing, have been developed over the past two decades (FHWA 2005; MCEER 2005). These techniques can be used to provide an existing reinforced concrete (RC) column with effective confinement so that the column will not collapse during a strong earthquake event (Mander et al. 1988). Strengthening alone, however, is unlikely to improve the column performance under moderate earthquake events. This is because significant strains must be developed in the column before a jacketing technique is effectively engaged as part of the strengthened column system. It is, therefore, desirable to develop a new retrofitting technology that can meet multiple performance objectives in the context of performance-based design of structures (FEMA 1997; MCEER 2005).

In recent years, FRP jacketing has become increasingly popular for seismic retrofitting of bridge columns. Due to the confinement, the concrete strength increases and the columns become more ductile, which can meet the seismic demand (Mander 1998; FHWA 2005; MCEER 2005). Over the past decade, extensive research has been

conducted to investigate the behavior of RC columns strengthened with FRP composites (Matsuda et al. 1990; Priestley and Seible 1991; Saadatmanesh et al. 1994; Seible et al. 1995; Xiao and Ma 1997; Mirmiran and Shahawy 1997; Xiao et al. 1999; Pantelides et al. 1999; Liu et al. 2000). More recently, Chen et al. (2006) introduced a constrained VE layer wrapped by FRP jacketing to a rectangular RC column. They did some experimental studies to understand the characteristics of column responses under such a system (Huang 2005; Chen et al. 2006). The system consists of one or more FRP sheets (inner) wrapped around column, a VE layer attached on the FRP sheets, and another FRP sheet (outer) outside the VE layer that is anchored at one end into the connecting member (beam or footing) of the column.

PAPER

1. Surface Damping Effect on the Bending Vibration of Simply Supported Beams under Different Configurations of Constrained Viscoelastic Layers

Kazi R. Karim[1] and Genda Chen[2][*], F. ASCE

Abstract: VE materials are commonly used to control vibration-induced fatigue in airframes and for general vibration suppression. This study investigates the effect of surface damping treatment on the bending vibration of simply supported beams under different configurations of constrained VE layers. Emphasis was given to formulating the analytical solution for bending vibration of a simply supported beam with VE layers anchored at one-end as well as at both-end. First, the equation of bending vibration of the beam was formulated based on analytical approach and the responses for different configurations of the VE layers were obtained in the form of acceleration ratio based on steady state analysis. It was observed that a VE layer with both-end anchorage is more effective than that of the other configurations. This new technique is expected to be very useful for vibration suppression, particularly in civil, mechanical and aerospace structures.

[1] Structural Engineer, Kirkpatrick Forest Curtis PC, 205 NW 63rd St Suite 390, Oklahoma City, OK 73116, E-mail: krk2q4@mst.edu
[2] Professor of Civil Engineering and Interim Director of the Center for Infrastructure Engineering Studies, Missouri University of Science and Technology, 224 Engineering Research Laboratory, 500 W. 16th Street, Rolla, MO 65409, E-mail: gchen@mst.edu
[*] Corresponding author

CE Database subject headings: VE material; Simply supported beam; Surface damping; Bending vibration.

Introduction

Since the middle of the 20th century, sandwich materials have been used more and more in the industry. In 1959, Kerwin (1959) established the expression of the bending rigidity of a sandwich beam by adopting a linear longitudinal displacement field in each layer and considering the viscoelastic (VE) layer shearing effects. Mead (1962), while following the same approach as Kerwin (1959), generalized the result to a simply supported sandwich plate. Nowadays, sandwich plates and shells are very widely used in building and in industries such as car making, sporting equipments, ship building and aeronautic and spacecrafts. The lightness and the reduction of vibrations by energy dissipation contribute to the success of and the large use of sandwich materials.

In fact, the use of VE materials in sandwich structures increases their dissipative character. The energy dissipations generated mainly by shear effect are modeled by a hysteretic structural damping. While a significant amount of literature exists regarding the investigation and modeling of vibratory behavior of sandwich beams and plates with VE material cores, it has been generally understood that when designing a damping treatment, one has to consider five key points, viz. 1) the thickness of the VE material, 2) the modulus of the VE material, 3) the location of the VE material, 4) the thickness of the constraining layer, and 5) the modulus of the constraining layer, i.e. the type of material (Austin 1998; Wand 2001; Silva et al. 2005; Hao and Rao 2005; Hammami et al. 2005).

The design process consists of finding the combination of the above options that result in the maximum damping for the vibration modes of interest.

VE materials in distributed form were commonly used in mechanical engineering to control vibration-induced fatigue in airframes (Ross et al. 1959) and for general vibration suppression (Morgenthaler 1987: Gehling 1987). In civil engineering, however, VE materials were exclusively applied in VE dampers that can be installed between two adjacent floors in buildings. Most of the early investigations were included in Soong and Dargush (1997), Hanson and Soon (2001), and Soon and Spencer (2002). Original developments on this subject included the damper characterization (Zhang et al. 1989; Zhang and Soong 1992; Shen and Soon 1995), shake table tests of steel frames (Aiken et al. 1993; Bergman and Hanson 1993; Chang et al. 1992, 1995, 1996), laboratory tests on lightly-reinforced concrete frames (Foutch el al. 1993), and damper applications for retrofitting of buildings (Kasai et al. 1993; Chang et al. 1995). Chen et al. (2006) introduced a constrained VE layer wrapped by FRP jacketing to a cantilever RC column and investigated the response reduction due to distributed damping effect.

The focus of this study is to investigate the surface damping treatment to the bending vibration of a simply supported beam under different configurations of VE layers. Of particular interest is to formulate the analytical solution for bending vibration of a simply supported beam with VE layers anchored at one-end as well as at both-end. The effect of VE layer thickness as well as beam thickness is also investigated. Finally, the results are provided in the form of an acceleration ratio and compared for different configurations of VE layers.

Formulation of Equation of Motion

Fig. 1 shows different configurations of VE layers applied to a simply supported beam. In order to derive the equation of motion, an infinitesimal element is considered and its free-body-diagram (Inman 2001) is shown in Fig. 2. It should be noted that in Fig. 1, the VE layers are shown only at the top side of the beam. However, it should also be applied at the bottom side of the beam. This is due to the fact that when the beam vibrates, either the top or the bottom side of the beam is in tension and the VE layer is considered to be effective only in that tension side.

In Fig. 2, the axial force, *N(x, t)*, shear force, *V(x, t)*, and bending moment, *M(x, t)*, are applied at two ends of the free-body diagram of the element, following the beam sign convention (Chopra 2001). Both the average damping force, $c\,\partial y(x,t)/\partial t\,dx$, and the average shear force provided by the VE layer, $\tau(x,t)\,b\,dx$, are also included in the free-body diagram. When *dx* approaches to zero, the force equation and the moment equation of the free-body diagram can be respectively described by

$$\frac{\partial V(x,t)}{\partial x} = -m\frac{\partial^2 y(x,t)}{\partial t^2} - c\frac{\partial y(x,t)}{\partial t} + p(x,t) \tag{1}$$

$$V(x,t) = \frac{\tau(x,t)\,h\,b}{2} + \frac{\partial M(x,t)}{\partial x} \tag{2}$$

By substituting *V(x, t)* in Equation (2) into Equation (1) and introducing the moment-curvature relation, the equation of motion to describe the transverse vibration of the beam can be derived as

$$EI\frac{\partial^4 y(x,t)}{\partial x^4} + m\frac{\partial^2 y(x,t)}{\partial t^2} + c\frac{\partial y(x,t)}{\partial t} + \frac{\partial \tau(x,t)}{\partial x}\frac{hb}{2} = p(x,t) \tag{3}$$

in which $y(x,t)$ is the relative transverse displacement, $\tau(x,t)$ is the shear stress resulting from the shear deformation in the VE layer, EI is the flexural rigidity of the beam, b and h denote the width and depth of the beam cross section, m and c are the mass and damping coefficient per unit length, respectively, which are considered as constants in this study.

To relate the shear stress in the VE layer to the transverse displacement of the beam, a particular section A-B at a distance x is considered, as shown in Fig. 3. Now, let us consider the both-end anchorage case. Due to the bending vibration, A-B will rotate and let us consider this rotation as $\theta(x)$. However, since both ends are anchored, there will be a constant rotation at both ends. Let us consider these rotations as θ_a and θ_b for the left-end and right-end, respectively. From Fig. 3, the shear strain for the two VE layers can be derived as

$$\gamma_1(x,t) = \frac{h}{2t_v}\left(\frac{\partial y(x,t)}{\partial x} - \theta_a\right) \tag{4}$$

$$\gamma_2 = \left(\frac{h}{2t_v} + 1\right)(\theta_b - \theta_a) \tag{5}$$

When the applied force $p(x,t) = A(x)e^{i\omega t} = Ae^{i\omega t}$, the transverse displacement and the shear strain in the VE layer, Equation (4), can respectively be expressed as

$$y(x,t) = \phi(x)e^{i\omega t} \tag{6}$$

$$\gamma_1(x,t) = \frac{h}{2t_v}\left(\frac{d\phi(x)}{dx}e^{i\omega t} - \theta_a\right) \tag{7}$$

where A is the amplitude of the applied force, ω is the excitation frequency, t denotes the time instance, and $i = \sqrt{-1}$ represents a complex number, and $\phi(x)$ is a displacement

function. Therefore, the stress in the VE layer can be expressed as (Soong and Dargush 1997)

$$\tau_1\left(x,t\right) = \frac{h}{2t_v}\frac{G_v'}{\cos\delta}e^{i\delta}\left(\frac{d\phi(x)}{dx}e^{i\omega t} - \theta_a\right) \tag{8}$$

in which G_v' is the shear storage modulus and δ is the loss factor of the VE material. In general, they are both functions of the excitation frequency as well as Durometer of the materials. With a known Poisson ratio μ, the shear storage modulus can be determined from the Young's Modulus, $E_v(\omega)$, by $G_v'(\omega) = 0.5\,E_v(\omega)/(1+\mu)$. Note that the expression for τ_2 is not shown since it will be cancelled out in the derivative term of $\tau(x,t)$ in Equation (3).

After the harmonic base excitation and the shear stress in Equation (8) are introduced, Equation (3) becomes

$$\frac{d^4\phi(x)}{dx^4} + \frac{b\,h^2\,E_v(\omega)(1+i\tan\delta)}{8t_v\,EI\,(1+\mu)}\frac{d^2\phi(x)}{dx^2} + \frac{-m\omega^2 + ic\omega}{EI}\phi(x) = \frac{A}{EI} \tag{9}$$

Solution Scheme

Now, Equation (9) holds true for the all configurations of VE layers as well as without VE layers and the solution is obtained following the same methodology as provided by Chen et al. (2006). However, only the boundary conditions for each case have to be changed, which are given as

Case-1: No VE layer (in this case, the second term of Equation (9) disappears)

i) $\phi(0) = \phi(L) = 0$

ii) $EI\phi''(0) = EI\phi''(L) = 0$

Case-2: VE layer with no anchorage

i) $\phi(0) = \phi(L) = 0$

ii) $EI\phi''(0) = EI\phi''(L) = 0$

Case-3: VE layer with one-end anchorage

i) $\phi(0) = \phi(L) = 0$

ii) $\phi'(0) = \theta_a$

iii) $\phi'(L) = \theta_b$

iv) $EI\phi''(0) = M_a$

v) $EI\phi''(L) = 0$

where $M_a = -F_a\left(\frac{h}{2} + t_v\right)$, $F_a = \frac{Gbh}{2t_v}\int\limits_0^L \left[\phi'(x) - \theta_a\right]dx$, and $G = \frac{E_v(1 + i\tan\delta)}{2(1+\mu)}$

Case-4: VE layer with both-end anchorage

i) $\phi(0) = \phi(L) = 0$

ii) $\phi'(0) = \theta_a$

iii) $\phi'(L) = \theta_b$

iv) $EI\phi''(0) = M_a$

v) $EI\phi''(L) = M_b$

where $\quad M_a = -(F_a + F_b)\left(\frac{h}{2} + t_v\right), \quad M_b = -F_b\left(\frac{h}{2} + 2t_v\right), \quad F_a = \frac{Gbh}{2t_v}\int\limits_0^L \left[\phi'(x) - \theta_a\right]dx,$

$F_b = Gb\left(\frac{h}{2t_v} + 1\right)\int\limits_0^L \left[\theta_b - \theta_a\right]dx$, and $G = \frac{E_v(1 + i\tan\delta)}{2(1+\mu)}$

Parametric Study

Following the solution procedure in Chen et al. (2006) and using the boundary conditions for a rectangular cross section as given in the preceding section, the responses of a simply supported beam as well as a simply supported plate-strip under different configurations of VE layers were obtained. The parameters for the example beam and plate-strip are shown in Table 1 and the engineering parameters of VE material that were obtained by Huang (2005) based on experimental study were used in this study and are shown in Fig. 4.

Effect of Different Configurations of Constrained VE Layer

Fig. 5 shows the harmonic displacement responses of a simply supported beam for the both no-anchorage and one-end anchorage cases and the results are shown at fundamental frequency level with a VE layer thickness, t_v equal to 0.48 cm. It can be seen that the displacement response amplitude for the no-anchorage case is higher than that of the one-end anchorage case. It should be noted that the responses were obtained from an externally applied harmonic excitation.

Fig. 6 shows the shear-strain distribution of the VE layer for both the no-anchorage and the one-end anchorage cases, and the results are shown at fundamental frequency level with a VE layer thickness, t_v equal to 0.48 cm. It can be seen that the shear strain of the VE layer for the no-anchorage case is at a maximum at the ends while it is zero at the mid-point. On the other hand, shear strain of the VE layer for the one-end anchorage case is at a minimum at the anchored point and following a cubic distribution, it is at a maximum at the other end. It should be noted that the shear force due to the VE layer for the one-end anchorage case is much higher than that of the no-anchorage case.

Fig. 7 shows the displacement responses of a simply supported beam for different configurations of VE layers and the results are shown at fundamental frequency level with a VE layer thickness, t_v equal to 0.48 cm. The displacement response with no VE layer is also shown in the same figure. It can be seen that the displacement response amplitude for the no VE layer case is higher when compared to the ones with VE layers. It can also be seen that the displacement response amplitude tends to be smaller from no VE layer case to VE layer with both-end anchorage. It should be noted that the responses were obtained from an externally applied harmonic excitation.

Figs. 8, 9 and 10 show the acceleration ratio of a simply supported beam for different configurations of the VE layers. Note that the acceleration ratio is defined as the ratio between the response acceleration of the beam and externally applied acceleration, i.e. excitation, and the definition holds true for the rest of the discussion. The results are shown for t_v equal to 0.48 cm, 0.32 cm, and 0.24 cm, respectively, with a beam thickness, h equal to 51 cm. For t_v equal to 0.48 cm, it can be seen (Fig. 8) that the amplitude is higher in the case of no VE layer than that of the other configurations with VE layers. The amplitude tends to decrease from no VE layer to VE layer with no anchorage to VE layer with one-end anchorage to VE layer with both-end anchorage, respectively. A similar trend has also been observed for t_v equal to 0.32 cm and 0.24 cm, respectively (Figs. 9 and 10). It suggests that a VE layer is more effective when it has been anchored at both ends than that of other configurations. In other words, if the VE layer is anchored either at one-end or at both-end, then it is more effective in comparison to the conventional case, i.e. VE with no anchorage.

Effect of Thickness of VE Layer

Figs. 11, 12 and 13 show the acceleration ratio for a simply supported beam for different thicknesses of VE layers. The results are shown for no-anchorage, one-end anchorage and both-end anchorage cases, respectively, with a beam thickness, h equal to 51 cm. For the no anchorage case, it can be seen (Fig. 11) that the amplitude is higher in the case of a VE layer thickness t_v equal to 0.48 cm than that of the other thickness and it tends to be smaller from t_v equal to 0.48 cm to t_v equal to 0.32 cm to t_v equal to 0.24 cm, respectively. A similar trend has also been observed for one-end anchorage and both-end anchorage case, respectively (Figs. 12 and 13). The effect of different thickness t_v of VE layer is summarized in Fig. 14 and the results are shown for a simply supported beam with thickness h equal to 51 cm for a both-end anchorage case. The results are also shown for normalized t_v, which is normalized w.r.t. h. The results clearly suggest that the VE layer is more effective when the thickness is less and it is less effective as the thickness goes higher.

Figs. 15, 16, 17, 18, 19, and 20 show the acceleration ratio for a simply supported plate-strip for different configurations of VE layers with different thicknesses of the VE layers. The effect of different thicknesses t_v of VE layers is summarized in Fig. 21 and the results are shown for a simply supported palate-strip with thickness h equal to 2 cm for a both-end anchorage case. The results are also shown for normalized t_v, which is normalized w.r.t. h. For the plate-strip, the results show the same trend as observed in the case of a simply supported beam. In other words, the VE layer is more effective when

it is anchored at both ends and it is also more effective when the thickness of the VE layer is less.

Although it was observed that for both the beam and the plate-strip, the VE layer is more effective when it is anchored at both-end and it was also observed that the VE layer is more effective when the thickness t_v of the VE layer is less, however, considering the same anchorage system, it is also necessary to investigate whether the VE layer is more effective for a beam or a plate-strip. With this objective, the results are summarized in Fig. 22 for both the beam and the plate-strip with both-end anchorage case and the results are shown w.r.t. VE layer thickness t_v. Note that the fundamental frequencies for both the beam and the plate-strip are also shown in the same figure. It can be seen (Fig. 22) that the VE layer is more effective for the beam when compared to the plate-strip.

It should be noted that the thickness of the beam was considered as 51 cm while the thickness of the plate-strip was considered as 2 cm. Also, as shown in Fig. 22, the fundamental frequency of the beam is 4.2 Hz while for the plate-strip it is 9.9 Hz. Since the thickness and the fundamental frequency of both the beam and the plate-strip are different, it is expected that either the thickness or the fundamental frequency of the beam and the plate-strip may have influence on the VE layer effect. Another point is, fundamental frequency is a function of modulus of elasticity, E, moment of inertia, I, mass, m and length, L. Therefore, changing the value of any parameter or changing the values of any combination of the parameters will directly change the fundamental frequency. This implies that fundamental frequency may be one of the key factors to influence the VE layer effect.

Effect of Thickness of Beam and Plate-Strip

So far, the results for both the simply supported beam and the plate-strip with different configurations of VE layers as well as different thicknesses of VE layers while considering a constant thickness of both the beam and the plate strip have been discussed. As discussed earlier, however, it is also necessary to see the effect of the VE layer due to different thicknesses or fundamental frequencies of both the beam and plate-strip while considering a constant thickness of the VE layer as well as same anchorage system. With this objective, both the beam and the plate-strip were analyzed considering different thicknesses of the beam and the plate-strip; however, the analyses were restricted to only VE layers at both-end anchorage case with a VE layer thickness t_v of 0.24 cm.

Fig. 23 shows the acceleration ratio for different thicknesses of a beam and the results are summarized in Fig. 24. Note that the acceleration ratios are also shown w.r.t. normalized h, which is normalized w.r.t. t_v. It can be seen (Fig. 24) that as the thickness of the beam goes higher, the acceleration amplitude also goes higher. This implies that keeping the same thickness t_v of the VE layer, if the thickness of the beam is increased then the effect of the VE layer is less and if the thickness of the beam is decreased then the effect of the VE layer is more. Fig. 25 shows the acceleration ratio for different thicknesses of a plate-strip and the results are summarized in Fig. 26. Note that the acceleration ratios are also shown w.r.t. normalized h, which is normalized w.r.t. t_v. It can be seen (Fig. 26) that as the thickness of the plate-strip goes higher, the acceleration amplitude also goes higher. This implies that keeping the same thickness t_v of the VE layer, if the thickness of the plate-strip is increased then the effect of the VE layer is less and if the thickness of the plate-strip is decreased then the effect of the VE layer is more.

With the above observations, the relationship between the acceleration ratio and the fundamental frequency was also obtained considering the acceleration ratios obtained for both the beam and the plate-strip and the relationship is shown in Fig. 27. Note that the relationships between the acceleration ratio and the fundamental frequency that were obtained separately for both the beam and the plate-strip are also shown in the same figure. Looking at Fig. 27, it can be seen that the acceleration ratio is related to the fundamental frequency irrespective of the type of beam or plate-strip analyzed and that the acceleration amplitude goes higher as the fundamental frequency goes higher. This implies that the VE layer is more effective when the fundamental frequency is less and it is less effective when the fundamental frequency goes higher. This is also supported from the observation that the VE layer was more effective for the beam in comparison with the plate-strip as shown in Fig. 22, where it can be seen that the fundamental frequency of the beam is less (4.2 Hz) than the plate-strip (9.9 Hz). It was also observed (Fig. 27) the relationship follow the Kasai et al. (1993) model, which was used to understand the characteristics of the engineering properties of the VE materials (Huang 2007).

The observation of acceleration ratio as a function of fundamental frequency of the beam and the plate-strip clearly suggests that keeping the same configuration of the VE layer as well as the same thickness of the VE layer, the effect depends on the fundamental frequency of either the beam or the plate-strip under consideration.

Conclusions

In this study, the responses due to externally applied excitation of a simply supported beam and a plate-strip with different configurations of VE layers were investigated. First,

the equation of bending vibration was formulated and the responses were obtained in the form of acceleration ratios based on the steady state analysis. The acceleration ratio was defined as the ratio between response acceleration of the beam or plate-strip and externally applied acceleration, i.e. excitation. The responses were also obtained for different thicknesses of VE layers as well as different thicknesses of the beam. Based on the results in this study, the following conclusions can be made:

- VE layer with both-end anchorage case is more effective than that of the other configurations.

- VE layer with smaller thickness is more effective than that of the larger thickness.

- With the same VE layer configuration as well as the same VE layer thickness, the VE layer is more effective when the fundamental frequency of the beam is less and it is less effective when the fundamental frequency goes higher.

The new both-end anchored constrained VE layer technique is expected to be very useful in vibration suppression, particularly, in civil, mechanical and aerospace structures. Since the results are provided based on an analytical approach, it is also necessary to verify the results based on experimental testing and a further study is recommended in this regard.

Acknowledgement

References

Aiken, I. D., Nims, D. K., Whittaker, A. S., and Kelly, J. M. (1993). "Testing of passive energy dissipation systems." *Earthquake Spectra*, 9(3), 335-370.

Aprile, A., Inaudi, J. A., and Kelly, J. M. (1997). "Evolutionary model of viscoelastic dampers for structural applications." *Journal of Engineering Mechanics*, ASCE, 123(6), 551-560.

Austin, E. M. (1998). "Influences of higher order modeling techniques on the analysis of layered viscoelastic damping treatments." Ph.D. dissertation, Virginia Polytechnic Institute and State University, Blacksburg, VA.

Bergman, D. M., and Hanson, R. D. (1993). "Viscoelastic mechanical damping devices tested at real earthquake displacements." *Earthquake Spectra*, 9(3), 389-418.

Chang, K. C., Soong, T. T., Oh, S. T., and Lai, M. L. (1992). "Effect of ambient temperature on viscoelastically damped structures." *ASCE Journal Structural Engineering*, 118(7), 1955-1973.

Chang, K. C., Soong, T. T., Oh, S. T., and Lai, M. L. (1995). "Seismic behavior of steel frame with added viscoelastic dampers." *ASCE Journal of Structural Engineering*, 121(10), 1418-1426.

Chang, K. C., Chen, S. J., and Lai, M. L. (1996). "Inelastic behavior of steel frames with added viscoelastic dampers." *ASCE Journal of Structural Engineering*, 122(10), 1178-1186.

Chen, G., Wang, W. and Huang, X. (2006). "Optimal design of RC column seismic retrofitting for multiple performance objectives with an integrated damping and strengthening methodology." *8th National Conference on Earthquake Engineering* (CD-ROM), San Francisco, CA.

Chen, G. and Karim, K. R. (2006). "Damping-enhanced seismic strengthening of RC columns for multiple performance objectives." *5th National Seismic Conference of Bridges and Highways*, San Francisco, CA, Paper No B24.

Chopra, A. K. (2001). *Dynamics of structures*, Prentice Hall, New York, NY.

Foutch, D. A., Wood, S.L., and Beady, P. A. (1993). "Seismic retrofit for nonductile reinforced concrete frames using viscoelastic dampers." *Proceedings of Applied Technology Council ATC-17-1 Seminar on Seismic Isolation, Passive Energy Dissipation and Active Control*, 2, 605-616.

Gehling, R. N. (1987). "Large space structure damping treatment performance: analytic and test results." *Role of Damping in Vibration and Noise Control*, ASME, New York, NY, 93-100.

Hammami, L., Zghal, B., Fakhfakh, T., and Haddar, M. (2005). "Characterization of modal damping of sandwich plates." *Journal of Vibration and Accoustics*, 127, 431-440.

Hanson, R. D., and Soong, T. T. (2001). "Seismic design with supplemental energy dissipation devices." *EERI Monograph*, Oakland, CA.

Hao, M., and Rao, M. D. (2005). "Vibration and damping analysis of a sandwich beam containing a viscoelastic layer." *Journal of Composite Materials*, 39(18), 16211643.

Huang, X. (2005). "An integrated VE damping and FRP strengthening system for performance-based seismic retrofit of RC columns." Ph.D. dissertation, University of Missouri-Rolla, Rolla, MO.

Inman, D. J. (2001). *Engineering vibration*, Prentice Hall, Upper Saddle River, NJ.

Kasai, K., Munshi, J. A., Lai, M. L., and Maison, B. F. (1993). "Viscoelastic damper's hysteretic modal theory, experiment, and application." *Proceedings of Applied Technology Council ATC-17-1 Seminar on Seismic Isolation, Passive Energy Dissipation and Active Control*, 2, 521-532.

Kerwin, E. M. Jr. (1959). "Damping of flexural waves by a constrained viscoelastic layer." *J. Accoust. Soc. Am.*, 31(7), 952-962.

Lin, W. H., and Chopra, A. K. (2003). "Earthquake response of elastic single-degree-of-freedom systems with nonlinear viscoelastic dampers." *ASCE Journal of Engineering Mechanics*, 129(6), 597-606.

Mead, D. J. (1962). "The double skin damping configuration." Report No. AASU, University of Southampton, UK.

Morgenthaler, D. R. (1987). "Design and analysis of passive damped large space structures." *Role of Damping in Vibration and Noise Control*, ASME, New York, NY, 1-8.

Ross, D., Ungar, E. E., and Kerwin, E. W. (1959). "Damping of plate flexural vibrations by means of viscoelastic laminar." *Structural Damping* (ed, Ruzicka, E.J.), ASME.

Shen, K. L., and Soong, T. T. (1995). "Modeling of viscoelastic dampers for structural applications." *ASCE Journal of Engineering Mechanics*, 121(6), 694-701.

Silva, L. A., Austin, E. M., and Inman, D. J. (2005). "Time-varying controller for temperature-dependent viscoelasticity." *Journal of vibration and acoustics*, 127, 215-222.

Soong, T. T., and Dargush, G. F. (1997). *Passive energy dissipation system in structural engineering*, John Wiley & Sons, New York, NY.

Soong, T. T., and Spencer, B. F. (2002). "Supplemental energy dissipation: state-of-the-art and state-of-the-practice." *Engineering Structures*, 24, 243-259.

Wang, G. (2001). "Analyses of sandwich beams and plates with viscoelastic cores." Ph.D. dissertation, University of Maryland, College Park, MD.

Zhang, R. H., Soong, T. T., and Mahmoodi, P. (1989). "Seismic response of steel frame structures with added viscoelastic dampers." *Earthquake Engineering and Structural Dynamics*, 18, 389-396.

Zhang, R. H., and Soong, T. T. (1992). "Seismic design of viscoelastic dampers for structural applications." *ASCE Journal of Structural Engineering*, 118(5), 1375-1392.

Table 1. Beam and plate-strip parameters.

Item	Length, L (cm)	Cross-section		Young's modulus, E (N/cm^2)	Poisson's ratio, μ	Mass, m (N-s^2/cm/cm)	Damping coefficient, c (N-s/cm/cm)
		Width, b (cm)	Depth, h (cm)				
Beam	610	51	51	2.1E+6	0.4	0.06	0.73
Plate-strip	122	11	2.0	6.0E+6	0.3	0.00025	0.0023
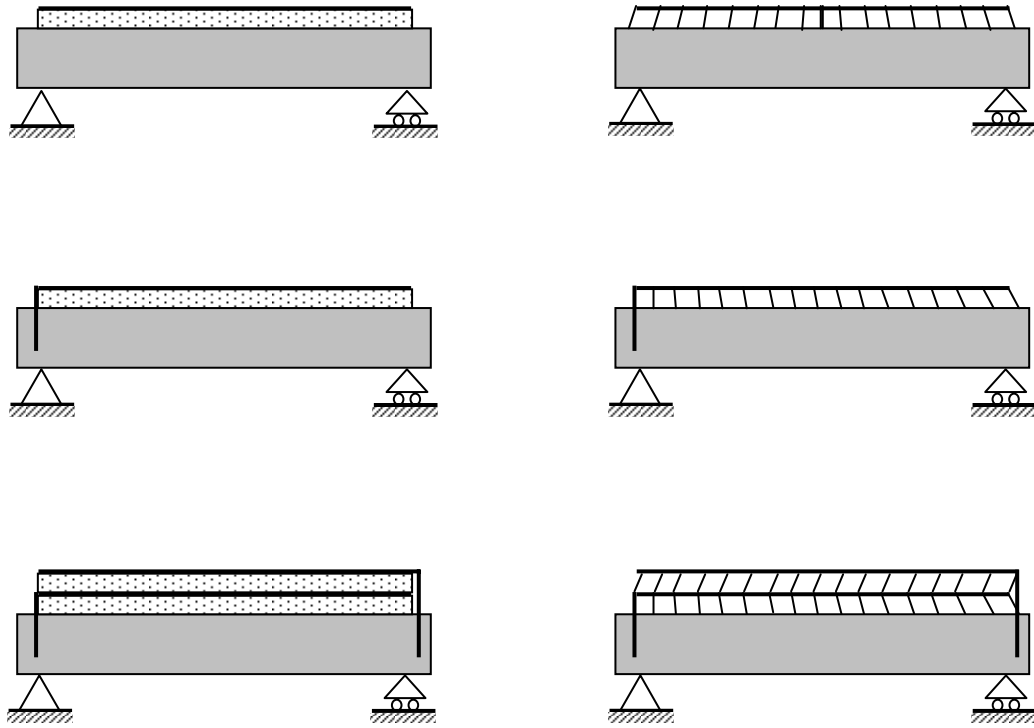
Fig. 1. Arrangement of different constraining layers (left) and their shear deformation (right). The arrangement follows as: no anchorage (top), one-end anchorage (middle), and both-end anchorage (bottom).
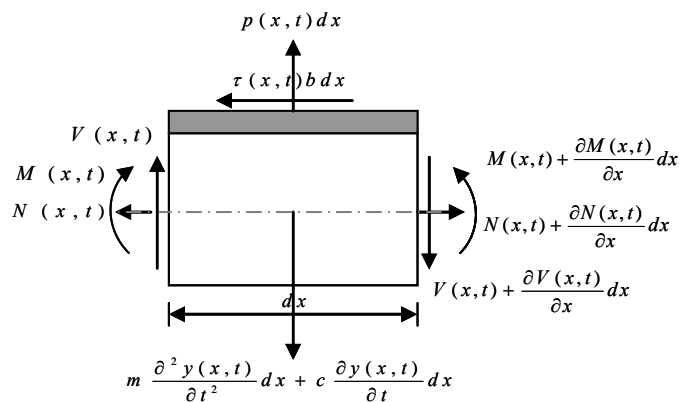
Fig. 2. Free body diagram of an infinitesimal element dx.
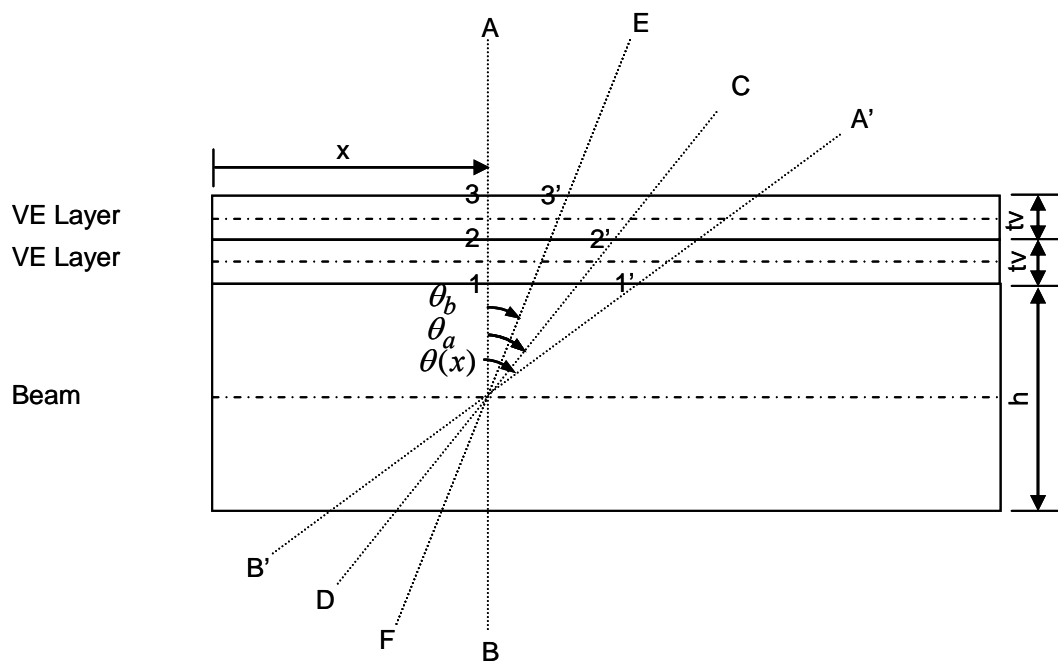
Fig. 3. Deformation of beam and VE layers for calculation of shear strain.
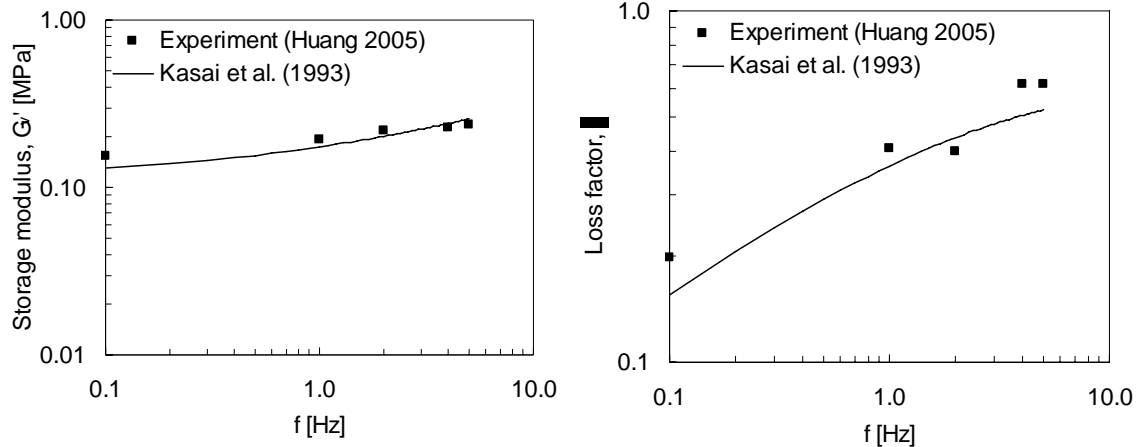
(a) Storage modulus.   (b) Loss factor.

Fig. 4. Engineering parameters of VE material obtained from experiments.
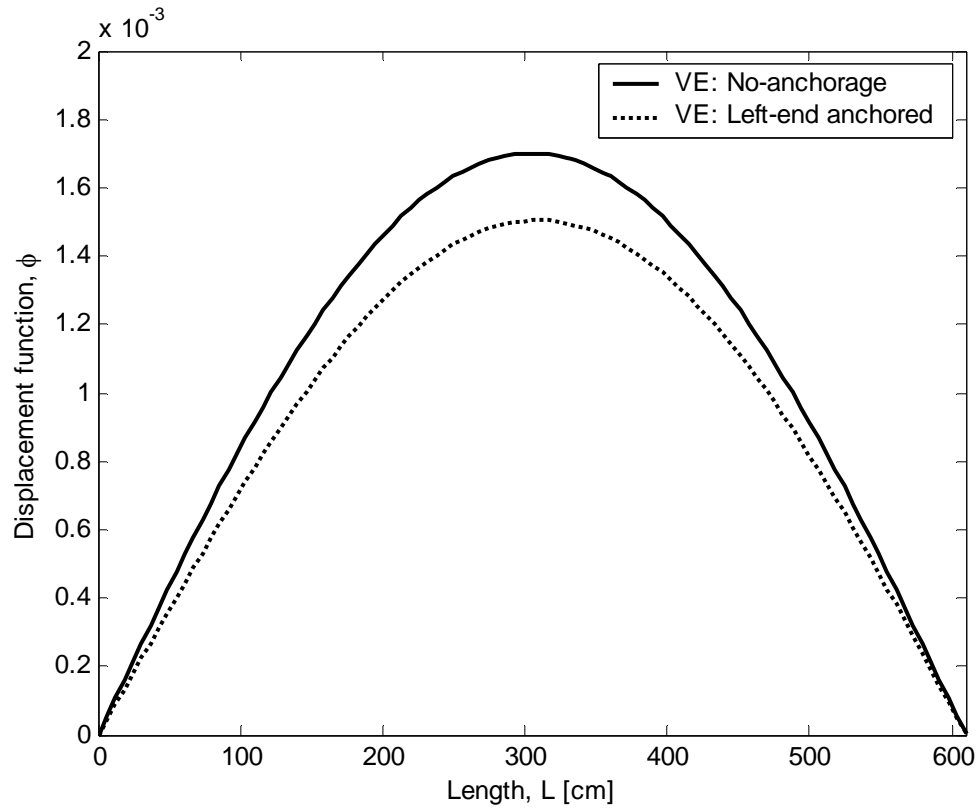
Fig. 5. Displacement functions of a simply supported beam with VE layer for both no-anchorage and one-end anchorage cases. The results are shown at fundamental frequency level for a beam with 51 cm thickness with t_v equal to 0.48 cm.
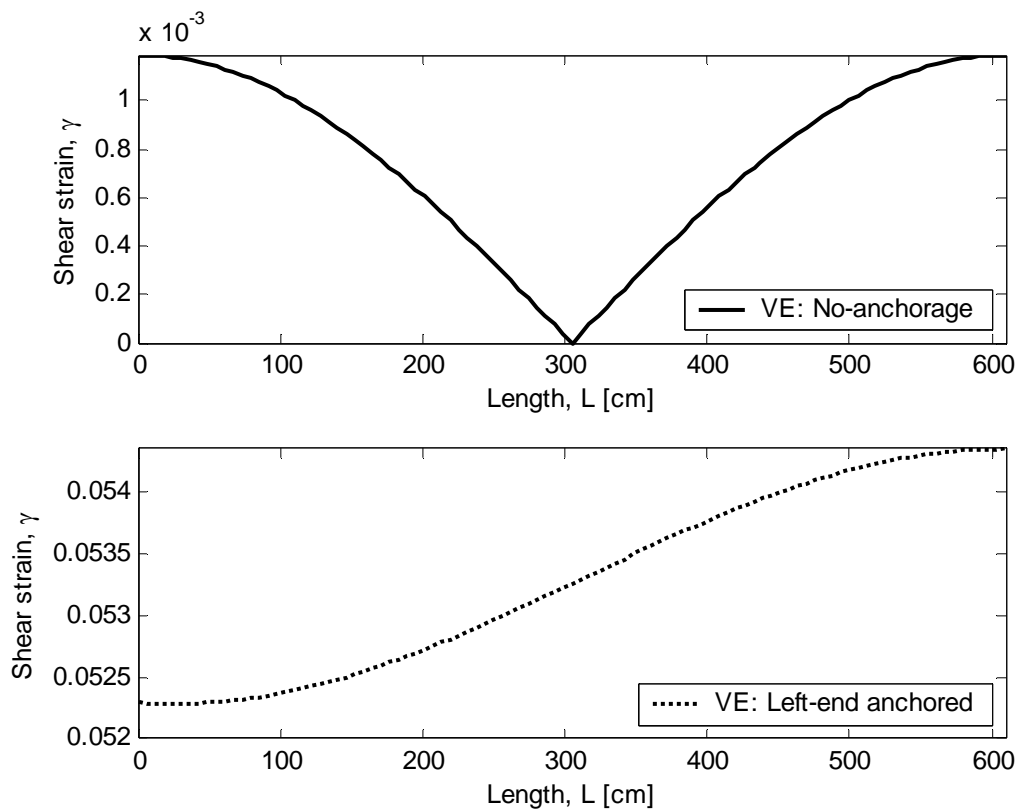
Fig. 6. Shear-strain distribution of a simply supported beam with VE layer for both no-anchorage and one-end anchorage cases. The results are shown at fundamental frequency level for a beam with 51 cm thickness with t_v equal to 0.48 cm.
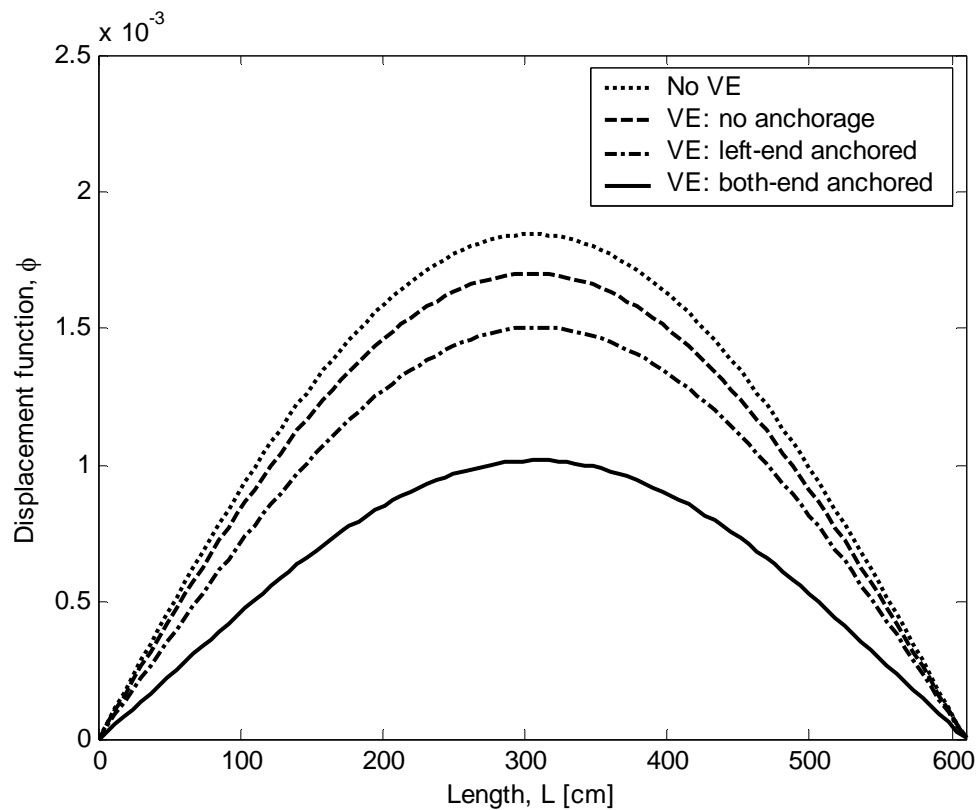
Fig. 7. Displacement functions of a simply supported beam for different configurations of VE layers. The results are shown at fundamental frequency level for a beam with 51 cm thickness with t_v equal to 0.48 cm.
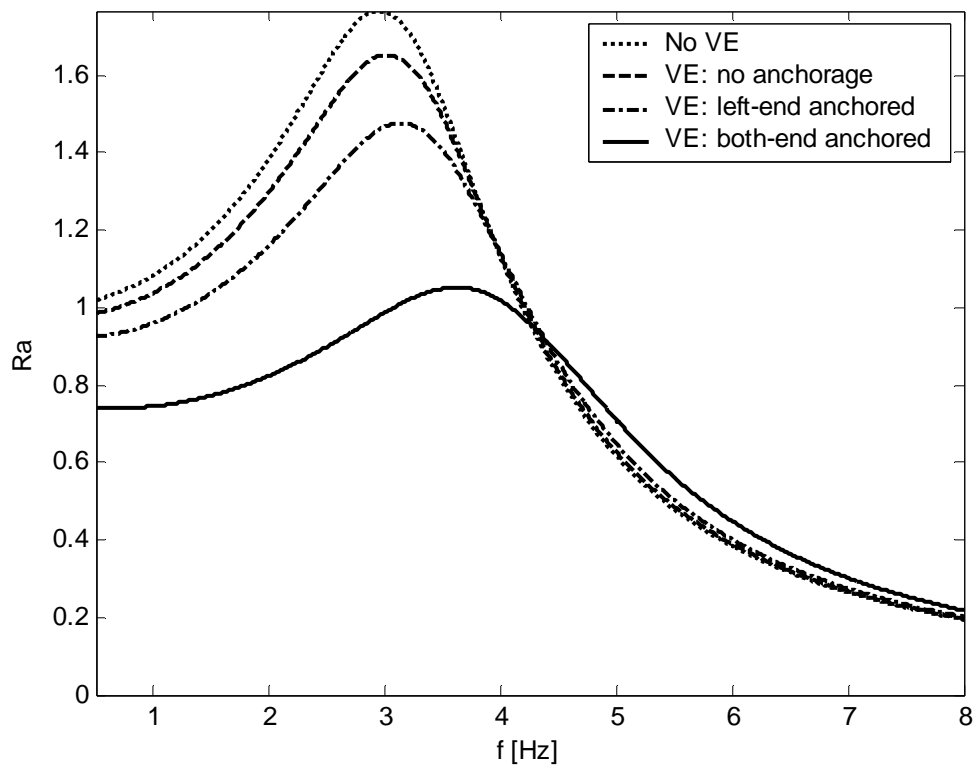
Fig. 8. Acceleration ratio for a simply supported beam for different configurations of VE layers with t_v equal to 0.48 cm including no VE layer case. The results are shown for a beam with 51 cm thickness.
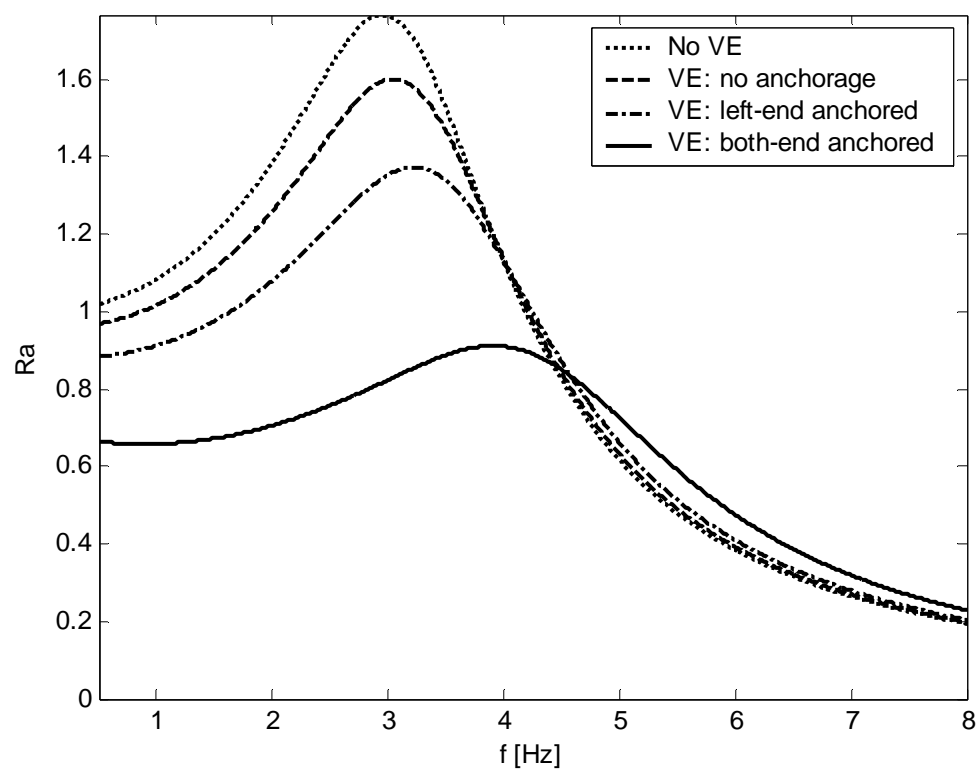
Fig. 9. Acceleration ratio for a simply supported beam for different configurations of VE layers with t_v equal to 0.32 cm including no VE layer case. The results are shown for a beam with 51 cm thickness.
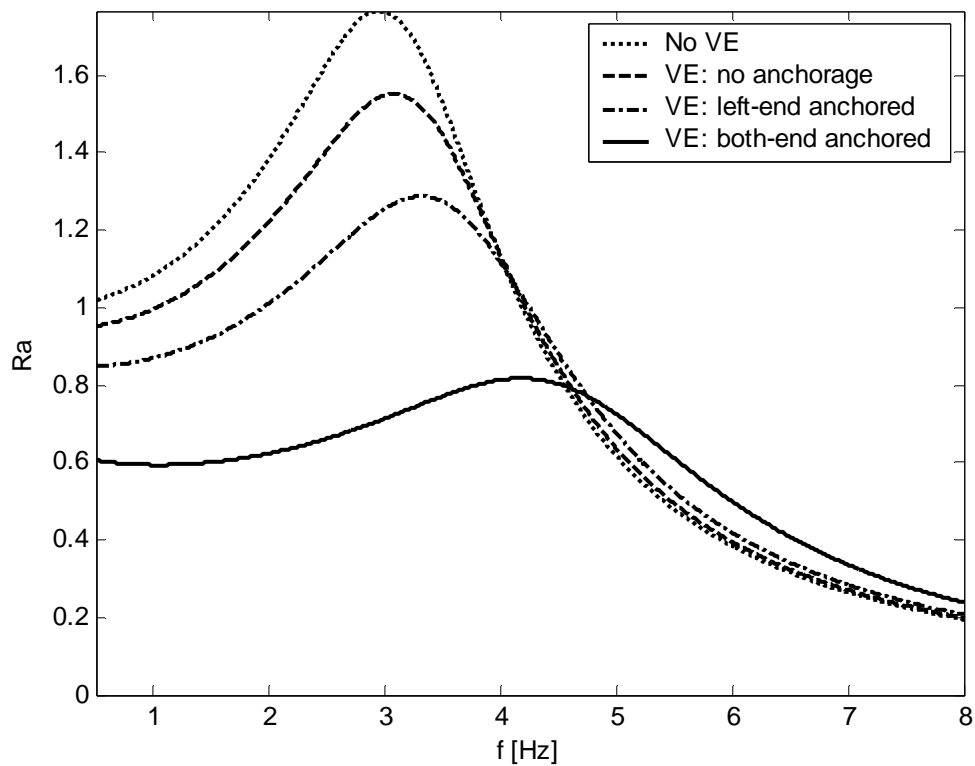
Fig. 10. Acceleration ratio for a simply supported beam for different configurations of VE layers with t_v equal to 0.24 cm including no VE layer case. The results are shown for a beam with 51 cm thickness.
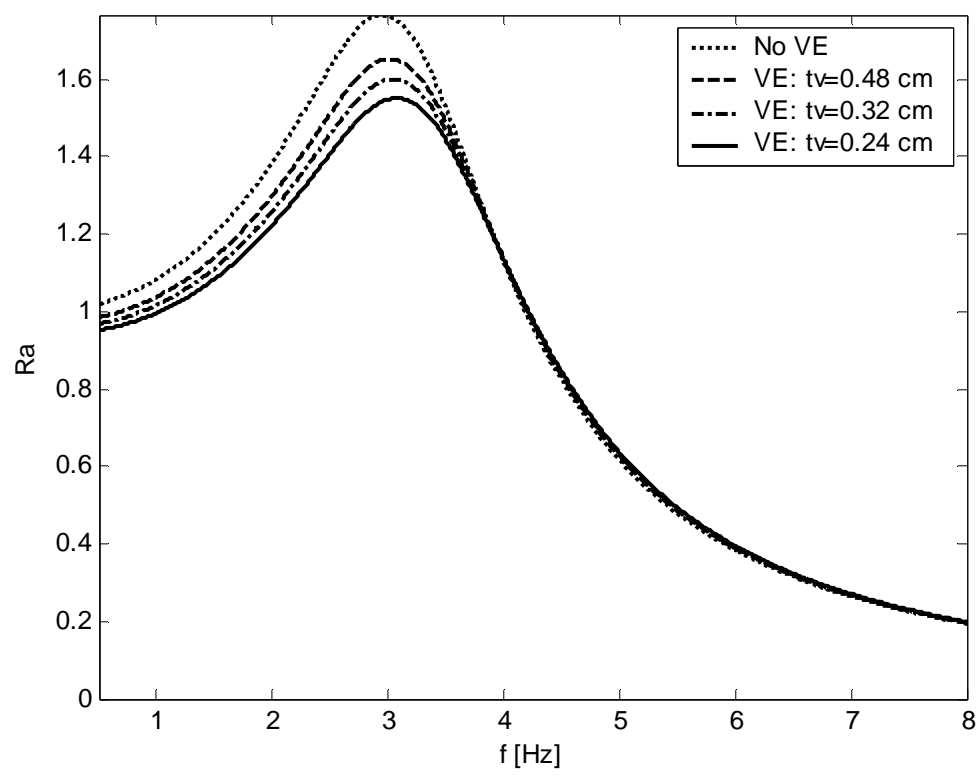
Fig. 11. Acceleration ratio for a simply supported beam with no anchorage case for different thickness of VE layers including no VE layer case. The results are shown for a beam with 51 cm thickness.
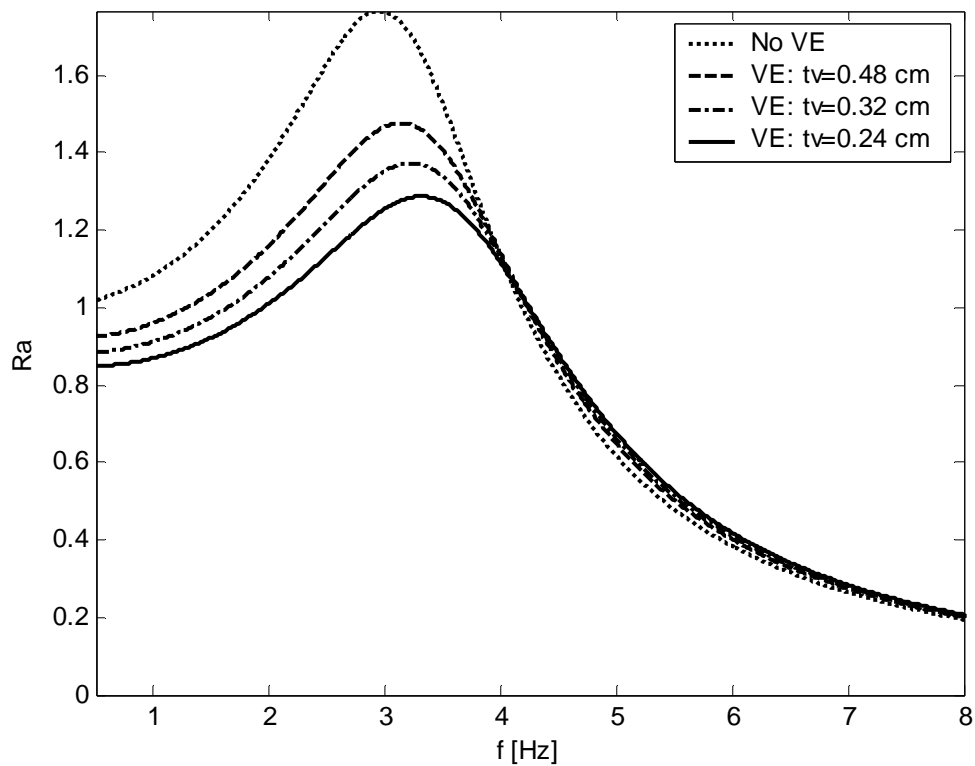
Fig. 12. Acceleration ratio for a simply supported beam with left-end anchorage case for different thickness of VE layers including no VE layer case. The results are shown for a beam with 51 cm thickness.
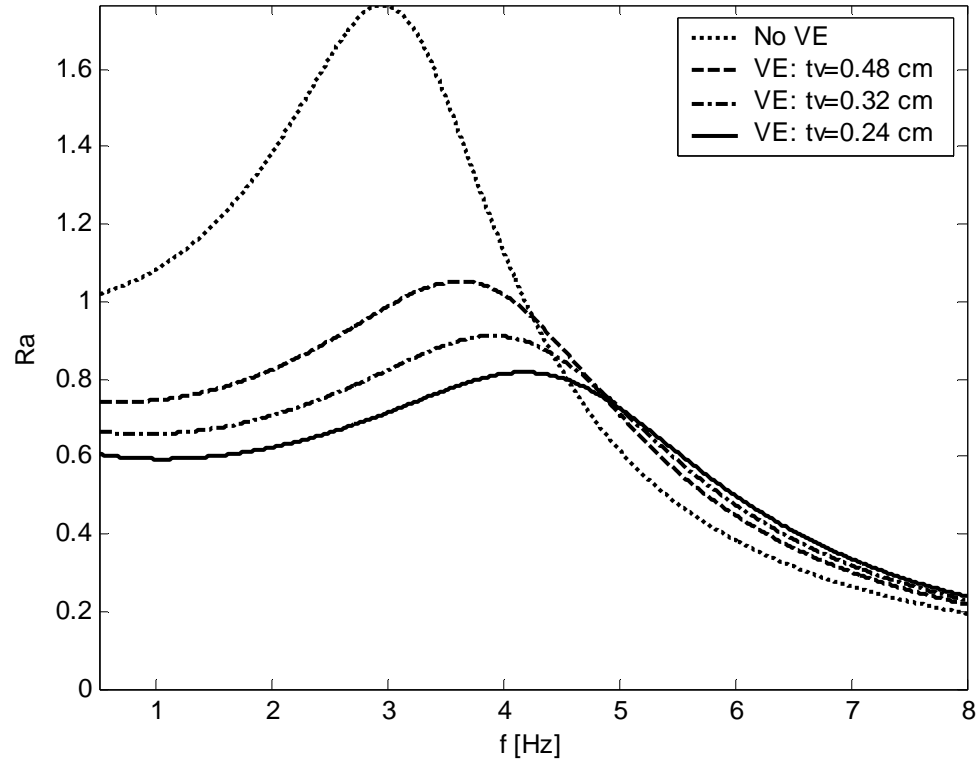
Fig. 13. Acceleration ratio for a simply supported beam with both-end anchorage case for different thickness of VE layers including no VE layer case. The results are shown for a beam with 51 cm thickness.
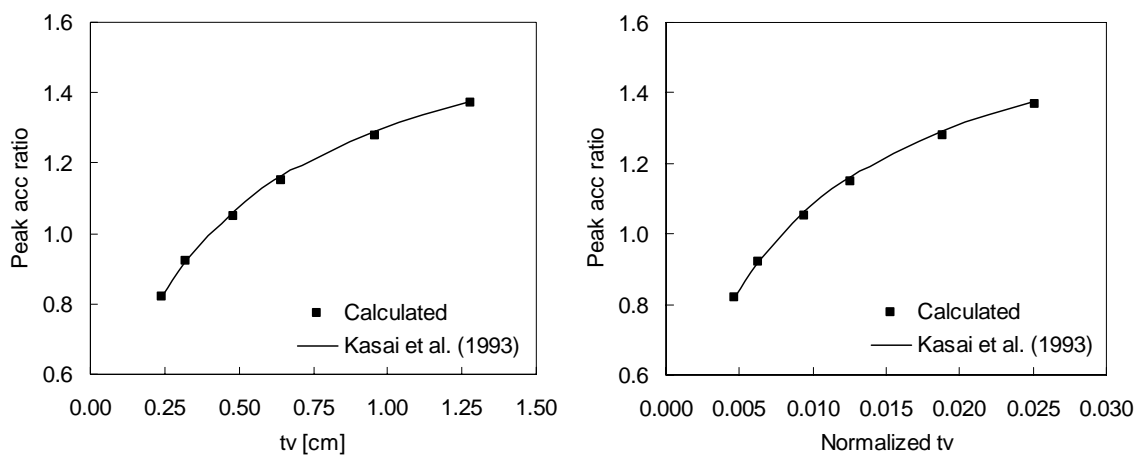
(a) Acceleration ratio w.r.t. VE layer thickness t_v.

(b) Acceleration ratio w.r.t. normalized t_v.

Fig. 14. Acceleration ratio for a simply supported beam with both-end anchorage case for different thickness of VE layers. The results are shown for a beam with thickness h equal to 51 cm and t_v is normalized w.r.t. h.
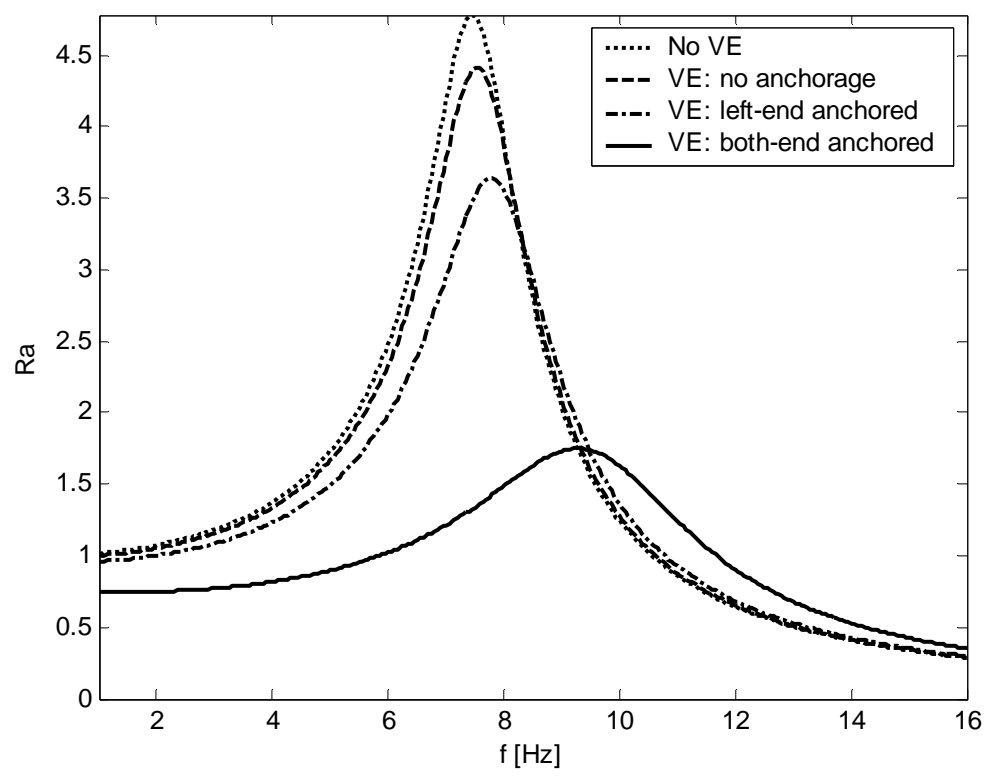
Fig. 15. Acceleration ratio for a simply supported plate-strip for different configurations of VE layers with t_v equal to 0.48 cm including no VE layer case. The results are shown for a plate-strip with 2 cm thickness.
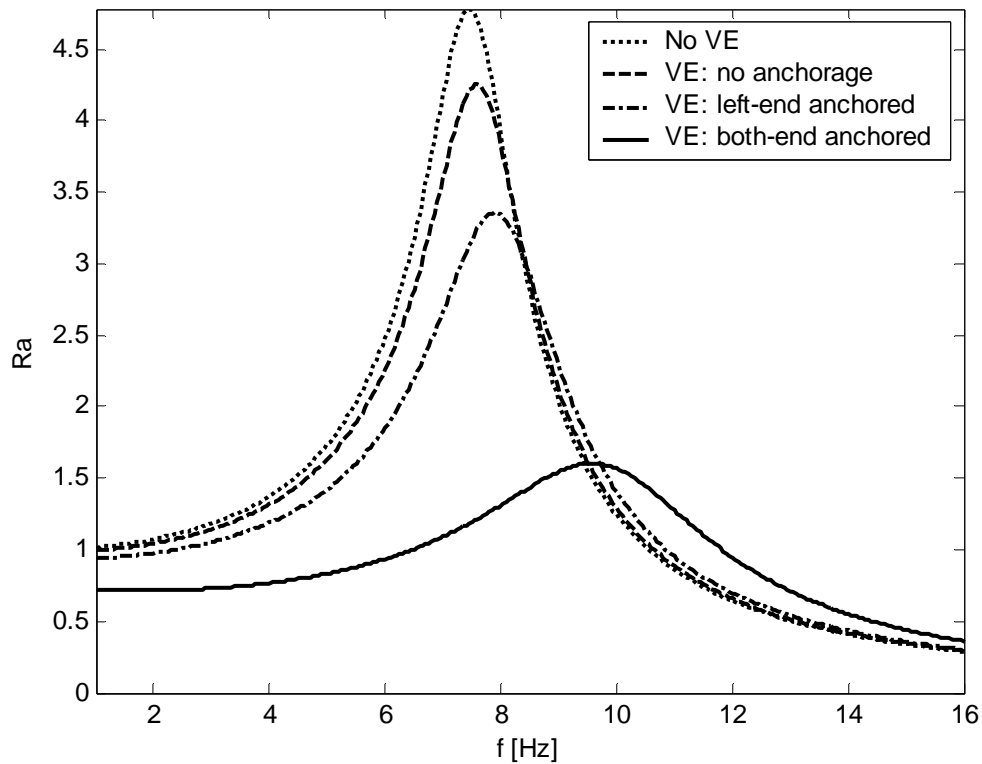
Fig. 16. Acceleration ratio for a simply supported plate-strip for different configurations of VE layers with t_v equal to 0.32 cm including no VE layer case. The results are shown for a plate-strip with 2 cm thickness.
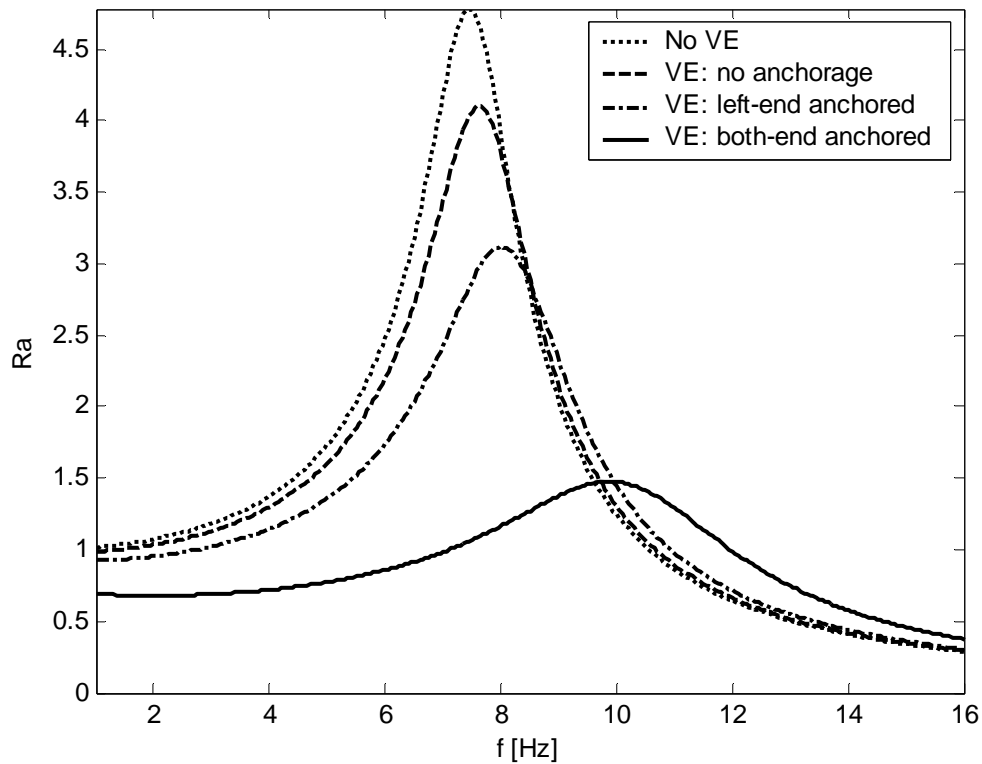
Fig. 17. Acceleration ratio for a simply supported plate-strip for different configurations of VE layers with t_v equal to 0.24 cm including no VE layer case. The results are shown for a plate-strip with 2 cm thickness.
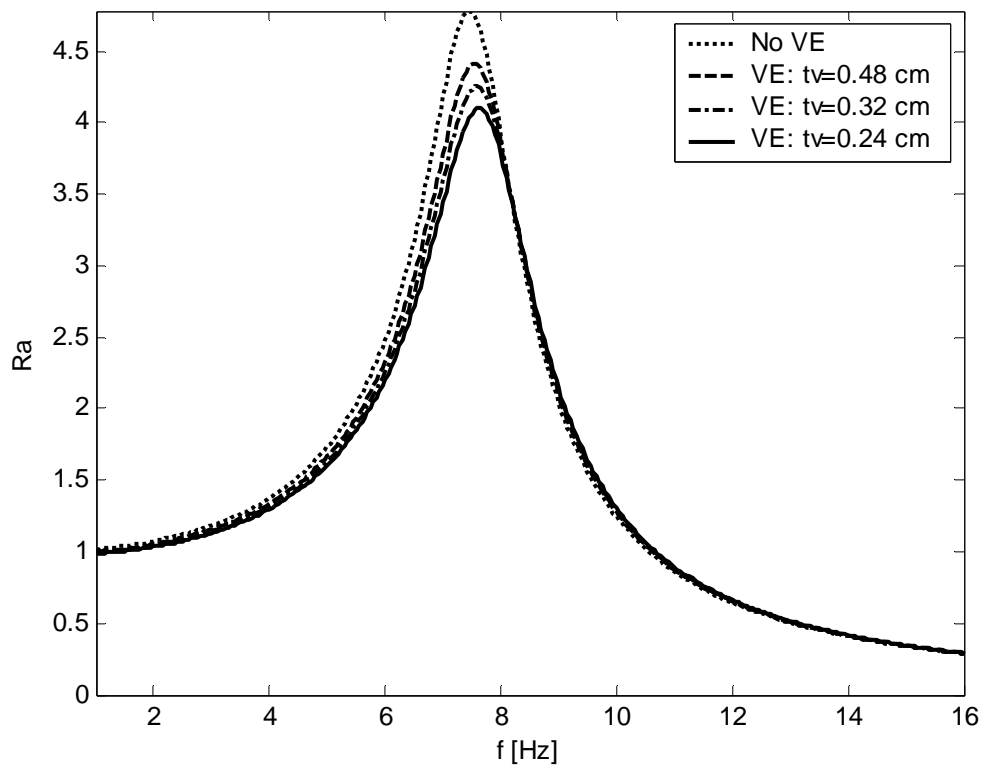
Fig. 18. Acceleration ratio for a simply supported plate-strip with no anchorage case for different thickness of VE layers including no VE layer case. The results are shown for a plate-strip with 2 cm thickness.
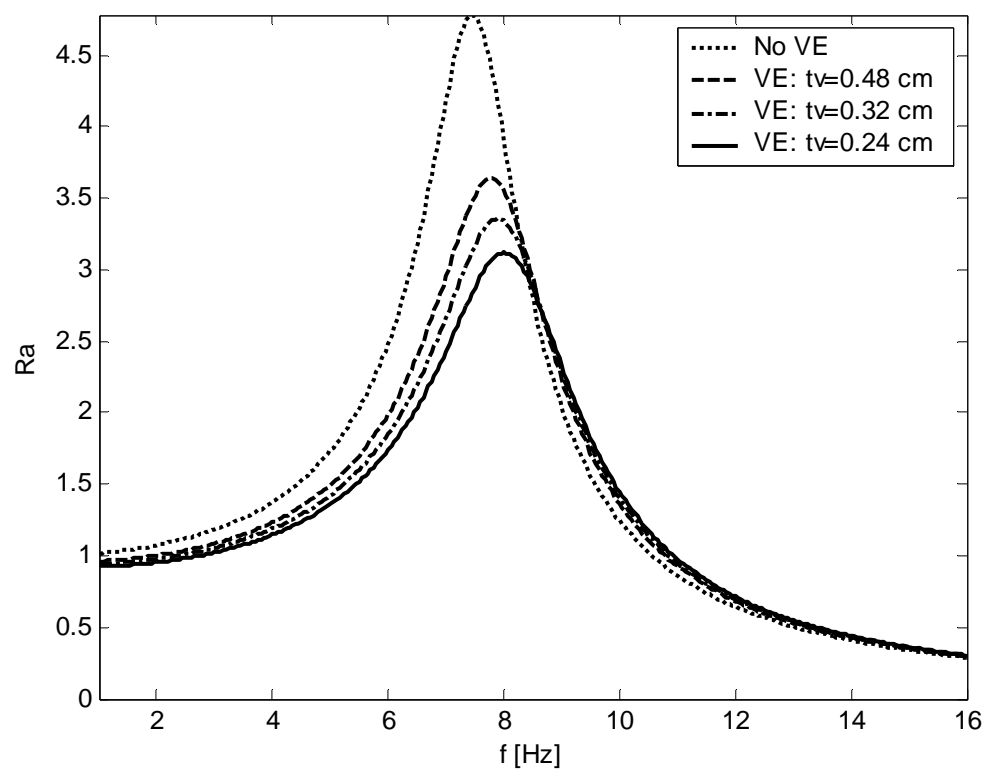
Fig. 19. Acceleration ratio for a simply supported plate-strip with left-end anchorage case for different thickness of VE layers including no VE layer case. The results are shown for a plate-strip with 2 cm thickness.
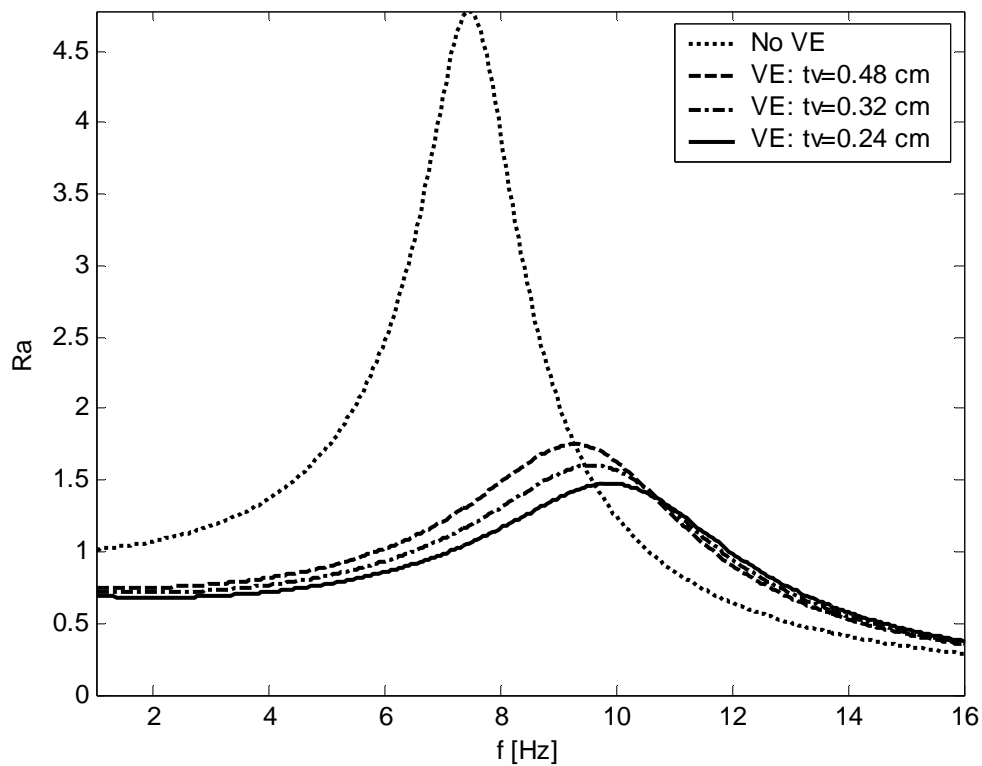
Fig. 20. Acceleration ratio for a simply supported plate-strip with both-end anchorage case for different thickness of VE layers including no VE layer case. The results are shown for a plate-strip with 2 cm thickness.
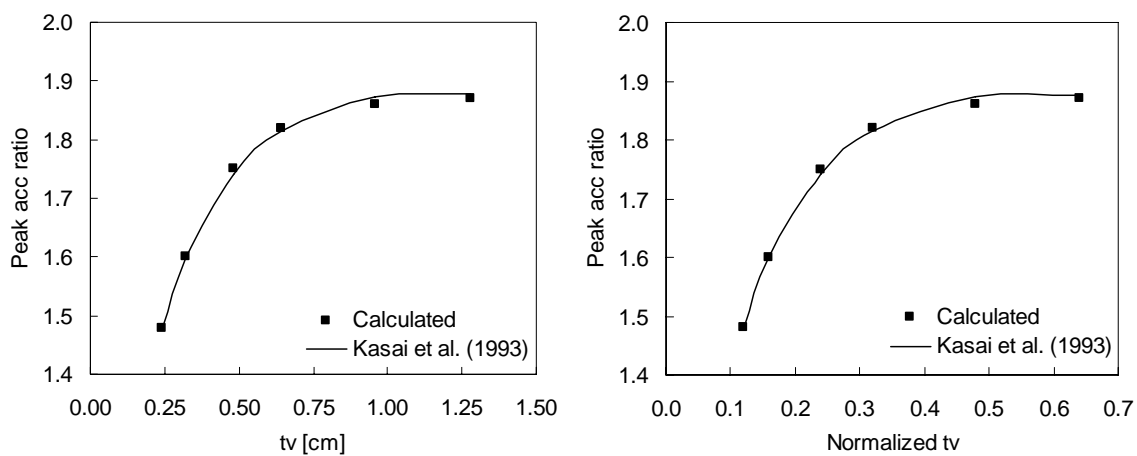
(a) Acceleration ratio w.r.t. VE layer thickness t_v.

(b) Acceleration ratio w.r.t. normalized t_v.

Fig. 21. Acceleration ratio for a simply supported plate-strip with both-end anchorage case for different thickness of VE layers. The results are shown for a plate-strip with thickness h equal to 2 cm and t_v is normalized w.r.t. h.
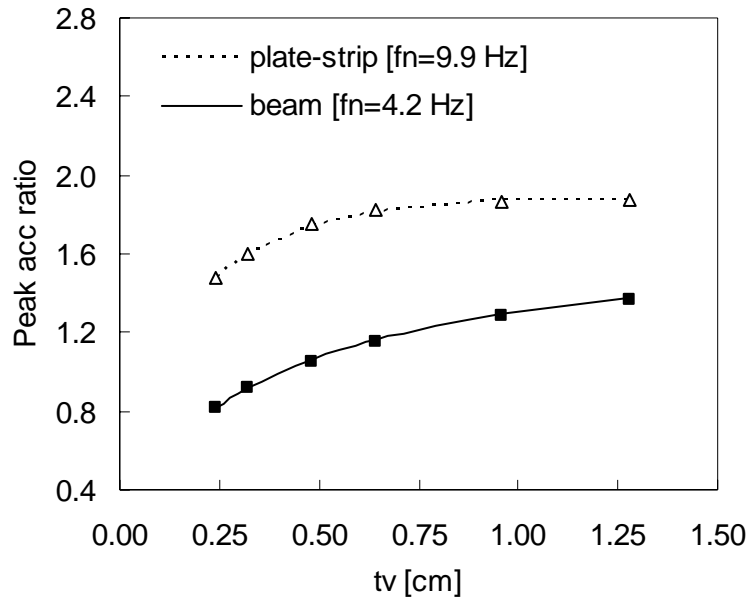
Fig. 22. Acceleration ratio for both simply supported beam and plate-strip with both-end anchorage case for different thickness of VE layers. The results are shown for a beam with 51 cm thickness and a plate-trip with 2 cm thickness.
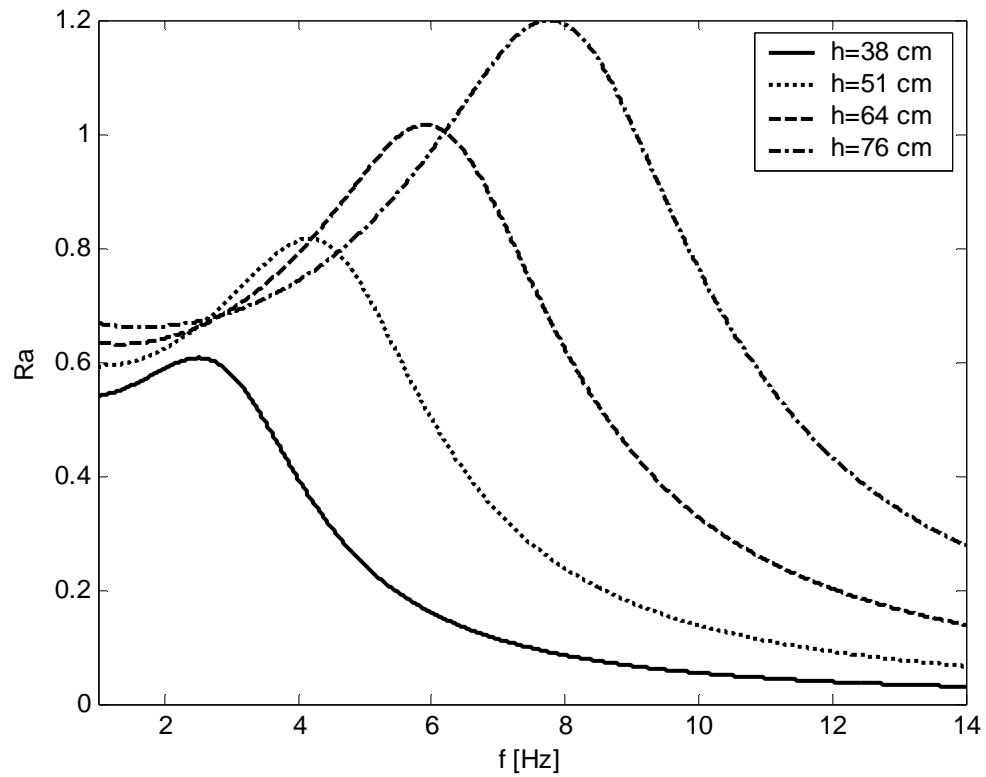
Fig. 23. Acceleration ratio for a simply supported beam with both-end anchorage case for different thickness of beam. The results are shown for a t_v equal to 0.24 cm.
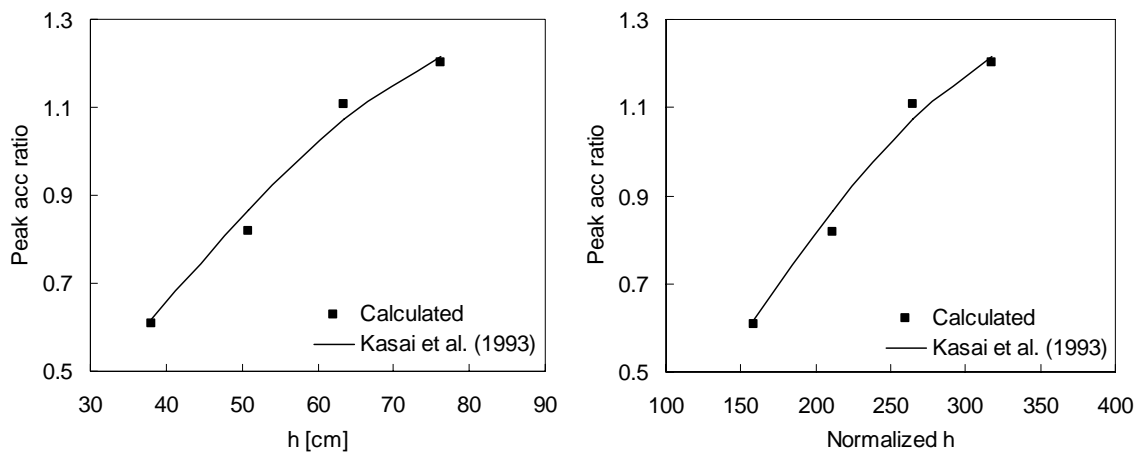
(a) Acceleration ratio w.r.t. beam thickness h.

(b) Acceleration ratio w.r.t. normalized h.

Fig. 24. Acceleration ratio for a simply supported beam with both-end anchorage case for different thickness of beam. The results are shown for a t_v equal to 0.24 cm and h is normalized w.r.t. t_v.
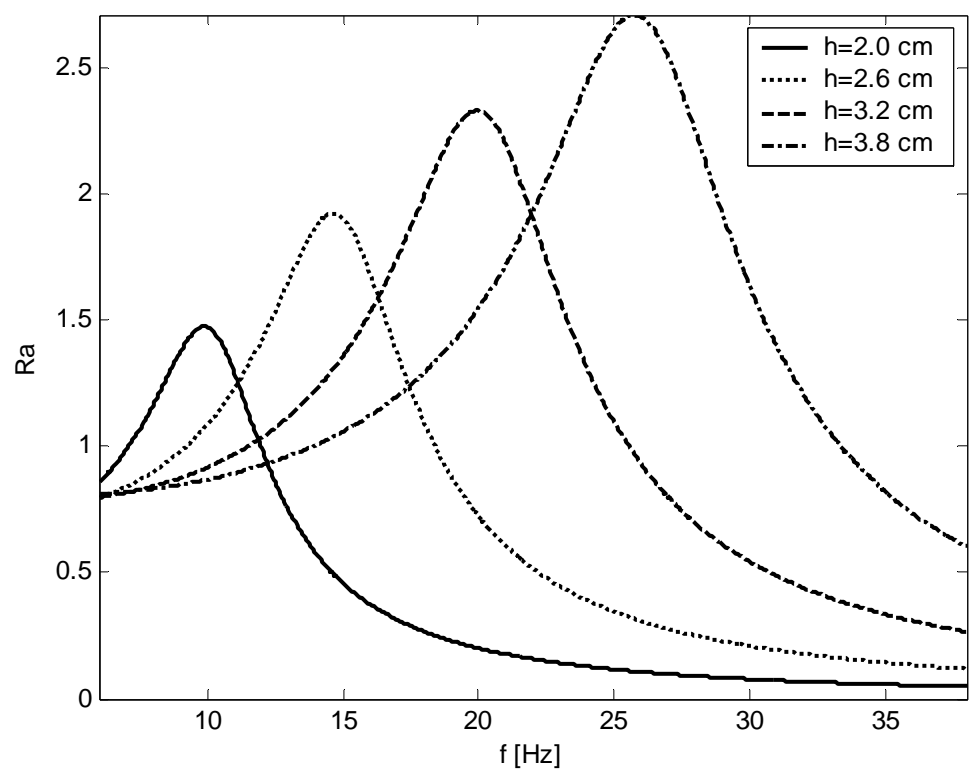
Fig. 25. Acceleration ratio for a simply supported plate-strip with both-end anchorage case for different thickness of plate-strip. The results are shown for a t_v equal to 0.24 cm.
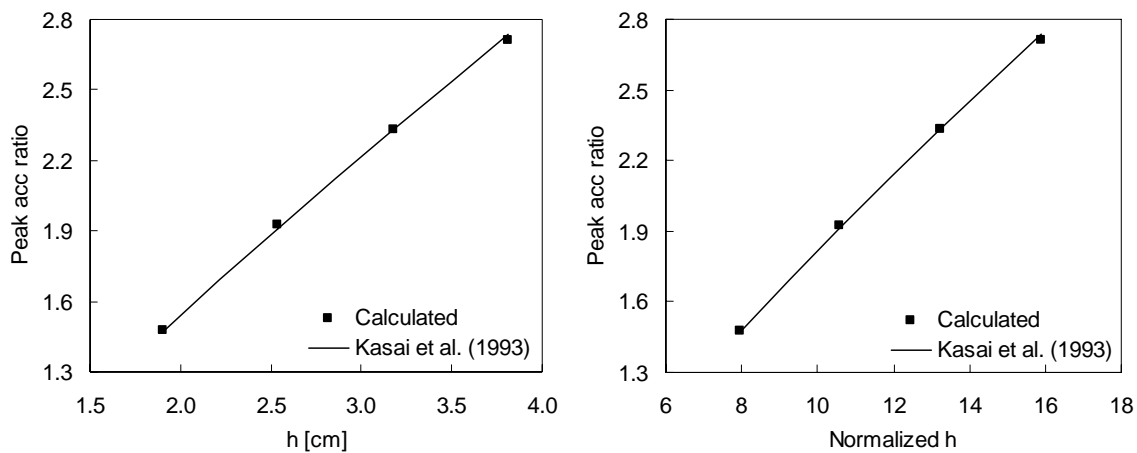
(a) Acceleration ratio w.r.t. plate-strip thickness h.

(b) Acceleration ratio w.r.t. normalized h.

Fig. 26. Acceleration ratio for a simply supported plate-strip with both-end anchorage case for different thickness of plate-strip. The results are shown for a t_v equal to 0.24 cm and h is normalized w.r.t. t_v.
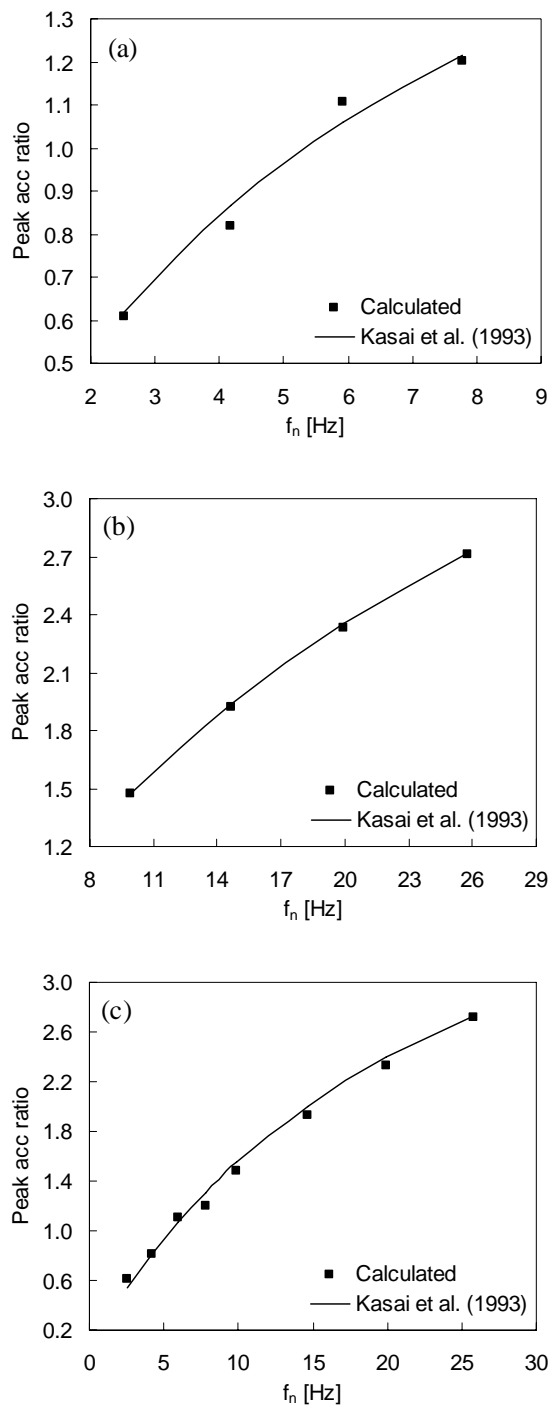
Fig. 27. Acceleration ratio w.r.t. fundamental frequency. The results are shown for (a) beam, (b) plate-strip, and (c) both beam and plate-strip for a both-end anchorage case with t_v equal to 0.24 cm.

2. Distributed Viscoelastic Layer Damping Effect on the Elastic Response of Highway Bridges

Kazi R. Karim[1] and Genda Chen[2*], F. ASCE

Abstract: In this study, VE layer in distributed form was applied to the Old St. Francis River Bridge, located in the new Madrid Seismic Zone, and the bridge responses under harmonic loading were investigated based on a finite element model. An emphasis was placed on the analytical derivation of the VE layer effects on responses of a circular column and modeling of the VE layers with discrete springs in a finite element model. The accuracy of the complex spring model was validated with an analytical solution under harmonic loading. The effect of single versus double curvatures was also investigated using the out-of-plane and in-plane motions. It was observed that a 2.38 mm VE layer covering the lower 40% of the column height can reduce the out-of-plane acceleration and displacement by 14% and the in-plane responses by approximately 11%. In comparison with the retrofit scheme at both ends of the columns, it was observed that retrofitting of one end of the columns with the same 40% VE coverage is more efficient compared to retrofitting at both ends. It was also observed that the VE layer is more effective for a range of 20% to 80% coverage of the column height. Finally, a simple

---

[1] Structural Engineer, Kirkpatrick Forest Curtis PC, 205 NW 63rd St Suite 390, Oklahoma City, OK 73116, E-mail: krk2q4@mst.edu

[2] Professor of Civil Engineering and Interim Director of the Center for Infrastructure Engineering Studies, Missouri University of Science and Technology, 224 Engineering Research Laboratory, 500 W. 16th Street, Rolla, MO 65409, E-mail: gchen@mst.edu

[*] Corresponding author

approach is proposed, which is expected to be useful in estimating the elastic responses of the bridge columns with VE layers.

CE Database subject headings: VE material; Highway bridge column; Elastic response; Surface damping.

Introduction

Over 50% of the bridges in the NBI database representing the 1970's construction methods which incorporate no seismic design considerations are structurally deficient (Chen et al. 2002). To respond to the ever-increasing retrofitting needs, several strengthening techniques, such as fiber reinforced polymer (FRP) jacketing, have been developed over the past two decades (FHWA 2005; MCEER 2005). These techniques can be used to provide an existing reinforced concrete (RC) column with effective confinement so that the column will not collapse during a strong earthquake event. Strengthening alone, however, is unlikely to improve the column performance under moderate earthquake events. This is because significant strains must be developed in the column before a jacketing technique is effectively engaged as part of the strengthened column system. It is, therefore, desirable to develop a new retrofitting technology that can meet multiple performance objectives in the context of performance-based design of structures (FEMA 1997; MCEER 2005).

VE materials in distributed form were commonly used in mechanical engineering to control vibration-introduced fatigue in airframes (Ross et al. 1959) and for general vibration suppression (Morgenthaler 1987; Gehling 1987; Kerwin and Ungar 1990). In civil engineering, however, VE materials were exclusively applied in VE dampers that

can be installed between two adjacent floors in buildings. Most of the early investigations were included in Aprile et al. (1997), Soong and Dargush (1997), Hanson and Soon (2001), Soon and Spencer (2002), and Lin and Chopra (2003). Original developments on this subject included the damper characterization (Zhang et al. 1989; Zhang and Soong 1992; Shen and Soon 1995), shake table test of steel frames (Aiken et al. 1993; Bergman and Hanson 1993; Chang et al. 1992, 1995, 1996), laboratory test on lightly-reinforced concrete frames (Foutch et al. 1993), and damper application for retrofitting of buildings (Kasai et al. 1993; Chang et al. 1995).

Chen et al. (2006) introduced a constrained VE layer wrapped by FRP jacketing to a cantilever RC column and investigated the response reduction due to distributed damping effect. The damping component of this new methodology is to reduce the bridge response under small to moderate earthquakes loading so that the operational performance level of the bridge is in compliance with design standards. Chen and Karim (2006) introduced an analytical derivation of the VE layer effects on circular column responses and modeling of the VE layers with discrete springs in a finite element model of a highway bridge.

The focus of this study is to apply VE layer in distributed form to a circular bridge column, formulate the equation of motion for a circular column that is retrofitted with VE layer, develop a discrete complex spring modeling technique for the distributed VE layer and apply the model in the finite element analysis of a single bent of a three-span continuous steel girder bridge. The accuracy of the complex spring model was validated with an analytical solution under harmonic loading. The effect of single versus double curvatures on the damping effect was investigated in detail using the out-of-plane and in-

plane motions of a three-column bent that represents a three-span regular highway bridge in the New Madrid Seismic Zone, Central United States.

Damping-Enhanced Strengthening (DES) System

Chen et al. (2006) introduced a constrained VE layer wrapped by FRP jacketing to a cantilever RC column, known as a damping-enhanced strengthening (DES) system. The system consists of one or more FRP sheets (inner) wrapped around the circular (or rectangular) RC column, a VE layer attached on the FRP sheets, and another FRP sheet (outer) outside the VE layer that is anchored at one end into the connecting member (beam or footing) of the column. The entire system is shown schematically in Fig. 1. The fibers of the inner FRP sheets are oriented along the perimeter of the column for confinement effect while those of the outer FRP sheet are oriented vertically along the length of the column. The VE layer is bonded to the inner and outer FRP sheets with epoxy. Both the inner FRP sheets and the VE layer stop approximately one inch away from the beam/footing.

Shear Mechanism of Anchored Constrained VE Layer in a DES System

When the column is bent to the right, the VE layer on the left side of the column undergoes significant shear deformation between the inner and the outer FRP sheets and dissipates energy while the deformation and energy dissipation of the remaining VE layer on the right side are small. The shear deformation may become more pronounced when the column starts separating from its connecting member (beam or footing) at the construction joint due to slippage of dowel bars as a result of debonding of the lap splices

or formation of a plastic hinge. The main design parameters of such an integrated system include the number and height of the inner FRP sheets, thickness and height of the VE layers, the ratio of Young's modulus between VE material and concrete, bond strength, embedment length of the outer FRP sheet for anchorage, and the location of anchorage.

Effect of Distributed Damping in a DES System

The proposed DES system has an integrated VE layer as distributed damping into the FRP jacketing of a cantilevered RC column. In performance-based seismic design, the intent of providing an enhanced distributed damping component is to reduce the seismic responses of the column under a small earthquake event for an improved functionality and performance level. In this case, the inelastic deformation of the column is very limited and the retrofitted system basically remains elastic, which is the main reason to focus on the damping effect on elastic responses in this study. It is worth noting that adding VE layers has virtually no extra installation cost.

Shear Strain Amplification Mechanism in the New Treatment

To understand why the new constrained layer treatment is more effective than the conventional way, consider the partially covered column in Fig. 1 subjected to a bending moment at the cantilever end. Fig. 2 presents the comparison of the shear stress distribution between the conventional and the new treatments. Under the end moment, the column experiences a constant moment or curvature along its height. When the constraining layer is not anchored, as shown in Fig. 2(a), the induced shear stress must be zero and therefore changes its direction at the middle height of the VE layer in order to

satisfy the zero vertical force equilibrium condition at the section below the VE layer. At any other point, the shear stress is proportional to the distance from the middle height point.

On the other hand, when the constraining layer is anchored into the column footing, as illustrated in Fig. 2(b), the shear stress induced linearly increases with the distance from the footing in the same direction. As a result, the maximum stress in the new treatment, shown with solid plus dotted arrows in Fig. 2(b), is more than twice that of the conventional way, as shown in Fig. 2(a). By superimposing the stress distribution in Fig. 2(a) with that in Fig. 2(b), the net stress difference gained with the anchored constraining layer is indicated by the solid arrows in Fig. 2(b), resulting in a three times more shear force counteracting the effect of the end moment. In a similar study by Karim and Chen (2009) for a simply supported beam, it was observed that the distributed damping is more effective when the VE layer is either anchored at one-end or both-end of the beam when compared to the conventional VE layer, i.e. VE layer with no-anchorage.

Discrete Spring Modeling of Distributed VE Layers

For simplicity of the following derivation, the neutral axis of the circular section is assumed to pass through the center of the section, as illustrated in Fig. 3(a). Considering the Euler beam theory, the longitudinal deformation at any point on the circumference of the cross section, as shown in Fig. 3(b), is linearly distributed with the distance from the neutral axis, also shown in Fig. 3(a). As a result, the shear strain in the VE layer at x distance from the top surface of the column footing is obtained by dividing the

longitudinal deformation by the thickness of the VE layer. The shear strain and its corresponding shear stress can be expressed as

$$\gamma(x,\theta,t) = \frac{d}{2t_v}\frac{\partial y(x,t)}{\partial x}\cos\theta = \gamma_{max}(x,t)\cos\theta \quad \text{and} \quad \tau(x,\theta,t) = \tau_{max}(x,t)\cos\theta \qquad (1)$$

in which d is the diameter of the column, t_v is the thickness of the VE layer, θ is the angle over the cross section measuring from a line perpendicular to the neutral axis, $y(x,t)$ is the relative transverse displacement with respect to the column base along the centerline of the column, $\gamma_{max}(x,t)$ and $\tau_{max}(x,t)$ are the maximum shear strain and stress, respectively, on the cross section x distance from the footing.

For a circular section, the moment of the shear force over the distance dx about the neutral axis can be determined by

$$2\int_0^{\pi/2}[\tau(x,\theta,t)(\frac{d}{2}d\theta)dx](\frac{d}{2}\cos\theta) = \frac{d^2}{2}\tau_{max}(x,t)\int_0^{\pi/2}\cos^2\theta d\theta dx = \frac{\pi d^2}{8}\tau_{max}(x,t)\,dx \quad (2)$$

Therefore, the equation of motion can be derived following the same procedure as used in Chen et al. (2006) and written as

$$EI\frac{\partial^4 y(x,t)}{\partial x^4} + m\frac{\partial^2 y(x,t)}{\partial t^2} + c\frac{\partial y(x,t)}{\partial t} + \frac{\partial \tau_{max}(x,t)}{\partial x}\frac{\pi d^2}{8} = -m\ddot{y}_0(t) \qquad (3)$$

in which, EI is the flexural rigidity of the RC column, m and c are the mass and damping coefficients per unit length, respectively, which are considered as constants in this paper, and $\ddot{y}_0(t)$ is the ground acceleration.

When the base excitation $\ddot{y}_0(t) = Ae^{i\omega t}$, the steady-state transverse displacement, the maximum shear strain and stress in the VE layer can respectively be expressed as

$$y(x,t) = \phi(x)e^{i\omega t}, \ \gamma_{max}(x,t) = \frac{d}{2t_v}\frac{d\phi(x)}{dx}e^{i\omega t}, \ \text{and} \ \tau_{max}(x,t) = \frac{d}{2t_v}\frac{d\phi(x)}{dx}\frac{G'(\omega)}{\cos\delta}e^{i(\omega t+\delta)} \ (4)$$

where A is the amplitude of the base acceleration, ω is the excitation frequency, t denotes the time instance, $i = \sqrt{-1}$ represents the imaginary unit of a complex number, $\phi(x)$ is a displacement function, G'_v is the shear storage modulus, and δ is the loss factor of the VE material. In general, they are both functions of the excitation frequency and the hardness of the materials. In this study, the shear storage modulus G'_v and loss factor δ were taken from the experimental study by Huang (2005) and are shown in Fig. 4.

Spring Representation of VE Layer Effects

The fourth term on the left side of Equation 3 represents the effect of the added VE layer. To facilitate the finite element analysis of a bridge structure, it is desirable to express that term as a function of the transverse displacement so that it can be modeled by discrete springs of complex coefficients. A closer examination on the fourth term in Equation 3 and the maximum stress expression in Equation 4 indicates that the shear stress at any point is proportional to the curvature at that point for the steady-state responses. Therefore, a relation between the curvature and the displacement needs to be established. In this study, an approximation of the ratio between the curvature and the displacement of the column, $r_1(x)$, is made by using the first mode shape of the cantilever column of consistent mass (Chopra 2001). That is,

$$r_1(x) = \beta_1^2 \frac{\cosh \beta_1 x + \cos \beta_1 x - a\,(\sinh \beta_1 x + \sin \beta_1 x)}{\cosh \beta_1 x - \cos \beta_1 x - a\,(\sinh \beta_1 x - \sin \beta_1 x)}, \quad a = \frac{\cosh \beta_1 L + \cos \beta_1 L}{\sinh \beta_1 L + \sin \beta_1 L} \quad (5)$$

where $\beta_1 = 1.8751/L$ is related to the fundamental frequency of a column of uniformly distributed mass, and L is the total length of the cantilever column.

With this approximation, the fourth term on the left side of Equation 3 can be simplified in the steady-state of vibration into the following:

$$\frac{\partial \tau_{\max}(x,t)}{\partial x} \frac{\pi d^2}{8} = \frac{\pi d^3}{16 t_v} \frac{d^2 \phi(x)}{dx^2} \frac{G'(\omega)}{\cos \delta} e^{i(\omega t + \delta)} \approx \frac{\pi d^3}{16 t_v} \frac{G'(\omega)}{\cos \delta} e^{i\delta} r_1(x) y(x,t) \qquad (6)$$

The effect of the VE layer now can be approximately modeled by continuous springs along the portion of the column that is covered by the VE layer. The spring constant per linear length, $k(x)$, is defined as

$$k(x) = \frac{\pi d^3}{16 t_v} \frac{G'(\omega)}{\cos \delta} e^{i\delta} r_1(x) \qquad (7)$$

which is a complex function. In the finite element model of a bridge structure, the effect of the VE layer can be further simplified by discrete springs. When a column is equally divided into many finite elements of Δx in length, the spring constant of the discrete element at x distance from the footing is equal to $k(x)\Delta x$ in force per length. The normalized shape function $\phi(x)$ and corresponding normalized curvature to displacement ratio $r_1(x)$ are shown in Fig. 5. It should be noted that in Fig. 5, height is normalized w.r.t. overall height of the column, $\phi(x)$ is normalized w.r.t. maximum value of $\phi(x)$, and $r_1(x)$ is normalized with respect to (w.r.t.) maximum value of $r_1(x)$ so that their maximum values cannot exceed 1.0 and can easily be visualized how they look like within the same frame.

Validation of Spring Representation with a 1/5-Scale Square RC Column

To validate the discrete spring model of VE layers, a 152.4 cm long, 20.32 cm×20.32 cm square column analytically studied in Chen et al. (2006) was analyzed using the finite

element model (FEM). When the column is evenly divided into finite elements of 2.54 cm long, the steady-state acceleration ratio between the top of the column and the ground is presented in Fig. 6 over a frequency range of 6.6 to 7.2. In the figure, two solid lines represent the solutions obtained by the analytical and two dotted lines indicate the FEM results. Two cases are presented: a_5=0, i.e. no VE layers, and a_5=0.4, i.e. 40% coverage of the column height with VE layers. It can be observed that for either case, the FEM solution agrees well with the analytical results over the entire frequency range considered, particularly in the resonant range. The VE layer reduces the acceleration by approximately 5%.

Finite Element Modeling of Bridge Columns with VE Layers

Old St. Francis River Bridge over US60 in the New Madrid Seismic Zone

To apply VE layers as discrete springs in the FEM of bridge columns, the Old St. Francis River Bridge was considered as an example, which is presented in the following study. Designed in 1977 without seismic considerations, this 7.92m high bridge consisted of three spans supported by steel plate girders (Chen et al. 2002). The interior diaphragms and the cross-frames each consisted of two diagonals L3×2½×5/16 crossed over each other, top and bottom horizontal members L4×4×5/16. All interior diaphragms and cross-frames were placed parallel to the abutments of the bridge. The bridge, however, was skewed at a 20° angle, so the ends of the girders were offset from one another at the ends of the bridge. Therefore, these diaphragms and cross-frames were not perpendicular to the girders because of the angle of the structure.

The bridge superstructure is supported by two intermediate bents through one fixed bearing and one expansion bearing, along with two seat-type abutments at its ends. Each bent consisted of a RC cap beam and three RC columns. Both bents and abutments are supported by deep friction pile foundations. There are 12 piles, each approximately 5.79 m in length, for each column footing and 16 piles, each about 13.72 m in length, for each abutment footing. Two expansion joints were constructed at the ends of the bridge. This bridge used 27.58 MPa concrete for the superstructure and 20.68 MPa concrete for the substructure. For the reinforcing steel, 275.80 MPa was used.

The bridge was modeled with the finite element method in SAP2000. All of the components of the structure were included in the bridge model. Springs and dashpots were used at the base of each column and each abutment to model the soil and foundation effects. The periods for the first two vibration modes of the bridge were found to be 1.3173s and 0.4773s, respectively (Chen et al. 2002). The elevation and vibration modes of the bridge are shown in Figs. 7 and 8, respectively, and cross-sectional properties of one of the bridge columns are shown in Fig. 9(a).

To better understand the effect of VE layers, the bridge was first analyzed under two individual ground motions: along the traffic direction (longitudinal) and perpendicular to the traffic direction (transverse). Since the bridge is skewed to a small degree, the longitudinal and transverse motion can be approximately simulated by the out-of-plane and in-plane motion of the fixed bent as separately discussed below.

Single Curvatures

The out-of-plane behavior of the fixed bent is similar to a cantilever column that was subjected to single curvature, the same behavior as Fig. 6 indicates except for different scale. The frequency response function of the absolute acceleration at the bridge deck, normalized by the peak ground acceleration, is shown in Fig. 10(a). It is clearly seen from Fig. 10(a) that a 40% VE coverage (a_5=0.4) of the lower portion of the column can reduce the peak deck acceleration by 14%, which is significantly more effective than that presented in Fig. 6 due mainly to scale effect. Note that the natural frequency of the fixed bent is slightly increased due to the stiffening effect of the VE layer.

Double Curvatures

The in-plane motion of the fixed column involves a frame action of three columns. Each column is subjected a double curvature. Each column can then be modeled as illustrated in Fig. 9(b) with VE effects represented by continuous springs. A rigid element was introduced at each end of the element to facilitate the development of a spring modeling concept. At each end of the column, a distribution of stiff concrete was considered in the FEM.

In this case, the parameter L in Equation 5 represents the distance from the point of inflection to the footing for the lower portion or to the cap beam for the upper portion of the column. From a linear analysis of the frame under a concentrated load at the cap beam, it was found that the point of inflection is slightly above the mid height of the column. For simplicity, it was considered at the mid height of the column in the following analysis. Fig. 10(b) presents the acceleration ratio between the deck and the

ground for five cases: no VE layer (a_5=0), 20% coverage on the lower half ((a_5=0.2 [b])

of the column, 20% coverage on the upper half ((a_5=0.2 [t]) of the column, 20% coverage

on the both lower and upper half of the column (a_5=0.2 [t+b]), and 40% coverage on the

lower half ((a_5=0.4 [b]) of the column. In this case, it is clearly seen that the effect of VE

layers at top or bottom of the column is the same, each resulting about 2% reduction; the

introduction of VE layer both at the top and the bottom of the column, the total effect is

approximately 4%. The increase of this effect is due to the accumulative effect of shear

strain in VE layers.

It can also be seen from Fig. 10(b) that the 40% VE coverage can reduce the peak

acceleration by 11% when attached on the lower portion of the column, which is much

higher compared to the acceleration reduction when VE is applied 20% both on the lower

and upper portion of the column. These results indicate less effectiveness of VE layers

used to mitigate the in-plane responses with VE layers applied at both ends of the

column. Therefore, for mitigation purpose, it is better to apply VE layer only in one side

of the column, preferably, on the bottom half of the column.

Simple Expressions for Obtaining Responses in FEM

In the discrete spring representation of the VE layer, several factors are related, viz. %

coverage of the VE layer a_5, choice of Δx, VE layer thickness t_v, etc. While dealing with

these parameters in FEM, it is an extremely laborious task to provide those inputs in FEM.

Therefore, in this section, some procedures are given regarding how to use some simple

expressions in obtaining the steady state responses in FEM. It should be noted that the

responses considered are only the peak responses.

In order to do so, first, the responses were obtained w.r.t. a_5, Δx and t_v and they are shown in Figs. 11, 12, and 13, respectively. Fig. 14 summarizes the peak responses w.r.t. both Δx and t_v for $a_5 = 0.4$. Note that all values are shown w.r.t. normalized a_5, Δx and t_v for simplicity, where a_5 is normalized w.r.t. column height while both Δx and t_v are normalized w.r.t. column diameter. For instance, $a_5 = 0.4$ means VE layer coverage of 0.4h, i.e. 3.17m (height, h = 7.92m), $t_v = .0104$ means VE layer thickness of .0104d, i.e. 9.5mm (diameter, d=914mm), and $\Delta x = 0.03$ means discrete element of 0.03d, i.e. 27.4mm. Another reason to use normalized parameters is to avoid the possible conflict of using different unit systems. Therefore, the users have some flexibility in choosing any preferred unit system. Hereafter, the term "normalize" is omitted for simplicity.

Looking at Fig. 14, it is clear that the responses are correlated w.r.t. both Δx and t_v. A similar trend was also observed w.r.t. a_5 (not shown). This means that some scale factors can be applied in obtaining the responses. With this view, the scale factors are obtained w.r.t. Δx, t_v, and a_5, respectively, and they are shown in Fig. 15. The expressions for scale factors are summarized below. It should be noted that it is necessary to have the initial peak response to apply those scale factors. For simplicity, the initial response *Acco* w.r.t. Δx is considered for a $t_v = .0026$ and also shown below. It should also be noted that the subscripts refer to the corresponding scale factors.

$$Acco = a \exp^{b\Delta x} \tag{8}$$

$$sf_{\Delta x} = c \exp^{d\Delta x} \tag{9}$$

$$sf_{tv} = e^{\frac{(-f+g)tv^h \sin(h\pi/2)}{1+(f+g)tv^h \cos(h\pi/2)+fgtv^{2h}}} \tag{10}$$

$$sf_{a5} = ia_5^4 + ja_5^3 + ka_5^2 + la_5^1 + ma_5^0 \tag{11}$$

where the regression coefficients are obtained as a=22.56, b=-0.035, c=0.999, d=-0.035, e=1.0, f=0.1, g=26, h=0.582, i=-4.80, j=11.27, k=-8.85, l=2.33, and m=.885, respectively. Finally, using Equations (8), (9), (10) and (11), respectively, the final response Acc can be obtained as

$$Acc = [Acco][sf_{\Delta x}][sf_{tv}][sf_{a5}] \tag{12}$$

Therefore, using Equation (12), for any known values of a_5, Δx, and t_v, in other words, for a known combination of any values of a_5, Δx, and t_v, one can easily obtain the response without going for the FEM analysis where one needs to have input values for Δx, a_5, and t_v, which is a rather laborious task. As for the demonstration purpose, the peak accelerations are obtained using Equation (12) and summarized in Fig. 16 for an a_5 equal to 0.4, 0.5, 0.6 and 0.7, respectively.

It should be noted that the % of coverage of the VE layer was found effective between 20 to 80%, i.e. a_5 equal to 0.2 to 0.8. Therefore, to consider scale factor w.r.t. a_5, the value for a_5 should be taken somewhere between 0.2 and 0.8 (Fig. 11(b)). Care should be taken that the simple expression as given in Equation (12) is expected to be applicable only for a similar kind of bridge structure, particularly, having a bridge column with circular cross-section. At this point, it is not understood whether this simple expression may be applicable for other types of bridge structures or not, for instance, bridge structures with square columns. However, it is expected that simple expressions for other types of bridge structures may be derived following the same procedures as described in this section.

Conceptual Design for Seismic Retrofit of Highway Bridges

The proposed DES methodology is intended to allow engineers to design for multiple performance objectives simultaneously so that the designed structure has similar margins of performance under different earthquake hazards. The DES methodology has two components, viz. damping component and strengthening component. The damping component ensures the operational level of the bridge structure under a small earthquake and the strengthening component ensures the safety level of the bridge structure under a large earthquake. The results presented in this study are related to the effect of VE damping on a simplified bridge structure model, while the strengthening component is discussed in detail in a companion paper (Karim and Chen 2009).

Conclusions

The end goal of the proposed DES methodology is to enable engineers to retrofit a bridge structure for its normalized performances against multiple objectives under different levels of earthquake hazards. This paper presents one significant step towards that goal, developing a finite element modeling technique for the implementation of this methodology in practical application. Specifically, discrete springs were introduced to model the effects of distributed VE damping layers on the response of columns and the structural system at large. The discrete spring model was validated against the analytical solution derived from the previous study and found quite satisfactory.

The validated model was then applied to investigate the effect of VE layers on the out-of-plane and in-plane motion of the three-column bent from a three-span steel-girder bridge. It was observed that the 40% coverage of a circular column by one 2.38 mm VE

layer can reduce the peak acceleration at the bridge deck by 14% when the column is subjected to a single curvature action. In the case of double curvature action, with 40% VE coverage applied on the lower portion of the column will reduce responses by 11%. In comparison with the retrofit scheme at both ends of the columns, it was observed that retrofitting of one end of the column with the same 40% VE coverage is more efficient compared to retrofitting at both ends. It was also observed that the VE layer is more effective for a range of 20-80% coverage; however, a range of 40-70% coverage is recommended for practical application. Finally, some simple expressions are derived in estimating the elastic responses of the bridge columns with VE layers.

Acknowledgement

References

Aiken, I. D., Nims, D. K., Whittaker, A. S., and Kelly, J. M. (1993). "Testing of passive energy dissipation systems." *Earthquake Spectra*, 9(3), 335-370.

Aprile, A., Inaudi, J. A., and Kelly, J. M. (1997). "Evolutionary model of viscoelastic dampers for structural applications." *Journal of Engineering Mechanics*, ASCE, 123(6), 551-560.

ATC/MCEER Joint Venture (2008). *Recommended LRFD Guidelines for the Seismic Design of Highway Bridges*, Applied Technology Council, Redwood City, CA.

Bergman, D. M., and Hanson, R. D. (1993). "Viscoelastic mechanical damping devices tested at real earthquake displacements." *Earthquake Spectra*, 9(3), 389-418.

Chang, K. C., Soong, T. T., Oh, S. T., and Lai, M. L. (1992). "Effect of ambient temperature on viscoelastically damped structures." *ASCE Journal Structural Engineering*, 118(7), 1955-1973.

Chang, K. C., Soong, T. T., Oh, S. T., and Lai, M. L. (1995). "Seismic behavior of steel frame with added viscoelastic dampers." *ASCE Journal of Structural Engineering*, 121(10), 1418-1426.

Chang, K. C., Chen, S. J., and Lai, M. L. (1996). "Inelastic behavior of steel frames with added viscoelastic dampers." *ASCE Journal of Structural Engineering*, 122(10), 1178-1186.

Chen, G., Thebeau, P., and Mu, H., (2002). "Seismic vulnerability of highway bridges along a designated emergency vehicle access routes near the New Madrid seismic zone." *7th National Conference on Earthquake Engineering* (CD-ROM), Boston, MA.

Chen, G., Wang, W. and Huang, X. (2006). "Optimal design of RC column seismic retrofitting for multiple performance objectives with an integrated damping and strengthening methodology." *8th National Conference on Earthquake Engineering* (CD-ROM), San Francisco, CA.

Chen, G. and Karim, K. R. (2006). "Damping-enhanced seismic strengthening of RC columns for multiple performance objectives." *5th National Seismic Conference of Bridges and Highways*, San Francisco, CA, Paper No B24.

Chopra, A. K. (2001). *Dynamics of structures*, Prentice Hall, New York, NY.

Fajfar, P. (1999). "Capacity spectrum method based on inelastic demand spectra." *Earthquake Engineering and Structural Dynamics*, 28, 979-993.

FEMA-273. (1997), "NEHRP guidelines for the seismic rehabilitation of buildings." *Building Seismic Safety Council*, Washington, DC.

FHWA (2005). "Seismic retrofitting manual for highway bridges." *Federal Highway Administration*, Publication No. FHWA-RD-94-052.

Foutch, D. A., Wood, S.L., and Beady, P. A. (1993). "Seismic retrofit for nonductile reinforced concrete frames using viscoelastic dampers." *Proceedings of Applied Technology Council ATC-17-1 Seminar on Seismic Isolation, Passive Energy Dissipation and Active Control*, 2, 605-616.

Gehling, R. N. (1987). "Large space structure damping treatment performance: analytic and test results." *Role of Damping in Vibration and Noise Control*, ASME, New York, NY, 93-100.

Hammami, L., Zghal, B., Fakhfakh, T., and Haddar, M. (2005). "Characterization of modal damping of sandwich plates." *Journal of Vibration and Accoustics*, 127, 431-440.

Hanson, R. D., and Soong, T. T. (2001). "Seismic design with supplemental energy dissipation devices." *EERI Monograph*, Oakland, CA.

Huang, X. (2005). "An integrated VE damping and FRP strengthening system for performance-based seismic retrofit of RC columns." Ph.D. dissertation, University of Missouri-Rolla, Rolla, MO.

International Code Council (2006). *International Building Code*, International Code Council, Inc., Whittier, CA.

Karim, K. R., and Chen, G. (2009). "Surface damping effect on the bending vibration of simply supported beams under different configuration of constrained VE layers." *ASCE Journal of Structural Engineering* (to be submitted).

Karim, K. R., and Chen, G. (2009). "Damping-enhanced seismic strengthening of highway bridge columns for dual performance objectives." *ASCE Journal of Structural Engineering* (to be submitted).

Kasai, K., Munshi, J. A., Lai, M. L., and Maison, B. F. (1993). "Viscoelastic damper's hysteretic modal theory, experiment, and application." *Proceedings of Applied Technology Council ATC-17-1 Seminar on Seismic Isolation, Passive Energy Dissipation and Active Control*, 2, 521-532.

Kerwin, E. M. Jr. (1959). "Damping of flexural waves by a constrained viscoelastic layer." *J. Accoust. Soc. Am.*, 31(7), 952-962.

Lin, W. H., and Chopra, A. K. (2003). "Earthquake response of elastic single-degree-of-freedom systems with nonlinear viscoelastic dampers." *ASCE Journal of Engineering Mechanics*, 129(6), 597-606.

Lu, B. (2007). "Application of displacement-based design method to blast-resistant reinforced concrete structures." Ph.D. dissertation, University of Missouri-Rolla, Rolla, MO.

Mander, J. B., Priestley, M. J. N., and Park, R. (1988). "Theoretical stress-strain model for confined concrete." *ASCE Journal of Structural Engineering*, 114(8), 1804-1826.

MCEER (2005). "Seismic retrofitting manual for highway structures: part 1 – bridges." Working Draft, Prepared by the Multidisciplinary Center for Earthquake Engineering Research (MCEER) for Federal Highway Administration.

Morgenthaler, D. R. (1987). "Design and analysis of passive damped large space structures." *Role of Damping in Vibration and Noise Control*, ASME, New York, NY, 1-8.

Priestley, M. J. N., Seible, F., and Calvi, G. M. (1996). *Sesimic design and retrofit of bridges*, John Wiley & Sons, New York, NY.

Ross, D., Ungar, E. E., and Kerwin, E. W. (1959). "Damping of plate flexural vibrations by means of viscoelastic laminar." *Structural Damping* (ed, Ruzicka, E.J.), ASME.

SAP2000. "Integrated software for structural analysis & design." *Computers & Structures, Inc.*, Berkeley, CA.

Shen, K. L., and Soong, T. T. (1995). "Modeling of viscoelastic dampers for structural applications." *ASCE Journal of Engineering Mechanics*, 121(6), 694-701.

Silva, P. F., Erecson, N. J., and Chen, G. (2007). "Seismic retrofit of bridge joints in central U.S. with carbon fiber-reinforced polymer composites." *ACI Structural Journal*, 104(2), 207-217.

Soong, T. T., and Dargush, G. F. (1997). *Passive energy dissipation system in structural engineering*, John Wiley & Sons, New York, NY.

Soong, T. T., and Spencer, B. F. (2002). "Supplemental energy dissipation: state-of-the-art and state-of-the-practice." *Engineering Structures*, 24, 243-259.

Viti, S., Reinhorn, A. M., and Whittaker, A. S. (2002). "Retrofit of structures: strength reduction with damping enhancement." *KEERC-MCEER Joint Seminar on Retrofit Strategies for Critical Facilites*, Buffalo, NY.

Zhang, R. H., Soong, T. T., and Mahmoodi, P. (1989). "Seismic response of steel frame structures with added viscoelastic dampers." *Earthquake Engineering and Structural Dynamics*, 18, 389-396.

Zhang, R. H., and Soong, T. T. (1992). "Seismic design of viscoelastic dampers for structural applications." *ASCE Journal of Structural Engineering*, 118(5), 1375-1392.

Fig. 1. Composition of a DES system.
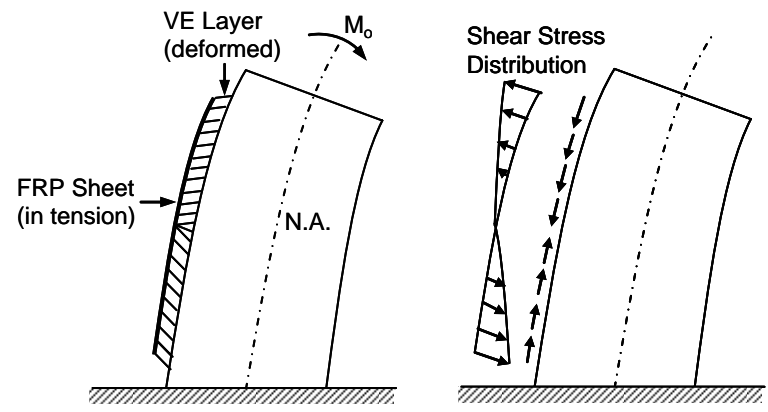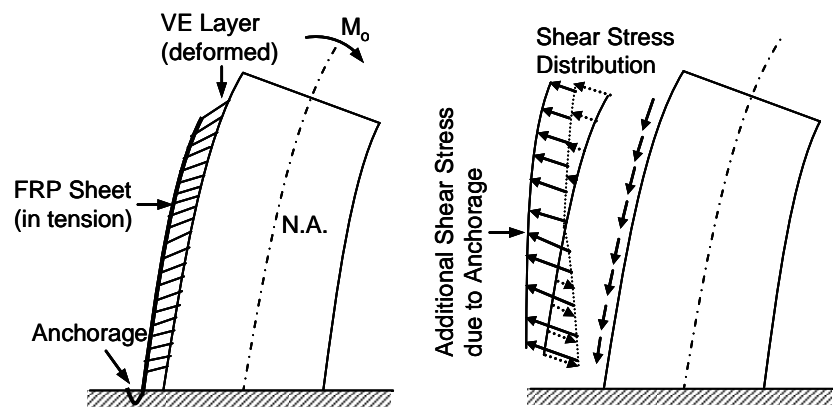
(a) Conventional constrained layer.

(b) Anchored constrained layer.

Fig. 2. Comparison of shear stress distributions in the conventional and the proposed layer treatments.

0

(a) Linear distribution of strain.   (b) Circular cross section.
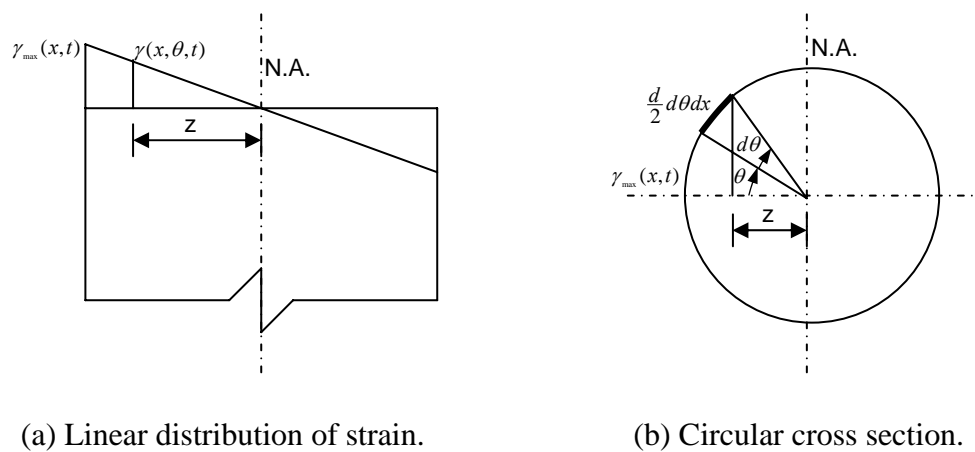
Fig. 3. Strain change over cross section.
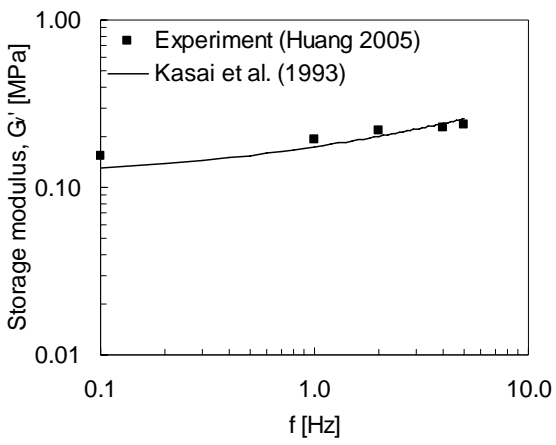
(a) Storage modulus.
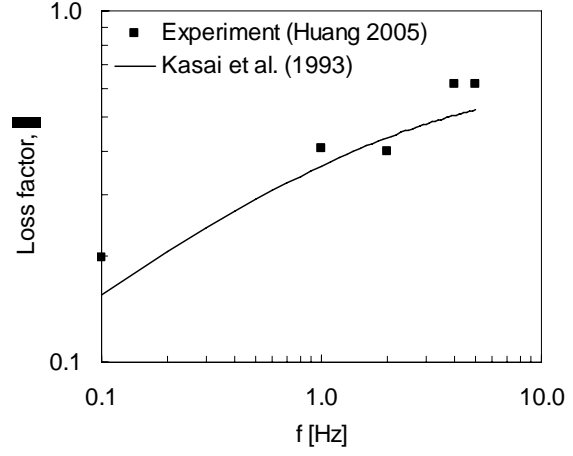
(b) Loss factor.

Fig. 4. Engineering parameters of VE material obtained from experiments.
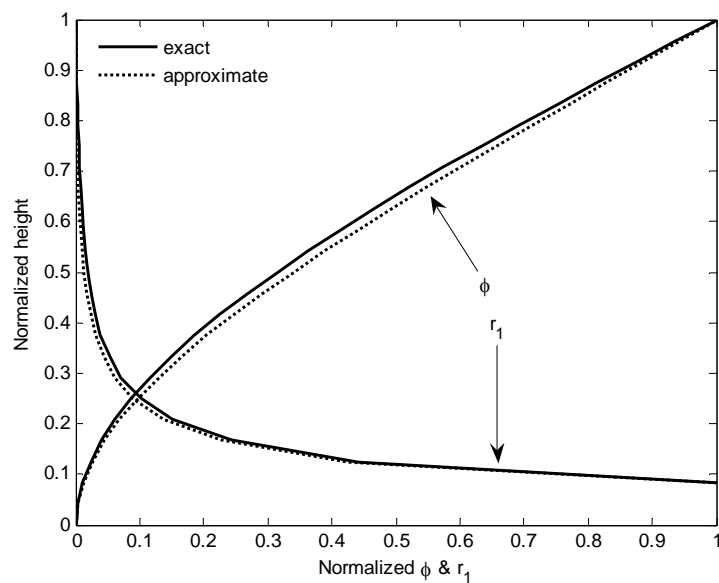
Fig. 5. Normalized shape functions (ϕ) and corresponding curvature to displacement ratios (r_1).
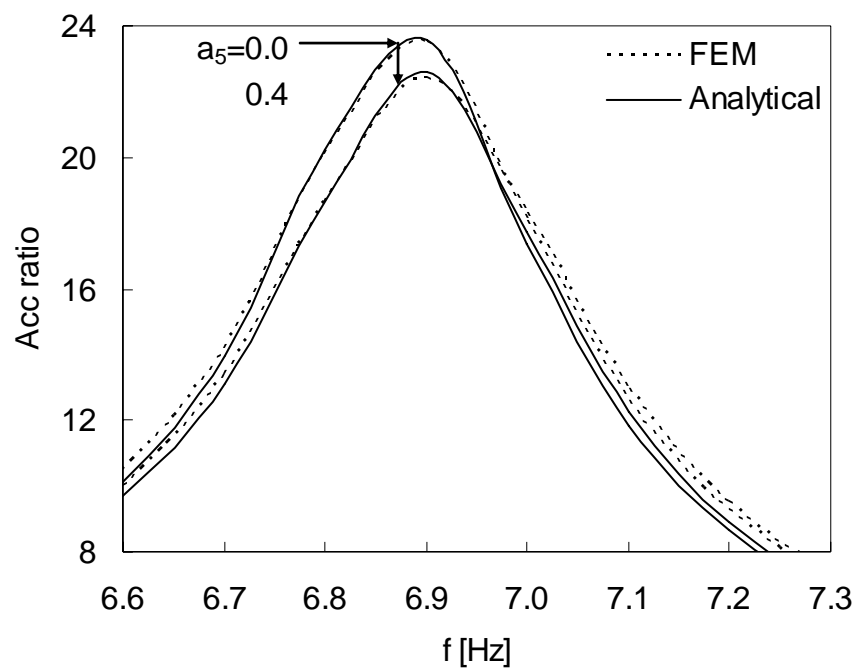
Fig. 6. Comparison of steady-state acceleration obtained from analytical model and FEM.
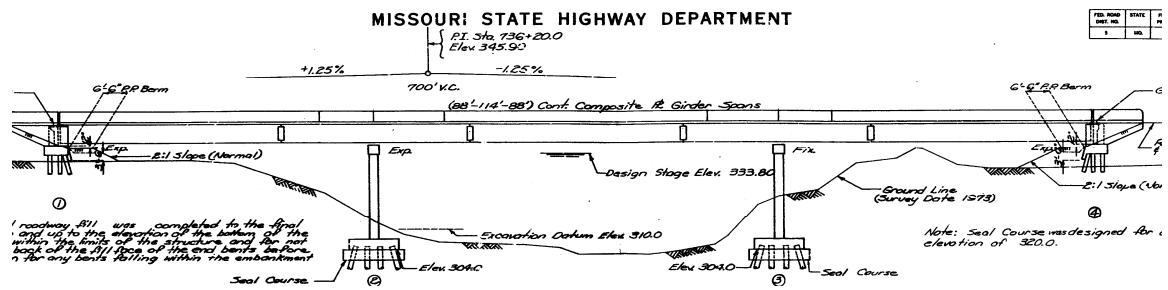
Fig. 7. Bridge elevation.
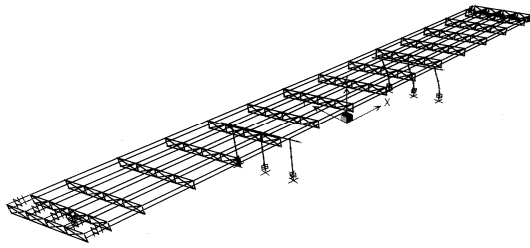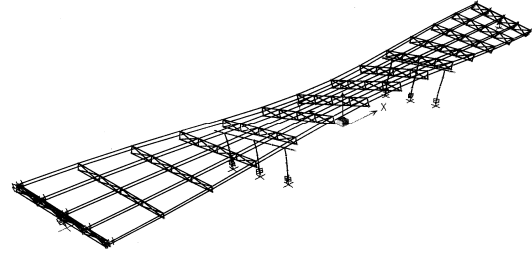
(a) mode 1, T=1.3173 s.   (b) mode 2, T=0.4773 s.

Fig. 8. Vibration period and mode shapes of the highway bridge.

(a) Bridge column.   (b) Double curvature action.
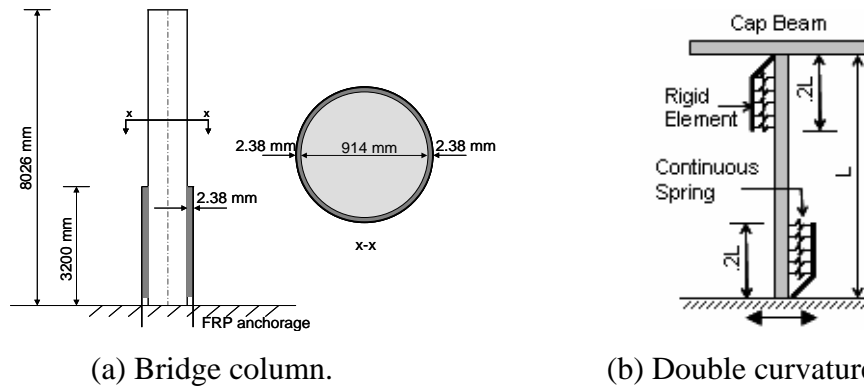
Fig. 9. Bridge column with VEM layer and modeling of VE layers for the case of double curvature action. The cross section of the column is also shown in the figure.
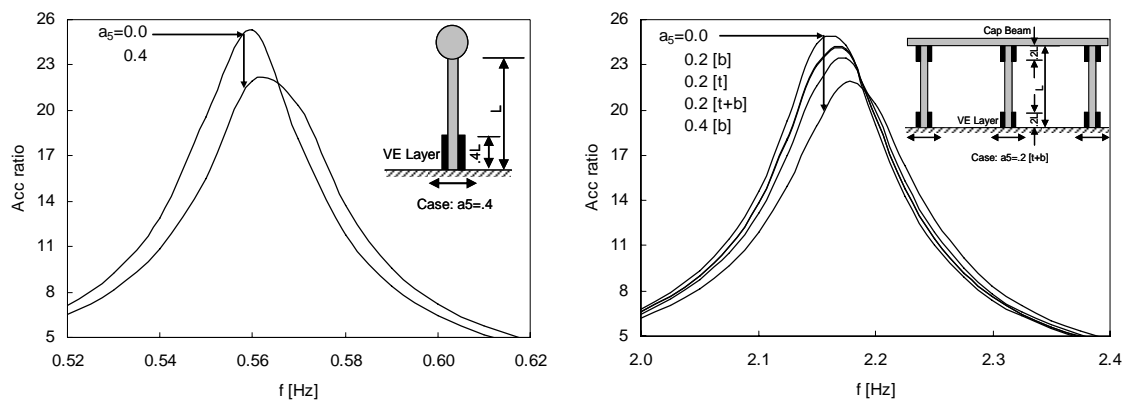
(a) Out-of-plane acceleration.   (b) In-plane acceleration.

Fig. 10. Steady-state acceleration for the both out-of-plane and in-plane motion for various configurations of VE layers.
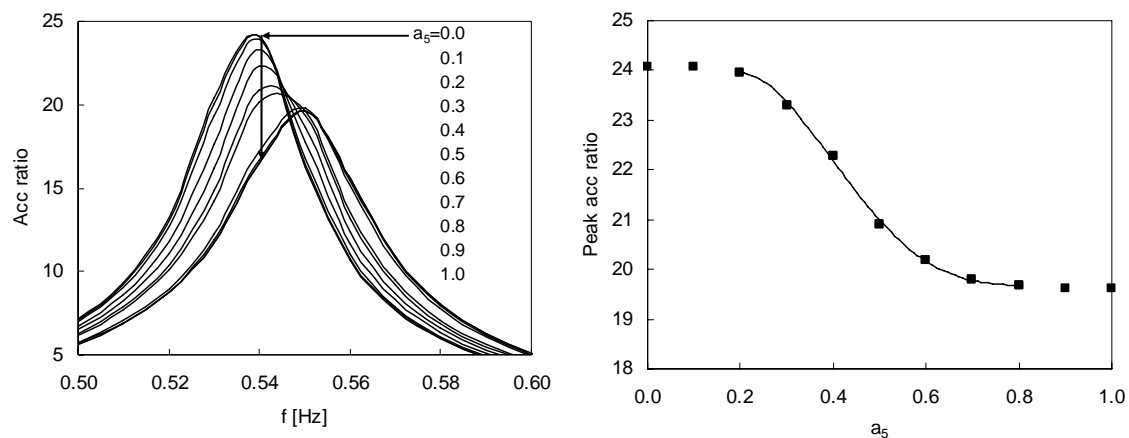
(a) Acceleration ratio. (b) Peak values.

Fig. 11. Acceleration ratio for different level of VE coverage a_5 (normalized w.r.t. column height) and corresponding peak values. The results are shown for a t_v=0.0026 (normalized w.r.t. column diameter).
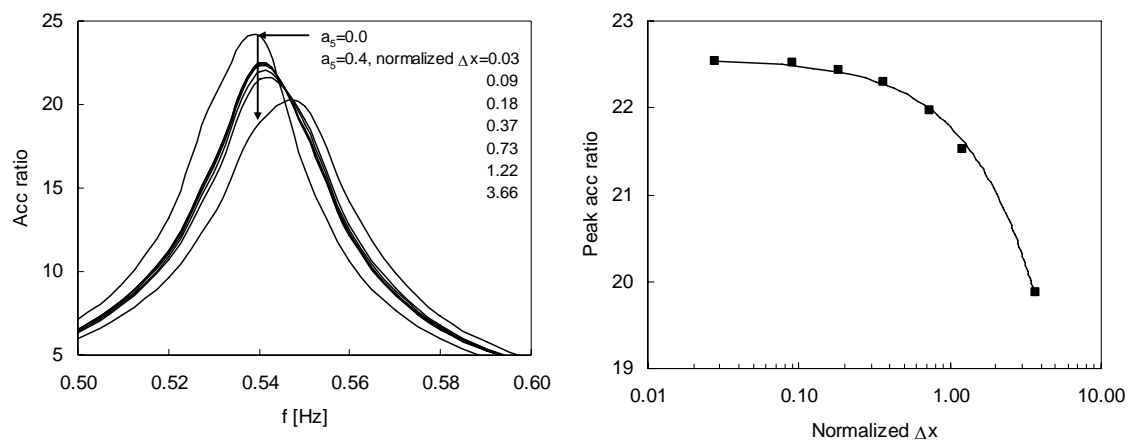
(a) Acceleration ratio.   (b) Peak values.

Fig. 12. Acceleration ratio for different Δx (normalized w.r.t. column diameter) and corresponding peak values for $a_5 = 0.4$ (normalized w.r.t. column height). The results are shown for a $t_v = 0.0026$ (normalized w.r.t. column diameter).
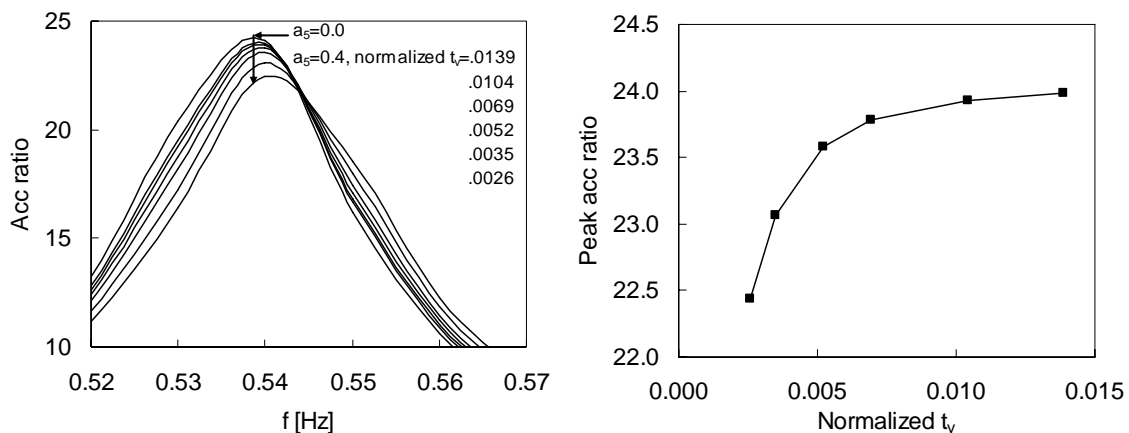
(a) Acceleration ratio.

(b) Peak values.

Fig. 13. Acceleration ratio for different t_v (normalized w.r.t. column diameter) and corresponding peak values for a_5 =0.4 (normalized w.r.t. column height). The results are shown for a Δx =0.18 (normalized w.r.t. column diameter).

(a) w.r.t. Δx.   (b) w.r.t. t_v.
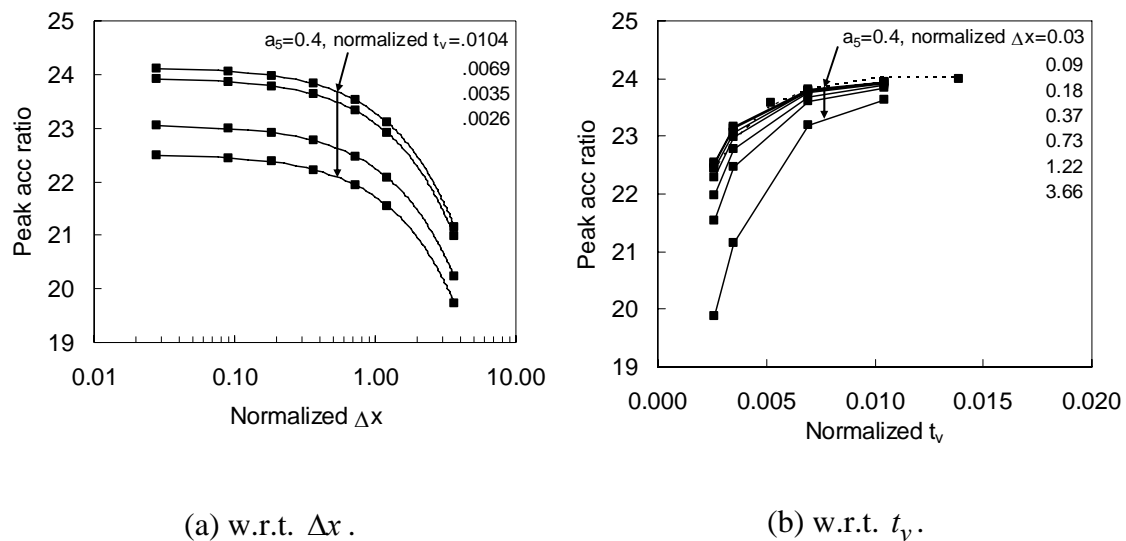
Fig. 14. Peak accelerations w.r.t. both Δx (normalized w.r.t. column diameter) and t_v (normalized w.r.t. column diameter) for $a_5 = 0.4$ (normalized w.r.t. column height).
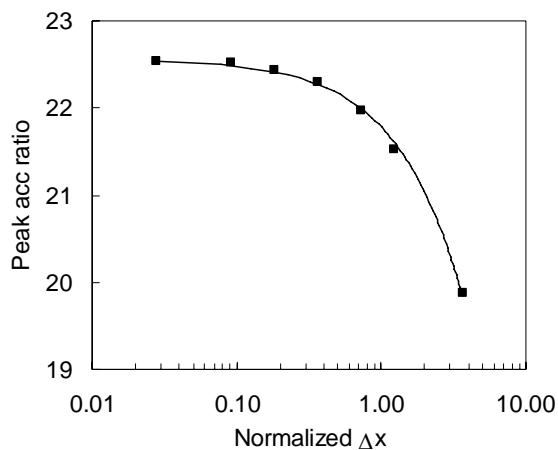
(a) Peak values w.r.t. Δx.
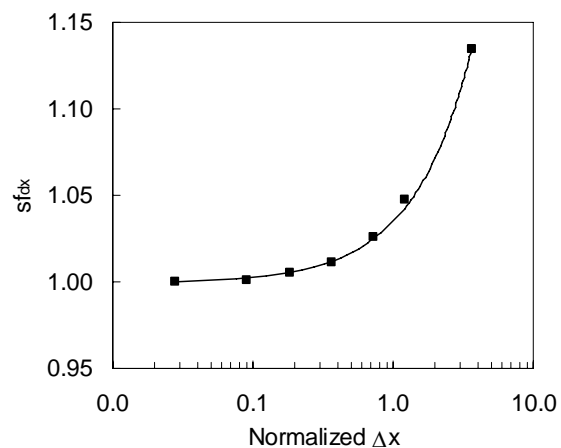
(b) Scale factor w.r.t. Δx.
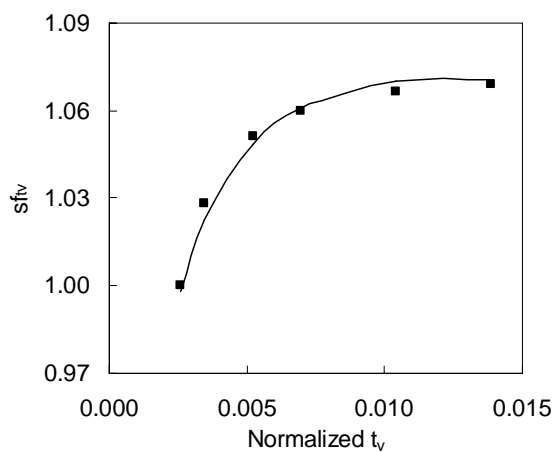
(c) Scale factor w.r.t. t_v.
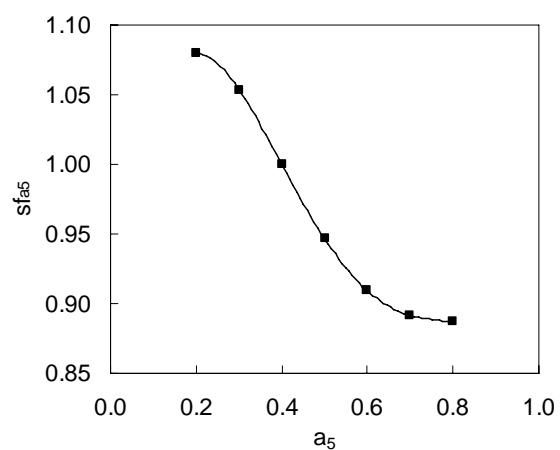
(d) Scale factor w.r.t. a_5.

Fig. 15. Peak values w.r.t. Δx (normalized w.r.t. column diameter) and corresponding scale factor. The results are shown for a t_v=0.0026 (normalized w.r.t. column diameter) and a_5=0.4 (normalized w.r.t. column height). The scale factors w.r.t. both t_v and a_5 are also shown in the figure.

(a) $a_5 = 0.4$.

(b) $a_5 = 0.5$.

(c) $a_5 = 0.6$.

(d) $a_5 = 0.7$.
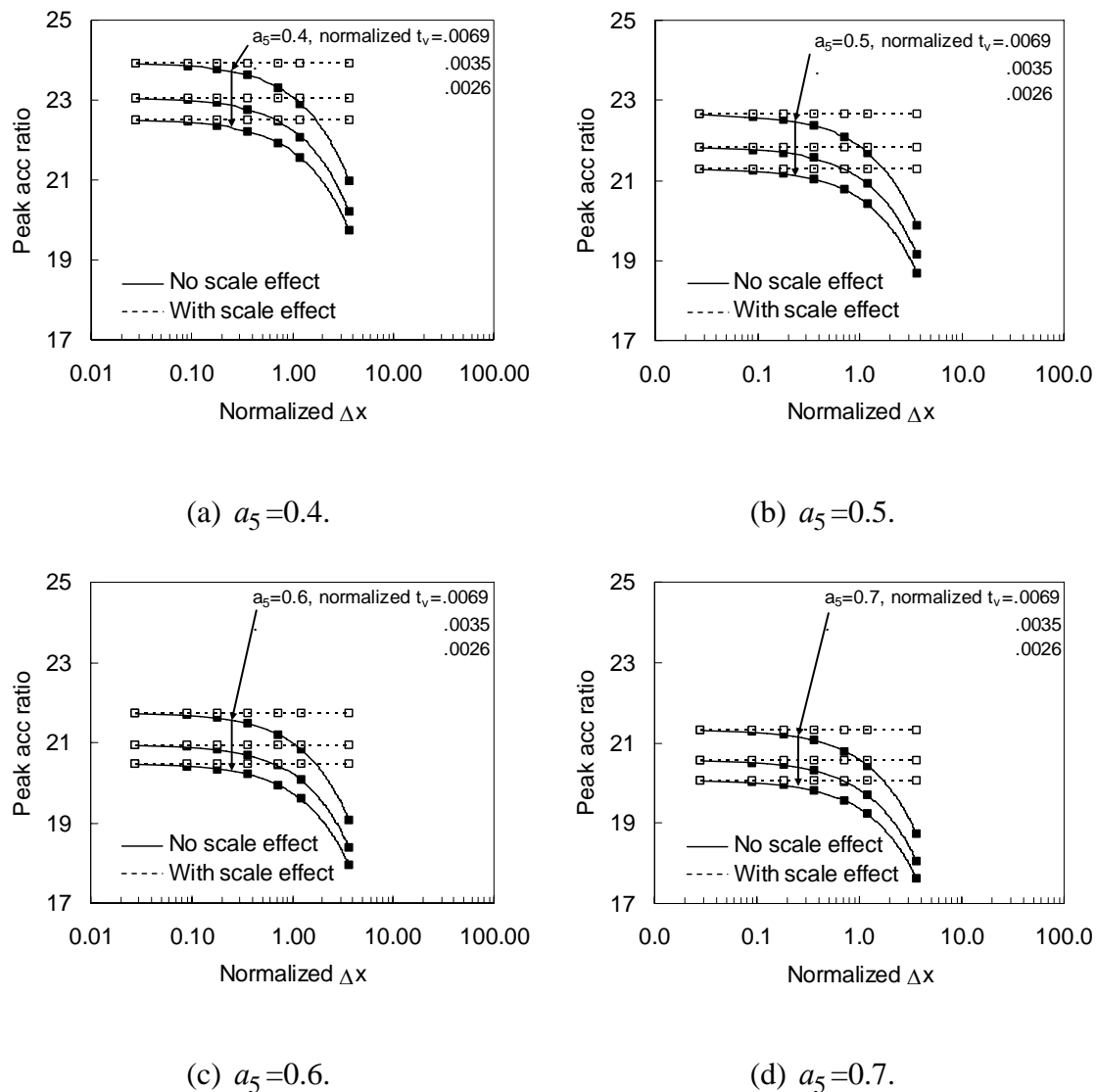
Fig. 16. Application of scale factors in obtaining peak values for different combination of Δx (normalized w.r.t. column diameter), t_v (normalized w.r.t. column diameter), and a_5 (normalized w.r.t. column height).

3. Damping-Enhanced Seismic Strengthening of Highway Bridge Columns for Dual Performance Objectives

Kazi R. Karim[1] and Genda Chen[2][*], F. ASCE

Abstract: In this study, a damping-enhanced seismic strengthening (DES) methodology with an integrated viscoelastic (VE) layer used for distributed damping in FRP jacketing for RC bridge columns is introduced. The proposed DES methodology was applied to the Old St. Francis River Bridge columns located in the new Madrid Seismic Zone. The column responses under harmonic loading were investigated based on a finite element model and presented in a companion paper. This paper primarily investigates the dual performance of the bridge columns for both out-of-plane and in-plane motions considering both damping and strengthening components of the DES strategy. It was observed that the damping component ensures the operational level under a small earthquake while the strengthening component ensures the safety level under a large earthquake. Therefore, both damping and strengthening satisfy dual performance objectives under both small and large earthquakes. It was also observed that for the bridge column under consideration, a 3ply of CFRP with full coverage of the VE layer is required to satisfy dual performance for out-of-plane motion, while either a 2ply of CFRP

[1] Structural Engineer, Kirkpatrick Forest Curtis PC, 205 NW 63rd St Suite 390, Oklahoma City, OK 73116, E-mail: krk2q4@mst.edu

[2] Professor of Civil Engineering and Interim Director of the Center for Infrastructure Engineering Studies, Missouri University of Science and Technology, 224 Engineering Research Laboratory, 500 W. 16th Street, Rolla, MO 65409, E-mail: gchen@mst.edu

[*] Corresponding author

with 40% coverage of the VE layer or a 1ply of CFRP with 80% coverage of the VE layer is required to satisfy dual performance for in-plane motion.

CE Database subject headings: VE layer; FRP jacketing, Bridge column; Elastic response; Surface damping; Seismic strengthening; Pushover Analysis; Normalized performance.

Introduction

The design concept of multiple performance objectives was introduced in FEMA (1997) and recommended load and resistance factor design (LRFD) guidelines for the seismic design of highway bridges (ATC/MCEER 2008). The current practice, however, is to design a structure for one performance level and check its adequacy for other levels if necessary. This practice could lead to an uneconomical design with inconsistent margins of compliance to different performance objectives. How to directly design for multiple performance objectives has never been discussed for both new design and retrofit projects.

Over 50% of the bridges in the NBI database representing the 1970's construction methods which incorporate no seismic design considerations are structurally deficient (Chen et al. 2002). To respond to ever-increasing retrofitting needs, several strengthening techniques, such as fiber-reinforced-polymer (FRP) jacketing, have been developed over the past two decades (FHWA 2005; MCEER 2005). These techniques can be used to provide an existing reinforced concrete (RC) column with effective confinement so that the column will not collapse during a strong earthquake event. Strengthening alone, however, is unlikely to improve the column performance under moderate earthquake

events. This is because significant strains must be developed in the column before a jacketing technique is effectively engaged as part of the strengthened column system. It is, therefore, desirable to develop a new retrofitting technology that can meet multiple performance objectives in the context of performance-based design of structures (FEMA 1997; MCEER 2005).

In this study, an integrated damping and strengthening methodology, called damping-enhanced seismic strengthening (DES), is introduced for bridge columns (Huang 2005; Chen et al. 2006). The proposed DES methodology is intended to allow engineers to design for multiple performance objectives simultaneously so that the designed structure has similar margins of performance under different earthquake hazards. The DES methodology has two components, viz. damping and strengthening components. The damping component ensures the operational level of a bridge structure under a small earthquake and the strengthening component ensures the safety level of a bridge structure under a large earthquake. Karim and Chen (2009) investigated the distributed VE layer damping effect on the elastic response of bridge columns and presented their findings in a companion paper.

The focus of this paper is to investigate the dual performance objectives of the Old St. Francis River Bridge columns under the considerations relevant to the DES methodology. With this objective, the columns were wrapped by different numbers of carbon-fiber-reinforced-polymer (CFRP) ply with different percentages of VE layer coverage. Both the out-of-plane and in-plane motions were considered in investigating the dual performance of bridge columns in both longitudinal and transverse directions. The damping component was taken from the study presented in the companion paper

(Karim and Chen 2009), while the strengthening component is investigated in this study based on nonlinear pushover analysis. Finally, the normalized performance for different combinations of number of CFRP ply and percentage of VE layer coverage is presented in tabular form. The intent is to select a suitable combination of materials that satisfy dual performance needs of the bridge column in both longitudinal and transverse direction.

The Concept of a DES Methodology

In earthquake engineering, performance-based design for multiple performance objectives has recently been introduced in retrofitting provisions (FEMA 1997; ATC/MCEER 2008). How to directly design for multiple performance objectives, however, has not been discussed in regard to both new design and retrofit specifications. Although FRP jacketing (FHWA 2005) can effectively confine an existing reinforced concrete (RC) column to prevent collapsing during a strong earthquake event, strengthening alone is unlikely to improve the column performance under moderate earthquake events. A new retrofitting technology to meet the multi-objective requirements in the performance-based design of structures is desirable.

Damping-Enhanced Strengthening (DES) System

Chen et al. (2006) introduced a constrained VE layer wrapped by FRP jacketing to a cantilever RC column, known as the DES system. The system consists of one or more FRP sheets (inner) wrapped around the circular (or rectangular) RC column, a VE layer attached on the FRP sheets, and another FRP sheet (outer) outside the VE layer that is anchored into the connecting member (beam or footing) of the column at one end. The

entire system is shown schematically in Fig. 1. The fibers of the inner FRP sheets are oriented along the perimeter of the column for a confinement effect while those of the outer FRP sheet are oriented vertically along the length of the column. The VE layer is bonded to the inner and outer FRP sheets with epoxy. Both the inner FRP sheets and the VE layer stop approximately one inch away from the beam/footing.

Shear Mechanism of Anchored Constrained VE Layer in a DES System

When the column is bent to the right, the VE layer on the left side of the column undergoes significant shear deformation between the inner and the outer FRP sheets and dissipates energy while the deformation and energy dissipation of the remaining VE layer on the right side are small. The shear deformation may become more pronounced when the column starts separating from its connecting member (beam or footing) at the construction joint due to slippage of dowel bars as a result of debonding of the lap splices or formation of a plastic hinge. The main design parameters of such an integrated system include the number and height of the inner FRP sheets, thickness and height of the VE layers, the ratio of Young's modulus between VE material and concrete, bond strength, embedment length of the outer FRP sheet for anchorage, and the location of anchorage.

Effect of Distributed Damping in a DES System

The proposed DES system has an integrated VE layer for distributed damping into the FRP jacketing of a cantilevered RC column. In performance-based seismic design, the intent of providing an enhanced distributed damping component is to reduce the seismic responses of the column for an improved functionality performance level under a small

earthquake event. In this case, the inelastic deformation of the column is very limited and the retrofitted system basically remains elastic, which is the main reason to investigate the damping effect on elastic responses in this study. On the other hand, the strengthening component is there to ensure that the column remains intact for a safety performance level under a strong earthquake event. It is worth noting that there is virtually no extra installation cost for adding VE layers.

Shear Strain Amplification Mechanism in the New Treatment

To understand why the new constrained layer treatment is more effective than the conventional way, consider the partially covered column in Fig. 1 subjected to a bending moment at the cantilever end. Fig. 2 presents the comparison of the shear stress distribution between the conventional and the new treatments. Under the end moment, the column experiences a constant moment or curvature along its height. When the constraining layer is not anchored, as shown in Fig. 2(a), the induced shear stress must be zero and changes its direction at the middle height of the VE layer in order to satisfy the zero vertical force equilibrium condition at the section below the VE layer. At any other point, the shear stress is proportional to the distance from the middle height point.

On the other hand, when the constraining layer is anchored into the column footing as illustrated in Fig. 2(b), the shear stress induced linearly increases with the distance from the footing in the same direction. As a result, the maximum stress in the new treatment, shown with solid plus dotted arrows in Fig. 2(b), is more than twice that of the conventional way, as shown in Fig. 2(a). By superimposing the stress distribution in Fig. 2(a) with that in Fig. 2(b), the net stress difference gained with the anchored

constraining layer is indicated by the solid arrows in Fig. 2(b), resulting in a three times more shear force counteracting the effect of the end moment.

Conceptual Design of the Seismic Retrofit of a Highway Bridge

The proposed DES methodology is intended to allow engineers to design for multiple performance objectives simultaneously so that the designed structure has similar margins of performance under different earthquake hazards. Following is a presentation of the step-by-step procedure for the implementation of the proposed methodology after a detailed assessment of the structural condition of the existing bridge. It is assumed that the safety performance or collapse prevention (CP) level and the operational performance (OP) level corresponding to the earthquake hazards at 2% and 10% probability of exceedance in 50 years, respectively, are considered for the retrofit of the bridge structures.

Structural Condition Evaluation of the Bridge

The capacity over demand ratio method was used to evaluate the structural condition of the Old St. Francis River Bridge (FHWA 2005). According to a detailed analysis (Chen et al. 2002), the bridge structure has the following deficiencies:

- Bearing failure in shear and insufficient anchorage
- Poor detailing at top and bottom of columns
- Moderate buckling of diaphragm/cross frame
- Column shear failure

- At the operational performance level

- At the safety performance level

Seismic Retrofit Design Procedure

Seismic retrofit of highway bridges using the proposed methodology can be performed with the following design procedure:

- Establish multiple performance objectives, e.g., operational and safety performance levels of the bridge example in this study

- Strengthen the inadequate columns for shear strength and confinement at their ends with FRP sheets to meet the safety performance level requirements

- Design VE layers to significantly reduce the earthquake-induced forces on bearings and diaphragm/cross frames so that they meet the operational performance level

- Evaluate the performance of the bridge structure retrofitted both with the damping layers and strengthening components. In this case, the VE layers will also reduce, to a certain degree, the earthquake forces on various structural components at the safety performance level.

Application of DES Methodology to Old St. Francis River Bridge Columns

With the above objectives, the Old St. Francis River Bridge Columns were considered to investigate dual performance objectives in the context of DES methodology. Designed in 1977 without seismic considerations, this 7.92m high bridge consisted of three spans supported by steel plate girders (Chen et al. 2002). The interior diaphragms and the cross-

frames each consisted of two diagonals L3×2½×5/16 crossed over each other, top and bottom horizontal members L4×4×5/16. All interior diaphragms and cross-frames were placed parallel to the abutments of the bridge. The bridge, however, was skewed at a 20° angle, so the ends of the girders were offset from one another at the ends of the bridge. Therefore, these diaphragms and cross-frames were not perpendicular to the girders because of the angle of the structure.

The bridge superstructure is supported by two intermediate bents through one fixed bearing and one expansion bearing, along with two seat-type abutments at its ends. Each bent consisted of a RC cap beam and three RC columns. Both bents and abutments are supported by deep friction pile foundations. There are 12 piles, each approximately 48.26 cm in length, for each column footing and 16 piles, each about 114.3 cm in length, for each abutment footing. Two expansion joints were constructed at the ends of the bridge. This bridge used 27.58 MPa concrete for the superstructure and 20.68 MPa concrete for the substructure. For the reinforcing steel, 275.80 MPa was used.

The bridge was modeled with the finite element method in SAP2000. All of the components of the structure were included in the bridge model. Springs and dashpots were used at the base of each column and each abutment to model the soil and foundation effects. The periods for the first two vibration modes of the bridge were found to be 1.3173s and 0.4773s, respectively (Chen et al. 2002). The elevation and vibration modes of the bridge are shown in Figs. 3 and 4, respectively.

Damping Effect on the Elastic Response of Bridge Columns

First, a possible damping effect on the column responses due to the distributed VE layer was investigated based on steady-state analysis and the details are presented in the companion paper (Karim and Chen 2009). The effect was investigated for both longitudinal and transverse directions considering both out-of-plane and in-plane motions. The investigation of a damping effect on column responses was one significant step towards the application of DES methodology to bridge columns. An emphasis was placed in developing a finite element modeling technique for the implementation of the DES methodology in practical application. Specifically, discrete springs were introduced to model the effects of distributed VE damping layers on the response of columns and the structural system at large (Karim and Chen 2009). Finally, this damping component was taken into account when applying the DES methodology to investigate the dual performance of the bridge columns under seismic loading in this study.

Seismic Strengthening of Bridge Columns by CFRP Jacketing

For seismic strengthening of bridge columns, different numbers of CFRP ply were applied to the bridge columns. Fig. 5(a) shows the stress-strain relationship of the concrete without retrofitting that was originally used in designing the column and with CFRP along with VE layers wrapped around the column. The confined stress-strain was obtained from the simple relationship originally proposed by Mander et al. (1988) and other parameters necessary in obtaining stress-strain relationship were adopted from Priestley et al. (1996). The CFRP parameters were taken from the study of Silva et al. (2007). The moment-curvature relationships were obtained using RESPONSE-2000 and

are shown in Fig. 5(b). The force-displacement relationships were obtained based on nonlinear pushover analysis (Bentz 2000).

Dual Performance of Bridge Columns in the Longitudinal Direction

In performance-based seismic design, a minimum design standard should be that the columns meet the OP level for small earthquakes and the CP level for large earthquakes. Other performance levels can be considered, however, in this study only the OP and CP performance levels are considered since they are the minimum design standards. Hereafter it is called dual performance.

There are two components in performance evaluation, viz. capacity and demand. In this study, the performance was evaluated based on the capacity and demand spectra. When both capacity and demand spectra meet each other, a performance point is obtained, and with the same token, when they do not meet each other, no performance point is obtained.

The capacity spectra were obtained from the force-displacement relationships of the bridge column. This was done by dividing the base shear with the appropriate mass applied at the top of the column. In obtaining the demand spectra, the IBC (2006) response spectra were considered in this study, and three levels of ground motion were considered, viz. small, design, and large earthquake.

While the spectrum for the design earthquake was obtained for the Old St. Francis River Bridge site following the same procedures given in the IBC (2006), both the small and the large earthquake spectra were obtained by applying some scale factors to design spectra to match the PGA level that were obtained from the site specific synthetic ground

motion of 10% and 2% probability of exceedance in 50 years, and they represent small and large earthquakes, respectively (Chen at el. 2002).

The inelastic demand spectra were obtained based on the procedures given in the study of Fajfar (1999) and the damping effects due to the distributed VE layers were then incorporated (Viti et al. 2002; Lu 2007). Hereafter, the first is called demand spectra without damping effect and the later is called demand spectra with damping effect. Note that the VE layer damping component was taken from the study of Karim and Chen (2009) and provided in the companion paper.

To investigate dual performance of the bridge column in the longitudinal direction, two cases were considered and discussed below, viz. 1) column wrapped by CFRP along with VE layer for a 40% coverage, i.e. $a_5 = 0.4$, and 2) column wrapped by CFRP along with VE layer for a 100% coverage, i.e. $a_5 = 1.0$.

Column Wrapped by CFRP along with VE Layer for 40% Coverage

Fig. 6(a) shows the force-displacement relationships of the column for $a_5 = 0.4$ in the longitudinal direction and the corresponding capacity spectra in acceleration-displacement-response-spectra (ADRS) format are shown in Fig. 6(b). The response spectra used in this study are shown in Fig. 7(a) and the spectra in ADRS format are shown in Fig. 7(b). Hereafter, ADRS spectra are called spectra for simplicity.

Fig. 8(a) shows the capacity-demand spectra without FRP and without damping while Fig. 8(b) shows the capacity-demand spectra without FRP and with damping effect for $a_5 = 0.4$. Note that both OP and CP levels are also shown in the same figures and they are defined as dy and du, respectively, where dy is the displacement at yield point and du

is the displacement at ultimate point. In Fig. 8(a), it is clearly seen that the column without FRP wrapping does not satisfy the OP level performance for any level of earthquakes if the damping effect is not considered; the same column satisfies CP level performance only for a small earthquake. It is also clearly seen (Fig. 8(b)) that the column without FRP wrapping does not satisfy the OP level performance for any level of earthquakes even after considering the damping effect, although it may survive during the small earthquake.

Therefore, it can be concluded that with the original capacity of the column, even after considering the damping effect, it does not meet the OP level for any level of earthquakes and it meets the CP level only for a small earthquake. Therefore, it is necessary to go forward with retrofitting of this column, which is done by applying VE layer around the column and wrapping with FRP sheets. It should be noted that the VE layer provides the damping effect and the FRP layer provides the strengthening effect.

In order to understand both the damping and strengthening effects, in this study, the column was retrofitted by applying 1ply, 2ply, 3ply, 4ply, 5ply and 6ply of CFRP along with VE layer around the column; the corresponding capacity-demand spectra for both with and without damping effects are shown in Figs. 9 to 14, respectively. Note that the explanation for the retrofitted column for all cases remains the same as discussed earlier for the case without FRP wrapping.

Now, following the same explanation and looking at Figs. 9 to 14, it can be seen that the retrofitted column with 5ply FRP (Fig. 13 (b)) satisfies the CP level for all level of earthquakes when damping effect is considered. However, the same retrofitted column still does not satisfy the OP level for any level of earthquake even though the damping

effect has been considered. Perhaps, the same column satisfies the CP level even without considering damping effect when it is wrapped by 6ply of CFRP (Fig. 14(a)).

Normalized Performance for 40% Coverage

Thus far, the performance was evaluated based on the actual displacements that were obtained for all cases. However, the capacity-demand spectra were also normalized w.r.t. OP. This was done in order to get the ductility of the bridge column, which is well known in the context of performance-based seismic design of structures. As an example, the normalized capacity-demand spectra are shown in Fig. 15 for the case of 40% coverage with 5ply FRP.

In the capacity-demand spectra, there are two components, viz. demand and capacity. After obtaining both demand and capacity displacements, they were normalized w.r.t. OP to get both demand and capacity ductility. Both the demand and capacity ductility for all cases considered were then summarized in a tabular form which is shown in Table 1. Note that the demand ductility was obtained based on performance point. Therefore, in Table 1, ductility demands are shown only for those cases that have performance points. Finally, the demand versus capacity ratios were obtained for all cases to see which case in the proposed DES methodology satisfy both OP and CP performance.

The idea of using demand versus capacity ratio is that it gives a better picture in understanding whether demand is more or less than the capacity. For instance, if the ratio falls below 1.0, it indicates that the demand is less than the capacity and if it falls above 1.0, it indicates that the demand is more than the capacity. The first one means that the

column capacity is insufficient to meet the demand while the later means that the column has sufficient capacity to meet the demand.

Looking at Table 1, it can be seen that none of the cases satisfy the OP level performance since the demand versus capacity ratios fall above 1.0. However, it can be seen that the CP level performance is satisfied for the case when only strengthening scheme is considered and a 6ply FRP is required in that case. With the same token, when the DES scheme is considered, the CP performance is satisfied for the case with 5ply FRP.

As explained earlier, the minimum design standard should be such that the column should meet the OP level for small earthquakes and it should meet the CP level for large earthquakes. Since the column only meets the CP level under large earthquakes (for 5ply of CFRP with DES scheme as shown in Fig. 13(b) or 6ply of CFRP with strengthening scheme as shown in Fig. 14(a)) but it still does not meet the OP level for any level of earthquakes. This means that 40% coverage is not sufficient to meet both OP and CP performance criteria, in other words, the dual performance is not satisfied for the case when the column is retrofitted by CFRP along with VE layer with 40% coverage in the longitudinal direction.

Column Wrapped by CFRP along with VE Layer for 100% Coverage

Fig. 16(a) shows the force-displacement relationships of the column for $a_5 = 1.0$ in the longitudinal direction and the corresponding capacity spectra are shown in Fig. 16(b). Fig. 17(a) shows the capacity-demand spectra without FRP and without damping while Fig. 17(b) shows the capacity-demand spectra without FRP and with damping effect for

$a_5 = 1.0$. It is clearly seen (Fig. 17(a)) that the column without FRP wrapping does not satisfy the OP level performance for any level of earthquake if damping effect is not considered and the same column satisfies CP level performance only for a small earthquake, but it does not satisfy CP level for the both design and large earthquakes. It is also clearly seen (Fig. 17(b)) that the column without FRP wrapping satisfies the OP level performance for a small earthquake when damping effect is considered, but it still does not satisfy CP level for the both design and large earthquakes even though the damping effect is considered.

Therefore, it can be concluded that with the original capacity of the column and with the consideration of damping effect, it meets the OP level for a small earthquake, but it does not meet the CP level for both design and large earthquakes even though the damping effect has been taken into account. Therefore, it is necessary to go forward with retrofitting of this column, which is done by applying VE layer around the column and wrapping with FRP sheets. The retrofitting was done by applying 1ply, 2ply, 3ply, 4ply, 5ply and 6ply of CFRP along with VE layer around the column, and the corresponding capacity-demand spectra for both without and with damping effects are shown in Figs. 18 to 23, respectively.

Looking at Figs. 18 to 23, it can be seen that the retrofitted column with 3ply of FRP and with consideration of damping effect (Fig. 20(b)), it satisfies OP level for a small earthquake and with the same token, it satisfies CP level for all level of earthquakes. Perhaps, the same column satisfies the CP level even without considering damping effect when it is wrapped by 5ply of CFRP (Fig. 22 (a)).

Normalized Performance for 100% Coverage

The capacity-demand spectra were normalized w.r.t. OP level for all cases following the same procedures as explained earlier and Fig. 24 shows the normalized capacity-demand spectra only for the case with 3ply of FRP. Both demand ductility and capacity ductility for all cases considered were summarized in a tabular form which is shown in Table 2. As explained earlier, in Table 2, ductility demands are shown only for those cases that have performance points. Finally, the demand versus capacity ratios were obtained for all cases to see which case in the proposed DES methodology satisfy both OP and CP performance.

Looking at Table 2, it can be seen that when the DES scheme is considered, both OP and CP level performance are satisfied for the cases when the column is retrofitted with 3 to 6ply of FRP, shown in the shaded area in the table. As explained earlier, the minimum design standard should be such that the column should meet the OP level for small earthquakes and it should meet the CP level for large earthquakes. Since the column meets the OP level under a small earthquake and the CP level under a large earthquake for 3 to 6ply of CFRP with DES scheme, as shown in the shaded area in Table 2, this implies that the dual performance is satisfied for the case when the column is wrapped by at least 3ply of CFRP along with VE layer with a 100% coverage in the longitudinal direction.

Comparison of Normalized Performance for 40% and 100% coverage

In order to compare the normalized performance for 40% and 100% coverage in the longitudinal direction, the relationship between normalized performance and number of

CFRP ply in the DES scheme were obtained for both cases, shown in Fig. 25. Note that the relationships for both cases are shown at CP level. It can be seen (Fig. 25) that at CP level the performance of the column is much better when it is retrofitted with 100% coverage than that of the 40% coverage. Perhaps, to meet the CP level, the column is required to be retrofitted with at least 5ply of CFRP when 40% coverage is considered. With the same token, the column is required to be retrofitted with at least 3ply of CFRP when 100% coverage is considered. At this point, and considering only CP level, either option can be considered in retrofitting the column. However, when dual performance is considered, i.e. when both OP and CP level are considered, then the column has to be retrofitted with 3ply of CFRP along with VE layer with full coverage.

Dual Performance of Bridge Columns in the Transverse Direction

To investigate the dual performance in the transverse direction, two cases are considered and discussed below, viz. 1) column wrapped by CFRP along with VE layer for a 40% coverage, i.e. $a_5 = 0.4$, and 2) column wrapped by CFRP along with VE layer for a 80% coverage, i.e. $a_5 = 0.8$.

Column Wrapped by CFRP along with VE Layer for 40% Coverage

Fig. 26(a) shows the force-displacement relationships of the column for $a_5 = 0.4$ in the transverse direction and the corresponding capacity spectra are shown in Fig. 26(b). Fig. 27(a) shows the capacity-demand spectra without FRP and without damping while Fig. 27(b) shows the capacity-demand spectra without FRP and with damping effect for $a_5 = 0.4$. It is clearly seen (Fig. 27(a)) that the column without FRP wrapping satisfies the

OP level performance for a small earthquake even without damping effect, however, the same column does not satisfy CP level when damping effect is not considered, although it satisfies the CP level for a design earthquake. It is also clearly seen (Fig. 27(b)) that the column without FRP wrapping satisfies the OP level for both small and design earthquakes with damping effect, however, it still does not satisfy the CP level for a large earthquake, even when damping effect is taken into account.

Therefore, it can be concluded that with the original capacity of the column, even after considering the damping effect, it does not meet the CP level for a large earthquake although it does satisfy the OP level for both small and design earthquakes. Therefore, it is necessary to go forward with retrofitting of this column, which is done by applying VE layer around the column and wrapping with FRP sheets. In this study, the column was retrofitted by applying 1ply, 2ply and 3ply of CFRP along with VE layer around the column, and the corresponding capacity-demand spectra for both with and without damping effects are shown in Figs. 28 to 30, respectively.

Note that explanation for the retrofitted column for all cases remains the same, as discussed earlier for the case without FRP wrapping. Now, following the same explanation and looking at Figs. 28 to 30, it can be seen that the retrofitted column with 1ply of FRP (Fig. 28 (b)) satisfies the OP level for both small and design earthquakes and it also satisfies the CP level for a large earthquake when damping effect is considered. Perhaps, the same column satisfies the CP level even without considering damping effect when it is wrapped by 2ply of CFRP (Fig. 29(a)).

Normalized Performance for 40% Coverage

The capacity-demand spectra were normalized w.r.t. OP level for all cases following the same procedures as explained earlier; Fig. 31 shows the normalized capacity-demand spectra only for the case with 1ply of FRP. Both demand ductility and capacity ductility for all cases considered were summarized in a tabular form which is shown in Table 3. As explained earlier, in Table 3, ductility demands are shown only for those cases that have performance points. Finally, the demand versus capacity ratios were obtained for all cases to see which case in the proposed DES methodology satisfy both OP and CP performance.

Looking at Table 3, it can be seen that when the DES scheme is considered, both OP and CP level performance are satisfied for the cases when the column is retrofitted with 1 to 3ply of FRP, shown in the shaded area in the table. Perhaps, the same column also satisfies both OP and CP levels when it is retrofitted with 2ply of FRP without considering damping effect. As explained earlier, the minimum design standard should be such that the column should meet the OP level for small earthquakes and it should meet the CP level for large earthquakes. Since the column meets the OP level under a small earthquake and CP level under a large earthquake for 1 to 3ply of CFRP with DES scheme, as shown in the shaded area in Table 3, this implies that the dual performance is satisfied for the case when the column is wrapped at least by 1ply of CFRP along with VE layer with a 40% coverage in the transverse direction.

Column Wrapped by CFRP along with VE Layer for 80% Coverage

Fig. 32(a) shows the force-displacement relationships of the column for a_5 =0.8 in the transverse direction and the corresponding capacity spectra are shown in Fig. 32(b). Fig. 33(a) shows the capacity-demand spectra without FRP and without damping while Fig. 33(b) shows the capacity-demand spectra without FRP and with damping effect for a_5 =0.8. It is clearly seen (Fig. 33(a)) that the column without FRP wrapping satisfies the OP level performance for a small earthquake even without damping effect, however, the same column does not satisfy the CP level when damping effect is not considered, although it satisfies the CP level for a design earthquake. It is also clearly seen (Fig. 33(b)) that the column without FRP wrapping satisfies the OP level for both small and design earthquakes with damping effect, however, it still does not satisfy the CP level for a large earthquake, even when damping effect is taken into account.

Therefore, it can be concluded that with the original capacity of the column, even after considering the damping effect, it does not meet the CP level for a large earthquake, although it does satisfy the OP level for both small and design earthquakes. Therefore, it is necessary to go forward with retrofitting of this column, which is done by applying VE layer around the column and wrapping with FRP sheets. In this study, the column was retrofitted by applying 1ply, 2ply and 3ply of CFRP along with VE layer around the column; the corresponding capacity-demand spectra for both with and without damping effects are shown in Figs. 34 to 36, respectively. Note that the explanation for the retrofitted column for all cases remains the same as discussed earlier for the case without FRP wrapping. Now, following the same explanation and looking at Figs. 34 to 36, it can be seen that the retrofitted column with 1ply of FRP (Fig. 34 (b)) satisfies the OP level

for both small and design earthquakes and it also satisfies the CP level for a large earthquake when damping effect is considered. Perhaps, the same column satisfies the OP and the CP level for a small and a large earthquake, respectively, even without considering damping effect when it is wrapped by 1ply of CFRP (Fig. 34(a)).

Normalized Performance for 80% Coverage

The capacity-demand spectra were normalized w.r.t. OP level for all cases following the same procedures as explained earlier; Fig. 37 shows the normalized capacity-demand spectra only for the case with 1ply of FRP. Both demand ductility and capacity ductility for all cases considered were summarized in a tabular form, which is shown in Table 4. As explained earlier, in Table 4, ductility demands are shown only for those cases that have performance points. Finally, the demand versus capacity ratios were obtained for all cases to see which case in the proposed DES methodology satisfy both the OP and CP performance.

Looking at Table 4, it can be seen that when the DES scheme is considered, both OP and CP level performance are satisfied for the cases when the column is retrofitted with 1 to 3ply of FRP, shown in the shaded area in the table. Perhaps, the same column also satisfies both the OP and CP level when it is retrofitted with both 1ply and 2ply of FRP without considering damping effect. As explained earlier, the minimum design standard should be such that the column should meet the OP level for small earthquakes and it should meet the CP level for large earthquakes. Since the column meets the OP level under a small earthquake and the CP level under a large earthquake for 1 to 3ply of CFRP with DES scheme, as shown in the shaded area in Table 4, this implies that the

dual performance is satisfied for the case when the column is wrapped at least by 1ply of CFRP along with VE layer with a 80% coverage in the transverse direction.

Comparison of Normalized Performance for 40% and 80% coverage

In order to compare the normalized performance for 40% and 80% coverage in the transverse direction, the relationship between normalized performance and number of CFRP ply in the DES scheme were obtained for both cases, shown in Fig. 38. Note that the relationships for both cases are shown at the CP level. It can be seen (Fig. 38) that at CP level the performance of the column is much better when it is retrofitted with 80% coverage than that of 40% coverage. Perhaps, to meet the CP level, the column is required to be retrofitted with at least 1ply of CFRP with 40% coverage, and in this case, it also meets the dual performance levels.

Conclusions

In this study, the DES methodology was applied to Old St. Francis River Bridge columns. The DES methodology consists of two components, viz. damping component and strengthening component. The damping component was obtained based on steady state analysis, which is presented in the companion paper, and the strengthening component was obtained in this study by retrofitting the columns with CFRP and performing nonlinear pushover analysis. Two performance levels were considered, viz. OP and CP levels since they are considered to be the minimum design standard in the context of performance-based seismic design. The performance was evaluated in both longitudinal

and transverse directions considering both out-of-plane and in-plane motions. Based on the results in this study, the following conclusions can be made:

- When the column is retrofitted with 5ply of CFRP along with VE layer with 40% coverage in the longitudinal direction, it does not satisfy the OP level under a small earthquake; however, it does satisfy the CP level under a large earthquake. This implies that the column does not meet dual performance objectives for 40% coverage in the longitudinal direction.

- When the column is retrofitted with 3ply of CFRP along with VE layer with 100% coverage in the longitudinal direction, it does satisfy the OP level under a small earthquake and it also satisfies the CP level under a large earthquake. This implies that the column meets dual performance objectives for 100% coverage in the longitudinal direction.

- When the column is retrofitted with 1ply of CFRP along with VE layer with 40% coverage in the transverse direction, it satisfies the OP level under a small earthquake and it also satisfies the CP level under a large earthquake. This implies that the column meets dual performance objectives for 40% coverage in the transverse direction.

- In order to meet dual performance objectives in both the longitudinal and transverse directions, the column is required to be retrofitted with 3ply of CFRP along with VE layer with full coverage. In that case, the damping component ensures the operational level under a small earthquake and the strengthening component ensures the safety level under a large earthquake in the both directions.

The proposed DES technique is expected to be very useful in performance-based seismic design and retrofit of highway bridges.

Acknowledgement

References

Aiken, I. D., Nims, D. K., Whittaker, A. S., and Kelly, J. M. (1993). "Testing of passive energy dissipation systems." *Earthquake Spectra*, 9(3), 335-370.

Aprile, A., Inaudi, J. A., and Kelly, J. M. (1997). "Evolutionary model of viscoelastic dampers for structural applications." *Journal of Engineering Mechanics*, ASCE, 123(6), 551-560.

ATC/MCEER Joint Venture (2008). *Recommended LRFD Guidelines for the Seismic Design of Highway Bridges*, Applied Technology Council, Redwood City, CA.

Bentz, E. C. (2000). "Sectional analysis of reinforced concrete." Ph.D. Dissertation, Department of Civil Engineering, University of Toronto, Toronto, Canada.

Bergman, D. M., and Hanson, R. D. (1993). "Viscoelastic mechanical damping devices tested at real earthquake displacements." *Earthquake Spectra*, 9(3), 389-418.

Chang, K. C., Soong, T. T., Oh, S. T., and Lai, M. L. (1992). "Effect of ambient temperature on viscoelastically damped structures." *ASCE Journal Structural Engineering*, 118(7), 1955-1973.

Chang, K. C., Soong, T. T., Oh, S. T., and Lai, M. L. (1995). "Seismic behavior of steel frame with added viscoelastic dampers." *ASCE Journal of Structural Engineering*, 121(10), 1418-1426.

Chang, K. C., Chen, S. J., and Lai, M. L. (1996). "Inelastic behavior of steel frames with added viscoelastic dampers." *ASCE Journal of Structural Engineering*, 122(10), 1178-1186.

Chen, G., Thebeau, P., and Mu, H., (2002). "Seismic vulnerability of highway bridges along a designated emergency vehicle access routes near the New Madrid seismic zone." *7th National Conference on Earthquake Engineering* (CD-ROM), Boston, MA.

Chen, G., Wang, W. and Huang, X. (2006). "Optimal design of RC column seismic retrofitting for multiple performance objectives with an integrated damping and strengthening methodology." *8th National Conference on Earthquake Engineering* (CD-ROM), San Francisco, CA.

Chen, G. and Karim, K. R. (2006). "Damping-enhanced seismic strengthening of RC columns for multiple performance objectives." *5th National Seismic Conference of Bridges and Highways*, San Francisco, CA, Paper No B24.

Chopra, A. K. (2001). *Dynamics of structures*, Prentice Hall, New York, NY.

Fajfar, P. (1999). "Capacity spectrum method based on inelastic demand spectra." *Earthquake Engineering and Structural Dynamics*, 28, 979-993.

FEMA-273. (1997), "NEHRP guidelines for the seismic rehabilitation of buildings." *Building Seismic Safety Council*, Washington, DC.

FHWA (2005). "Seismic retrofitting manual for highway bridges." *Federal Highway Administration*, Publication No. FHWA-RD-94-052.

Foutch, D. A., Wood, S.L., and Beady, P. A. (1993). "Seismic retrofit for nonductile reinforced concrete frames using viscoelastic dampers." *Proceedings of Applied Technology Council ATC-17-1 Seminar on Seismic Isolation, Passive Energy Dissipation and Active Control*, 2, 605-616.

Gehling, R. N. (1987). "Large space structure damping treatment performance: analytic and test results." *Role of Damping in Vibration and Noise Control*, ASME, New York, NY, 93-100.

Hammami, L., Zghal, B., Fakhfakh, T., and Haddar, M. (2005). "Characterization of modal damping of sandwich plates." *Journal of Vibration and Accoustics*, 127, 431-440.

Hanson, R. D., and Soong, T. T. (2001). "Seismic design with supplemental energy dissipation devices." *EERI Monograph*, Oakland, CA.

Huang, X. (2005). "An integrated VE damping and FRP strengthening system for performance-based seismic retrofit of RC columns." Ph.D. dissertation, University of Missouri-Rolla, Rolla, MO.

International Code Council (2006). *International Building Code*, International Code Council, Inc., Whittier, CA.

Karim, K. R., and Chen, G. (2009). "Distributed VE layer damping effect on the elastic response of highway bridges." *ASCE Journal of Structural Engineering* (to be submitted).

Kasai, K., Munshi, J. A., Lai, M. L., and Maison, B. F. (1993). "Viscoelastic damper's hysteretic modal theory, experiment, and application." *Proceedings of Applied Technology Council ATC-17-1 Seminar on Seismic Isolation, Passive Energy Dissipation and Active Control*, 2, 521-532.

Kerwin, E. M. Jr. (1959). "Damping of flexural waves by a constrained viscoelastic layer." *J. Accoust. Soc. Am.*, 31(7), 952-962.

Lin, W. H., and Chopra, A. K. (2003). "Earthquake response of elastic single-degree-of-freedom systems with nonlinear viscoelastic dampers." *ASCE Journal of Engineering Mechanics*, 129(6), 597-606.

Lu, B. (2007). "Application of displacement-based design method to blast-resistant reinforced concrete structures." Ph.D. dissertation, University of Missouri-Rolla, Rolla, MO.

Mander, J. B., Priestley, M. J. N., and Park, R. (1988). "Theoretical stress-strain model for confined concrete." *ASCE Journal of Structural Engineering*, 114(8), 1804-1826.

MCEER (2005). "Seismic retrofitting manual for highway structures: part 1 – bridges." Working Draft, Prepared by the Multidisciplinary Center for Earthquake Engineering Research (MCEER) for Federal Highway Administration.

Morgenthaler, D. R. (1987). "Design and analysis of passive damped large space structures." *Role of Damping in Vibration and Noise Control*, ASME, New York, NY, 1-8.

Priestley, M. J. N., Seible, F., and Calvi, G. M. (1996). *Sesimic design and retrofit of bridges*, John Wiley & Sons, New York, NY.

RESPONSE-2000 (2009). "Sectional analysis software for reinforced concrete." <http://www.ecf.utoronto.ca/~bentz/home.shtml>.

Ross, D., Ungar, E. E., and Kerwin, E. W. (1959). "Damping of plate flexural vibrations by means of viscoelastic laminar." *Structural Damping* (ed, Ruzicka, E.J.), ASME.

SAP2000. "Integrated software for structural analysis & design." *Computers & Structures, Inc*., Berkeley, CA.

Shen, K. L., and Soong, T. T. (1995). "Modeling of viscoelastic dampers for structural applications." *ASCE Journal of Engineering Mechanics*, 121(6), 694-701.

Silva, P. F., Erecson, N. J., and Chen, G. (2007). "Seismic retrofit of bridge joints in central U.S. with carbon fiber-reinforced polymer composites." *ACI Structural Journal*, 104(2), 207-217.

Soong, T. T., and Dargush, G. F. (1997). *Passive energy dissipation system in structural engineering*, John Wiley & Sons, New York, NY.

Soong, T. T., and Spencer, B. F. (2002). "Supplemental energy dissipation: state-of-the-art and state-of-the-practice." *Engineering Structures*, 24, 243-259.

Viti, S., Reinhorn, A. M., and Whittaker, A. S. (2002). "Retrofit of structures: strength reduction with damping enhancement." *KEERC-MCEER Joint Seminar on Retrofit Strategies for Critical Facilites*, Buffalo, NY.

Zhang, R. H., Soong, T. T., and Mahmoodi, P. (1989). "Seismic response of steel frame structures with added viscoelastic dampers." *Earthquake Engineering and Structural Dynamics*, 18, 389-396.

Zhang, R. H., and Soong, T. T. (1992). "Seismic design of viscoelastic dampers for structural applications." *ASCE Journal of Structural Engineering*, 118(5), 1375-1392.

Table 1. Normalized performance with different retrofit scheme for $a_5 = 0.4$ in the longitudinal direction.

Case	Retrofit Scheme		Ductility Demand[5]		Ductility Capacity		Demand/Capacity	
	VE	CFRP	OP[1]	CP[2]	OP[3]	CP[4]	OP	CP
No Retrofit	No	No	1.24	-	1.00	1.46	>1.00	-
Damping	Yes	No	1.10	-	1.00	1.46	>1.00	-
Strengthening	No	1ply	1.24	-	1.00	1.87	>1.00	-
	No	2ply	1.24	-	1.00	2.32	>1.00	-
	No	3ply	1.24	-	1.00	2.68	>1.00	-
	No	4ply	1.24	-	1.00	3.13	>1.00	-
	No	5ply	1.24	-	1.00	3.53	>1.00	-
	No	6ply	1.24	3.47	1.00	3.83	>1.00	0.91
Proposed DES	Yes	1ply	1.10	-	1.00	1.87	>1.00	-
	Yes	2ply	1.10	-	1.00	2.32	>1.00	-
	Yes	3ply	1.10	-	1.00	2.68	>1.00	-
	Yes	4ply	1.10	-	1.00	3.13	>1.00	-
	Yes	5ply	1.10	3.27	1.00	3.53	>1.00	0.93
	Yes	6ply	1.10	3.04	1.00	3.83	>1.00	0.79

[1]Seismic demand under small earthquakes, i.e. 10% probability of exceedance in 50 years; [2]Seismic demand under large earthquakes, i.e. 2% probability of exceedance in 50 years; [3]Ductiltiy at yield point; [4]Ductility at ultimate point; [5]Demand ductility is obtained based on performance point.

Table 2. Normalized performance with different retrofit scheme for $a_5 = 1.0$ in the longitudinal direction.

Case	Retrofit Scheme		Ductility Demand[5]		Ductility Capacity		Demand/Capacity	
	VE	CFRP	OP[1]	CP[2]	OP[3]	CP[4]	OP	CP
No Retrofit	No	No	1.24	-	1.00	1.46	>1.00	-
Damping	Yes	No	0.92	-	1.00	1.46	0.92	-
Strengthening	No	1ply	1.24	-	1.00	1.99	>1.00	-
	No	2ply	1.24	-	1.00	2.49	>1.00	-
	No	3ply	1.24	-	1.00	3.00	>1.00	-
	No	4ply	1.24	-	1.00	3.51	>1.00	-
	No	5ply	1.24	3.28	1.00	4.02	>1.00	0.82
	No	6ply	1.24	3.26	1.00	4.53	>1.00	0.72
Proposed DES	Yes	1ply	0.92	-	1.00	1.99	0.92	-
	Yes	2ply	0.92	-	1.00	2.49	0.92	-
	Yes	3ply	0.92	2.87	1.00	3.00	0.92	0.96
	Yes	4ply	0.92	2.51	1.00	3.51	0.92	0.71
	Yes	5ply	0.92	2.29	1.00	4.02	0.92	0.57
	Yes	6ply	0.92	2.27	1.00	4.53	0.92	0.50

[1]Seismic demand under small earthquakes, i.e. 10% probability of exceedance in 50 years; [2]Seismic demand under large earthquakes, i.e. 2% probability of exceedance in 50 years; [3]Ductiltiy at yield point; [4]Ductility at ultimate point; [5]Ductility demand based on performance point; Shaded area indicates retrofit scheme that satisfies both OP and CP criteria.

Table 3. Normalized performance with different retrofit scheme for $a_5 = 0.4$ in the transverse direction.

Case	Retrofit Scheme		Ductility Demand[5]		Ductility Capacity		Demand/Capacity	
	VE	CFRP	OP[1]	CP[2]	OP[3]	CP[4]	OP	CP
No Retrofit	No	No	0.57	-	1.00	1.48	0.57	-
Damping	Yes	No	0.50	-	1.00	1.48	0.50	-
Strengthening	No	1ply	0.57	-	1.00	1.87	0.57	-
	No	2ply	0.57	1.78	1.00	2.27	0.57	0.79
Proposed DES	Yes	1ply	0.50	1.57	1.00	1.87	0.50	0.84
	Yes	2ply	0.50	1.45	1.00	2.27	0.50	0.64
	Yes	2ply	0.50	1.45	1.00	2.73	0.50	0.53

[1]Seismic demand under small earthquakes, i.e. 10% probability of exceedance in 50 years; [2]Seismic demand under large earthquakes, i.e. 2% probability of exceedance in 50 years; [3]Ductiltiy at yield point; [4]Ductility at ultimate point; [5]Ductility demand based on performance point; Shaded area indicates retrofit scheme that satisfies both OP and CP criteria.

Table 4. Normalized performance with different retrofit scheme for $a_5 = 0.8$ in the transverse direction.

Case	Retrofit Scheme		Ductility Demand[5]		Ductility Capacity		Demand/Capacity	
	VE	CFRP	OP[1]	CP[2]	OP[3]	CP[4]	OP	CP
No Retrofit	No	No	0.57	-	1.00	1.48	0.57	-
Damping	Yes	No	0.43	-	1.00	1.48	0.43	-
Strengthening	No	1ply	0.57	1.75	1.00	2.00	0.57	0.88
	No	2ply	0.57	1.75	1.00	2.50	0.57	0.70
Proposed DES	Yes	1ply	0.43	1.05	1.00	2.00	0.43	0.53
	Yes	2ply	0.43	1.05	1.00	2.50	0.43	0.42
	Yes	3ply	0.43	1.05	1.00	3.00	0.43	0.35

[1]Seismic demand under small earthquakes, i.e. 10% probability of exceedance in 50 years; [2]Seismic demand under large earthquakes, i.e. 2% probability of exceedance in 50 years; [3]Ductiltiy at yield point; [4]Ductility at ultimate point; [5]Ductility demand based on performance point; Shaded area indicates retrofit scheme that satisfies both OP and CP criteria.
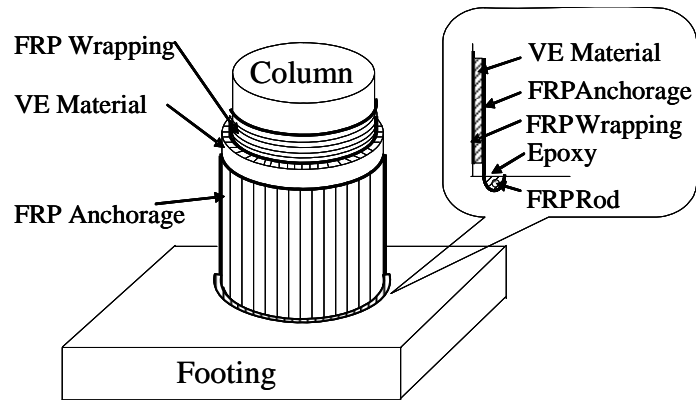
Fig. 1. Composition of a DES system.
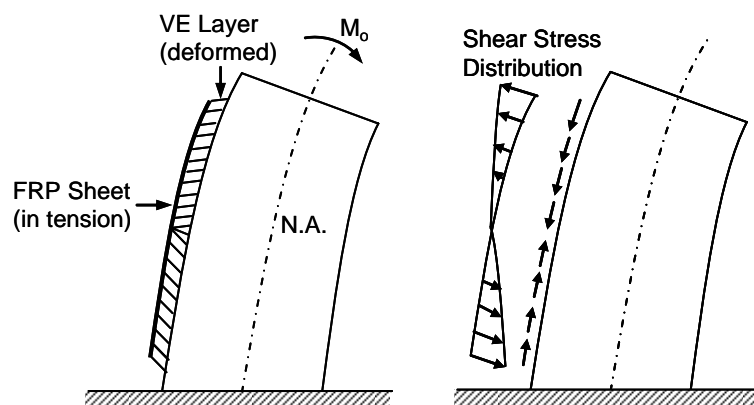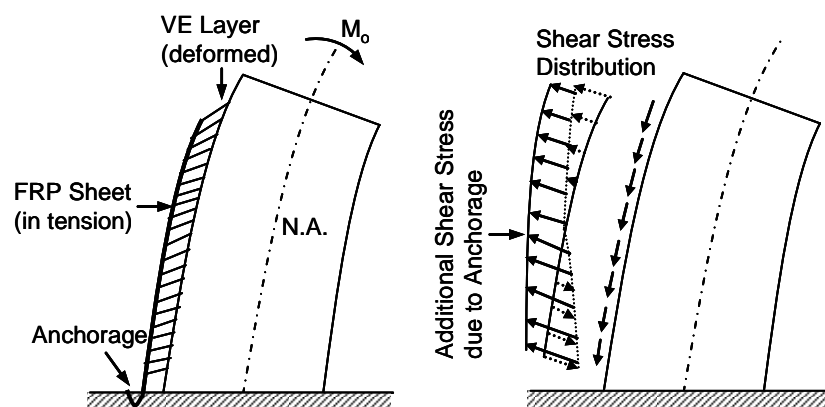
(a) Conventional constrained layer.

(b) Anchored constrained layer.

Fig. 2. Comparison of shear stress distributions in the conventional and the proposed layer treatments.
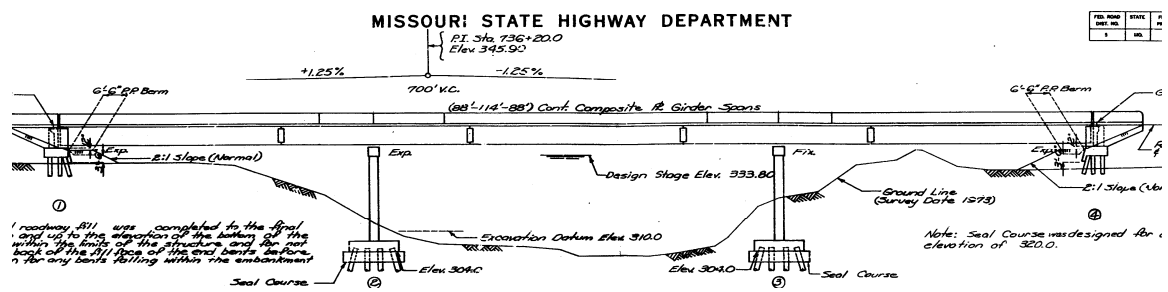
Fig. 3. Bridge elevation.
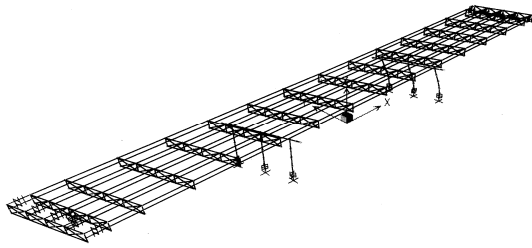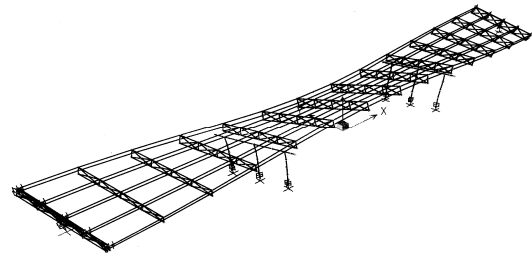
(a) mode 1, T=1.3173 s.   (b) mode 2, T=0.4773 s.

Fig. 4. Vibration period and mode shapes of the highway bridge.
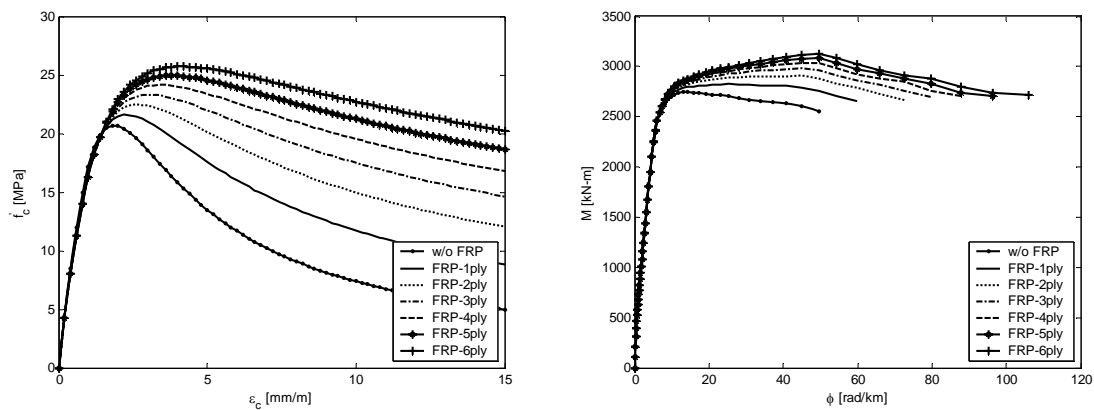
(a) Stress-strain relationship.   (b) Moment-curvature relationship.

Fig. 5. Concrete properties and corresponding moment-curvature relationship.
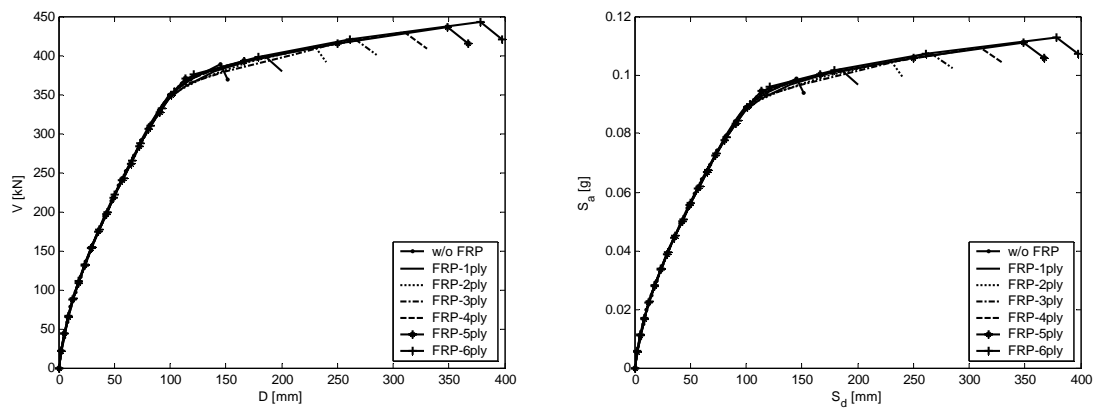
(a) Shear force-displacement relationship.   (b) Capacity spectrum.

Fig.6. Force-displacement and capacity spectrum obtained from pushover analysis for a_5 =0.4 in the longitudinal direction.
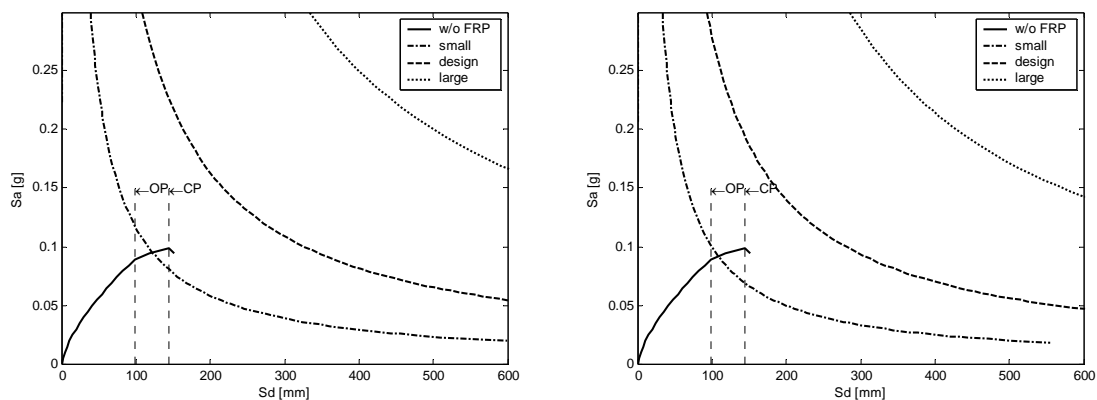
129

(a) Acceleration response spectra.

(b) Acceleration-displacement response spectra.

Fig. 7. IBC (2006) response spectra.

(a) Capacity-demand spectra without damping effect.

(b) Capacity-demand spectra with damping effect.

Fig. 8. Capacity-demand spectra without FRP for $a_5 = 0.4$ in the longitudinal direction.
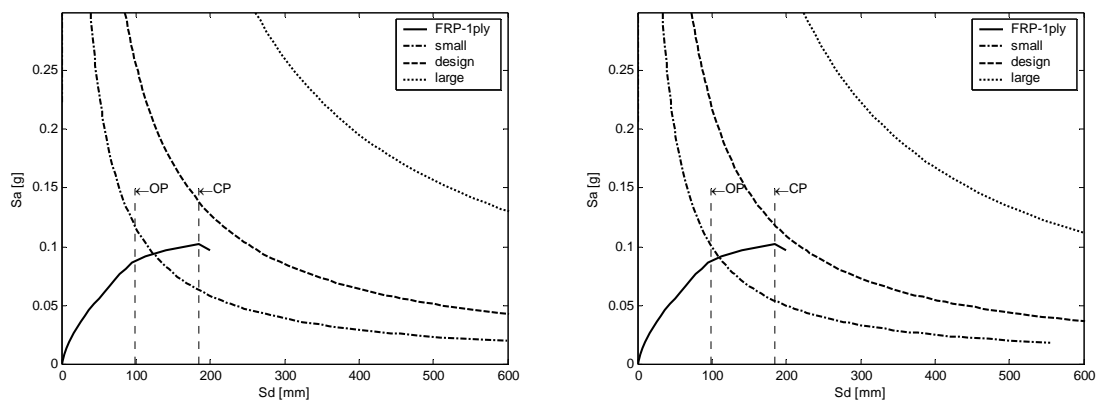
(a) Capacity-demand spectra without damping effect.
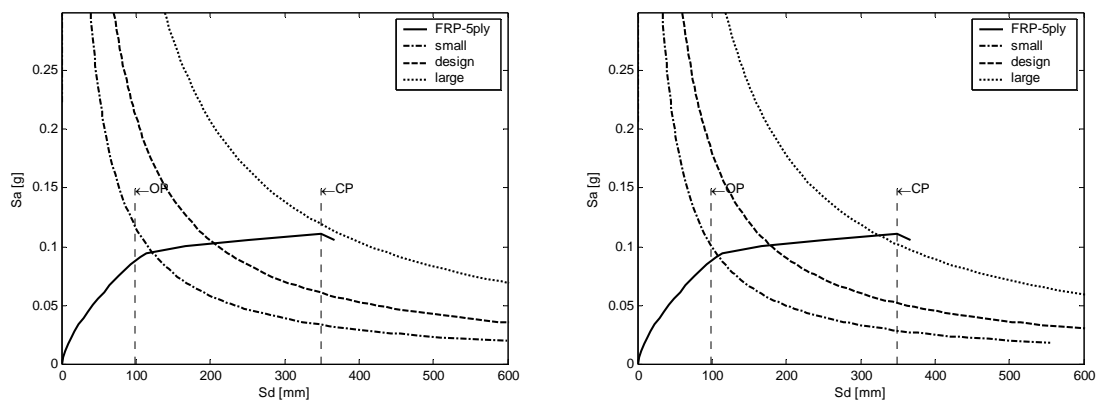
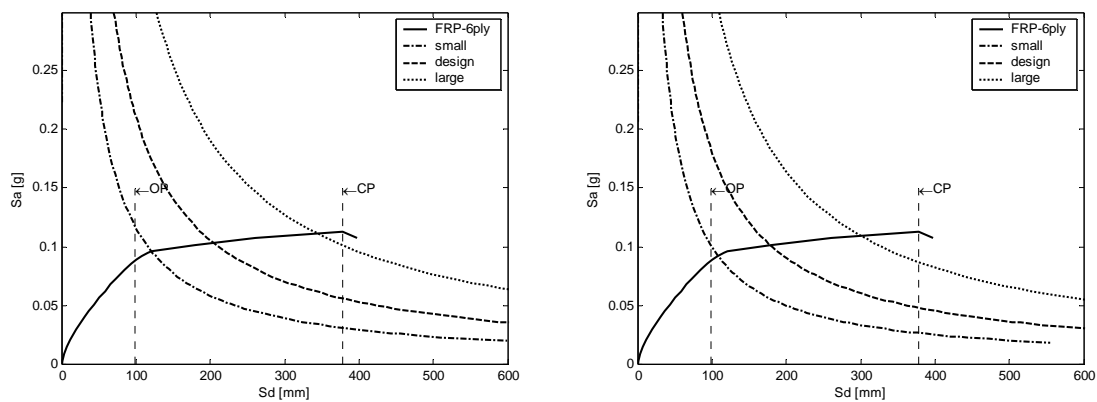(b) Capacity-demand spectra with damping effect.

Fig. 9. Capacity-demand spectra with 1ply FRP for $a_5 = 0.4$ in the longitudinal direction.
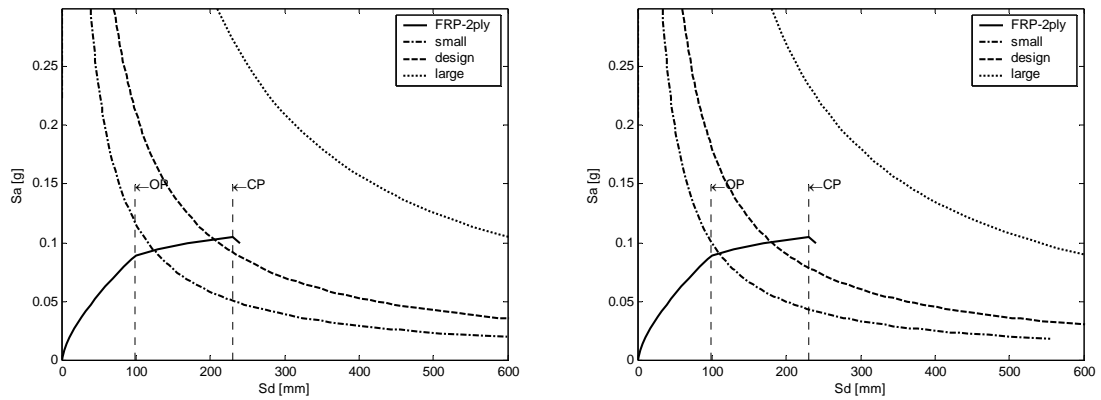
(a) Capacity-demand spectra without damping effect.

(b) Capacity-demand spectra with damping effect.

Fig. 10. Capacity-demand spectra with 2ply FRP for $a_5 =0.4$ in the longitudinal direction.
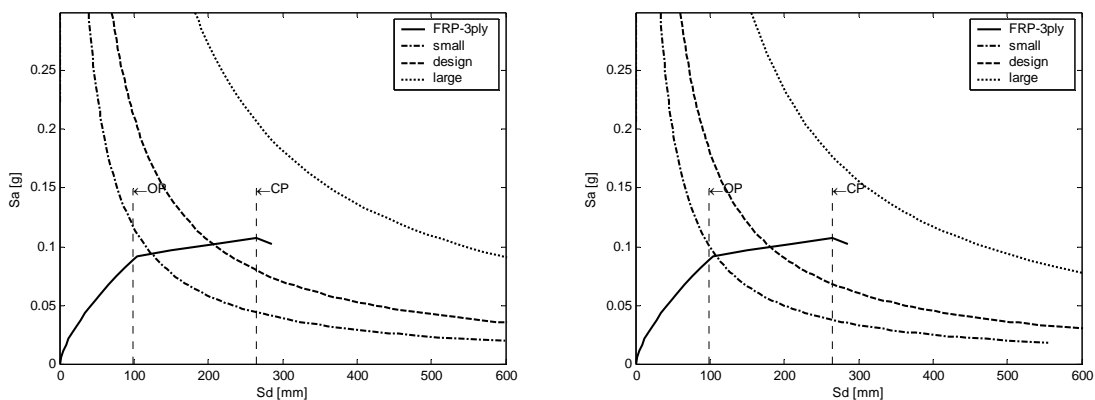
(a) Capacity-demand spectra without damping effect.
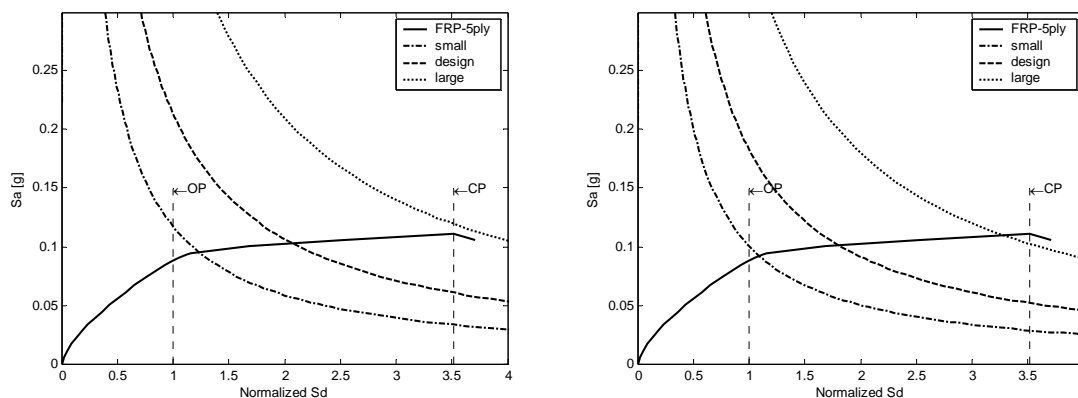
(b) Capacity-demand spectra with damping effect.

Fig. 11. Capacity-demand spectra with 3ply FRP for $a_5 = 0.4$ in the longitudinal direction.
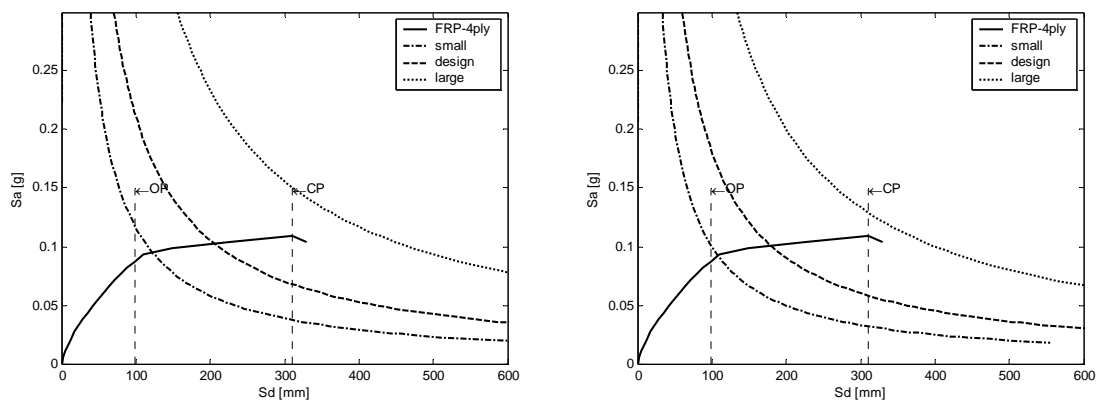
(a) Capacity-demand spectra without damping effect.

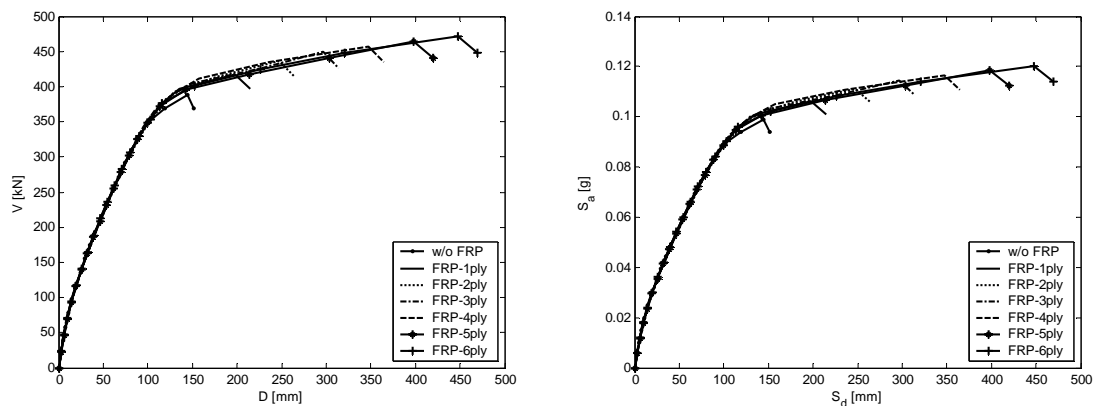(b) Capacity-demand spectra with damping effect.

Fig. 12. Capacity-demand spectra with 4ply FRP for $a_5 = 0.4$ in the longitudinal direction.

(a) Capacity-demand spectra without damping effect.

(b) Capacity-demand spectra with damping effect.

Fig. 13. Capacity-demand spectra with 5ply FRP for $a_5 = 0.4$ in the longitudinal direction.

(a) Capacity-demand spectra without damping effect.

(b) Capacity-demand spectra with damping effect.

Fig. 14. Capacity-demand spectra with 6ply FRP for $a_5 = 0.4$ in the longitudinal direction.

(a) Normalized capacity-demand spectra without damping effect.

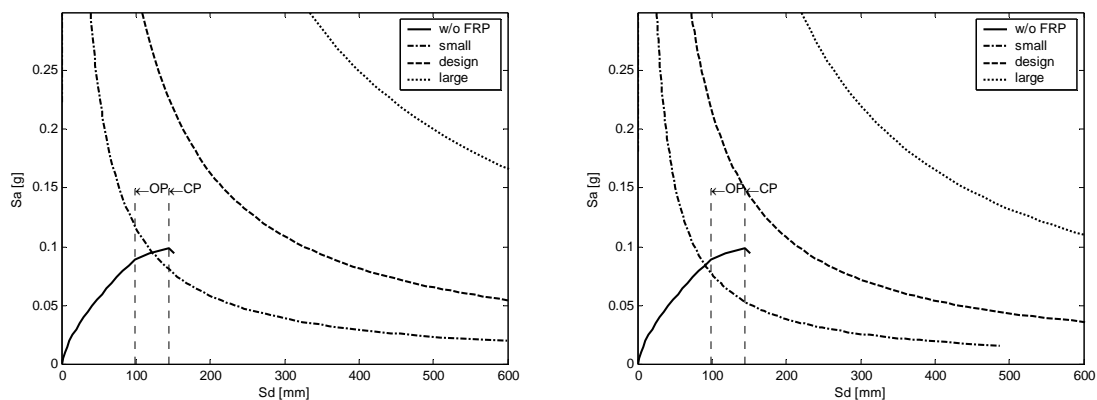(b) Normalized capacity-demand spectra with damping effect.

Fig. 15. Normalized capacity-demand spectra with 5ply FRP for $a_5 = 0.4$ in the longitudinal direction. Note that both capacity and demand spectra are normalized with respect to OP, which is defined as displacement at yield point.

(a) Shear force-displacement relationship.　　　　(b) Capacity spectrum.

Fig. 16. Force-displacement and capacity spectrum obtained from pushover analysis for $a_5 = 1.0$ in the longitudinal direction.

(a) Capacity-demand spectra without damping effect.

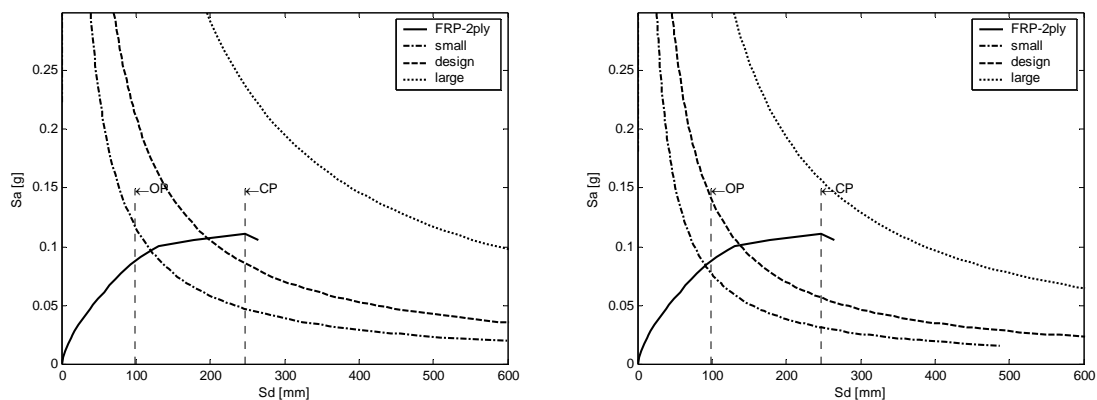(b) Capacity-demand spectra with damping effect.

Fig. 17. Capacity-demand spectra without FRP for $a_5 = 1.0$ in the longitudinal direction.
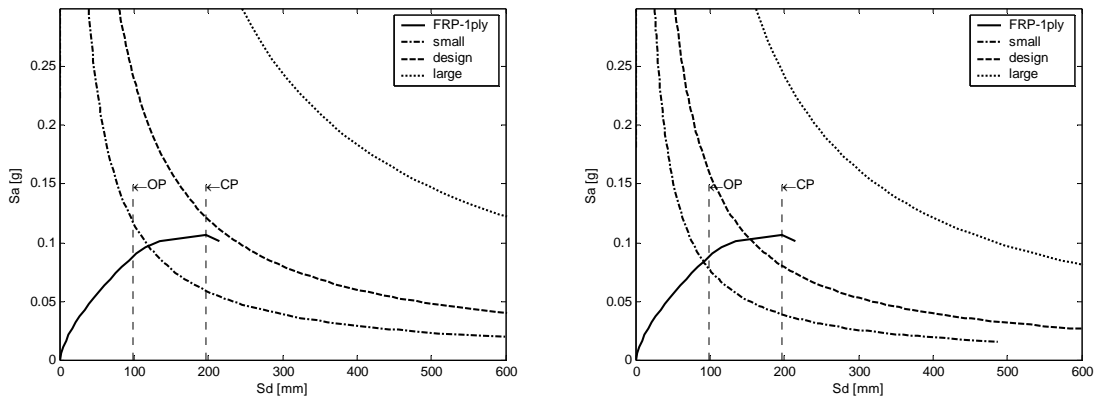
(a) Capacity-demand spectra without damping effect.

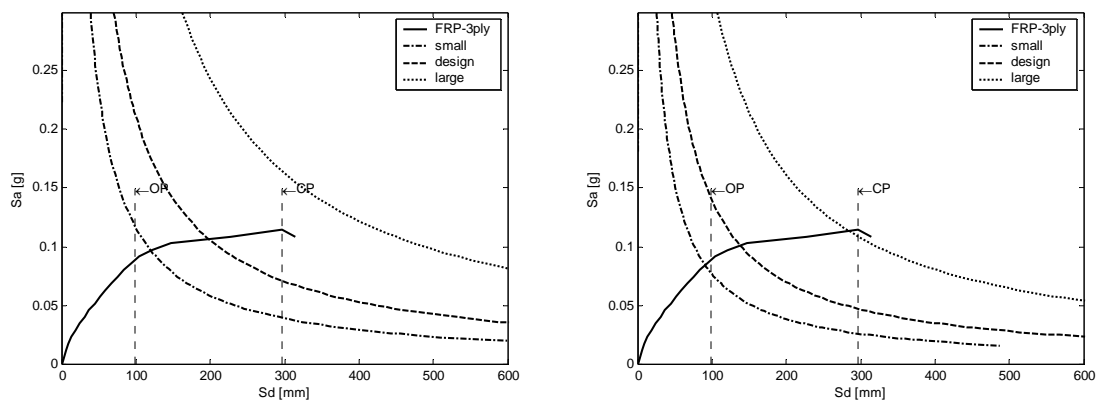(b) Capacity-demand spectra with damping effect.

Fig. 18. Capacity-demand spectra with 1ply FRP for $a_5 = 1.0$ in the longitudinal direction.

(a) Capacity-demand spectra without damping effect.

(b) Capacity-demand spectra with damping effect.

Fig. 19. Capacity-demand spectra with 2ply FRP for $a_5 = 1.0$ in the longitudinal direction.

(a) Capacity-demand spectra without damping effect.

(b) Capacity-demand spectra with damping effect.
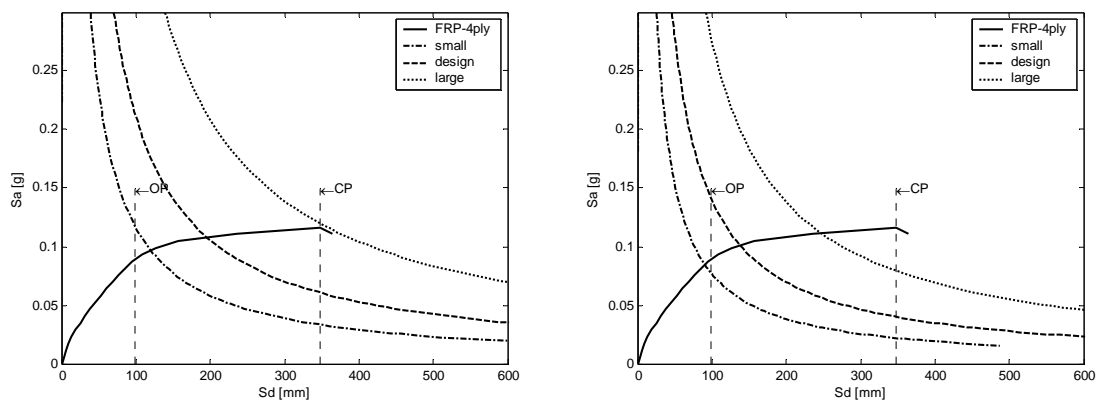
Fig. 20. Capacity-demand spectra with 3ply FRP for $a_5 = 1.0$ in the longitudinal direction.

(a) Capacity-demand spectra without damping effect.

(b) Capacity-demand spectra with damping effect.
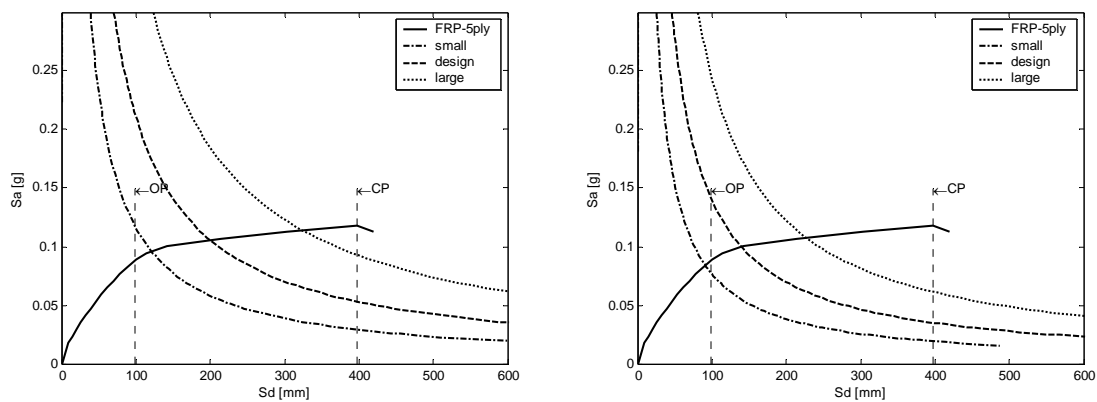
Fig. 21. Capacity-demand spectra with 4ply FRP for $a_5 = 1.0$ in the longitudinal direction.

(a) Capacity-demand spectra without damping effect.

(b) Capacity-demand spectra with damping effect.

Fig. 22. Capacity-demand spectra with 5ply FRP for $a_5 = 1.0$ in the longitudinal direction.

(a) Capacity-demand spectra without damping effect.

(b) Capacity-demand spectra with damping effect.
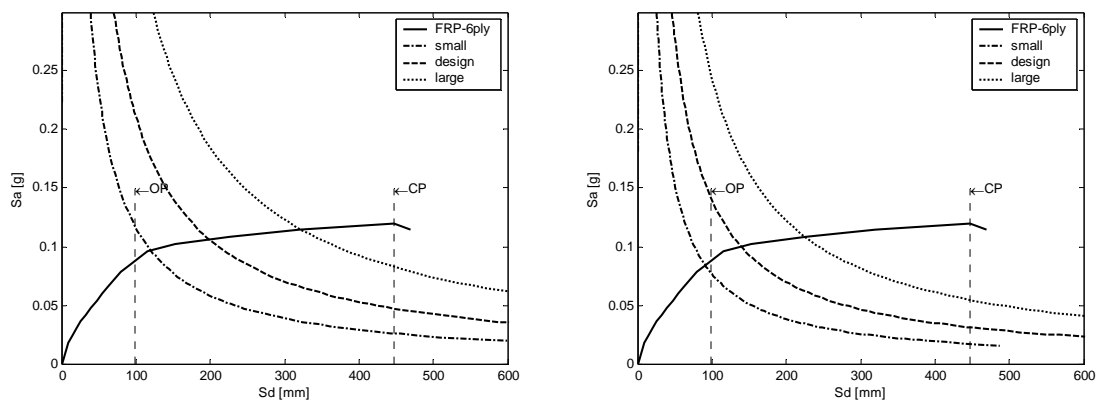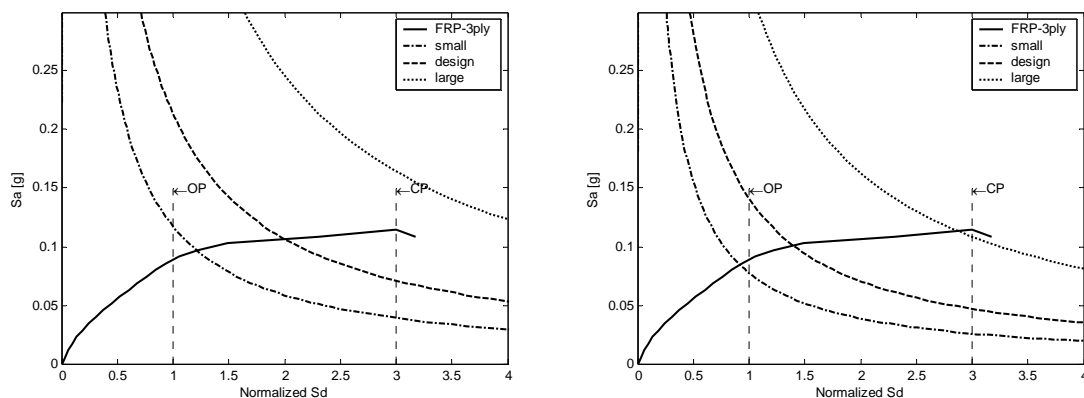
Fig. 23. Capacity-demand spectra with 6ply FRP for $a_5 = 1.0$ in the longitudinal direction.

(a) Normalized capacity-demand spectra without damping effect.

(b) Normalized capacity-demand spectra with damping effect.

Fig. 24. Normalized capacity-demand spectra with 3ply FRP for $a_5 = 1.0$ in the longitudinal direction. Note that both capacity and demand spectra are normalized with respect to OP, which is defined as displacement at yield point.
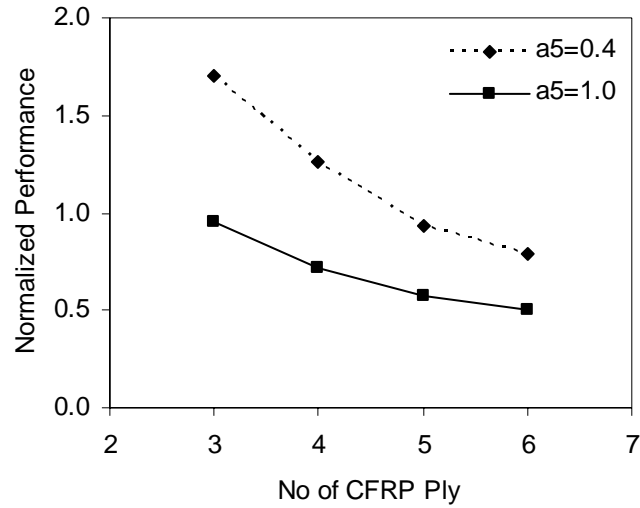
Fig. 25. Normalized performance (demand versus capacity ratio) in the longitudinal direction at CP level for a 40% (a_5=0.4) and 100% (a_5=1.0) coverage of CFRP ply around the bridge column for the proposed DES methodology that takes into account both damping and strengthening components.
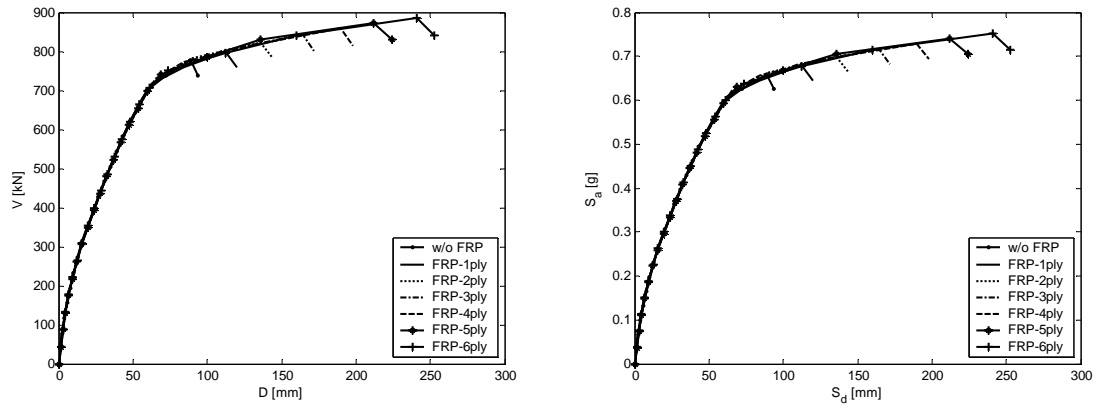
(a) Shear force-displacement relationship.   (b) Capacity spectrum.

Fig. 26. Force-displacement and capacity spectrum obtained from pushover analysis for $a_5 = 0.4$ in the transverse direction.
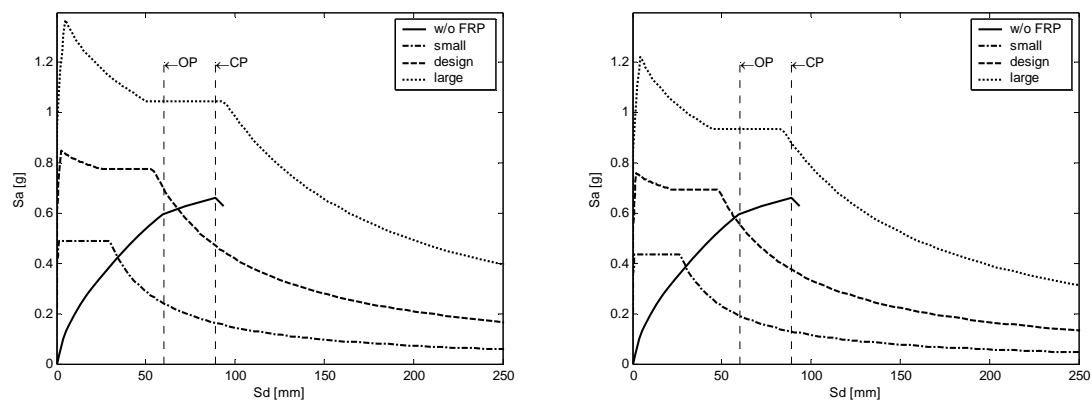
(a) Capacity-demand spectra without damping effect.

(b) Capacity-demand spectra with damping effect.

Fig. 27. Capacity-demand spectra without FRP for $a_5 = 0.4$ in the transverse direction.
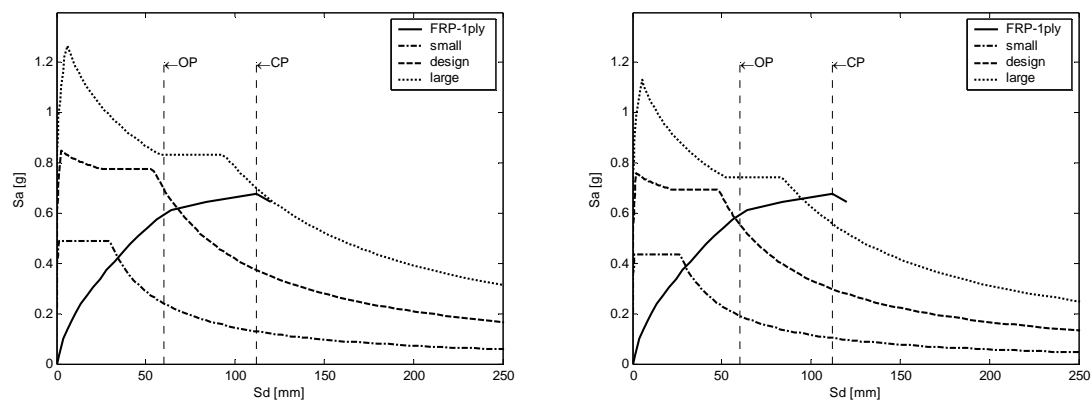
(a) Capacity-demand spectra without damping effect.

(b) Capacity-demand spectra with damping effect.

Fig. 28. Capacity-demand spectra with 1ply FRP for $a_5 = 0.4$ in the transverse direction.

(a) Capacity-demand spectra without damping effect.

(b) Capacity-demand spectra with damping effect.

Fig. 29. Capacity-demand spectra with 2ply FRP for $a_5 = 0.4$ in the transverse direction.

(a) Capacity-demand spectra without damping effect.

(b) Capacity-demand spectra with damping effect.

Fig. 30. Capacity-demand spectra with 3ply FRP for $a_5 = 0.4$ in the transverse direction.

(a) Normalized capacity-demand spectra without damping effect.

(b) Normalized capacity-demand spectra with damping effect.

Fig. 31. Normalized capacity-demand spectra with 1ply FRP for $a_5 = 0.4$ in the transverse direction. Note that both capacity and demand spectra are normalized with respect to OP, which is defined as displacement at yield point.

(a) Shear force-displacement relationship.　　　(b) Capacity spectrum.

Fig. 32. Force-displacement and capacity spectrum obtained from pushover analysis for a_5 =0.8 in the transverse direction.

(a) Capacity-demand spectra without damping effect.

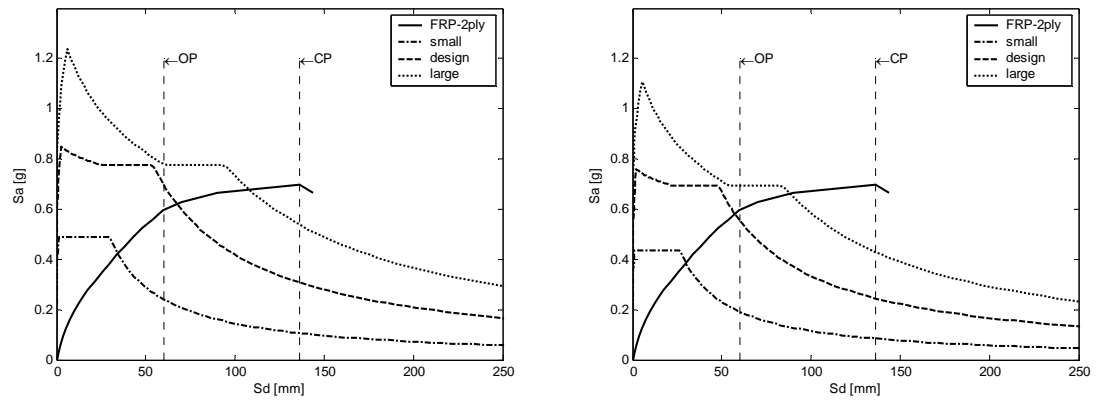(b) Capacity-demand spectra with damping effect.

Fig. 33. Capacity-demand spectra without FRP for $a_5 = 0.8$ in the transverse direction.
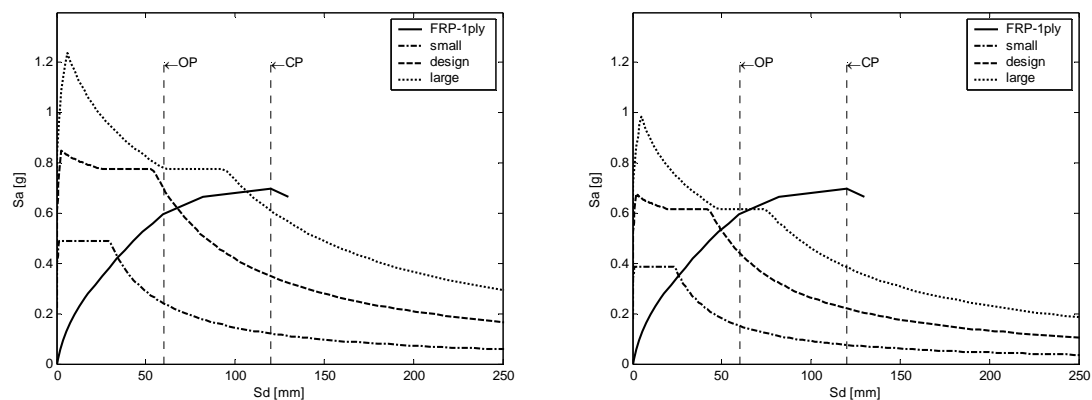
(a) Capacity-demand spectra without damping effect.

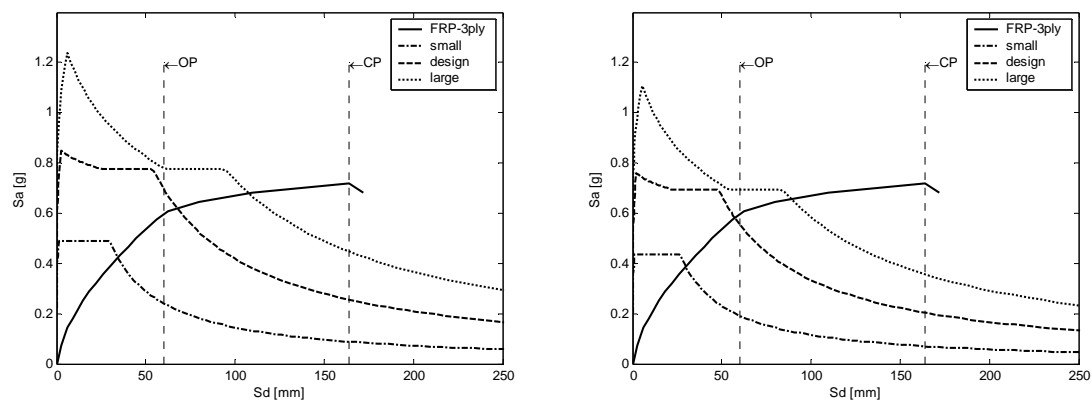(b) Capacity-demand spectra with damping effect.

Fig. 34. Capacity-demand spectra with 1ply FRP for $a_5 = 0.8$ in the transverse direction.
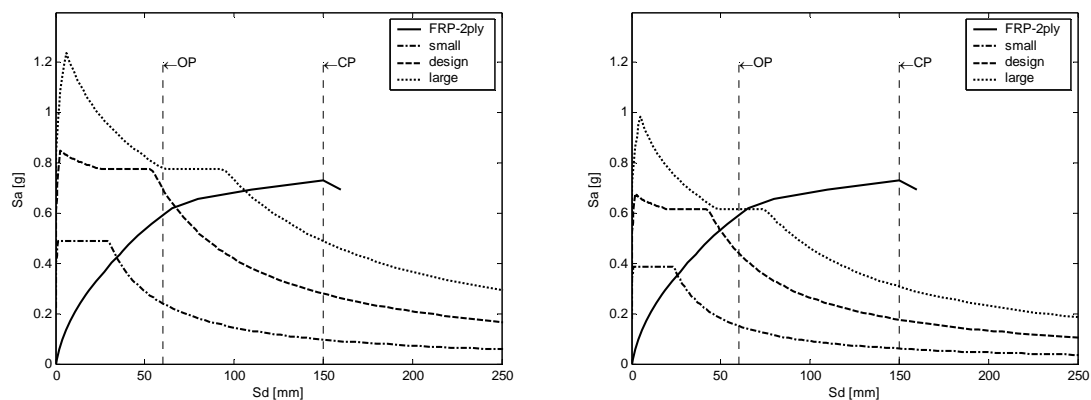
(a) Capacity-demand spectra without damping effect.

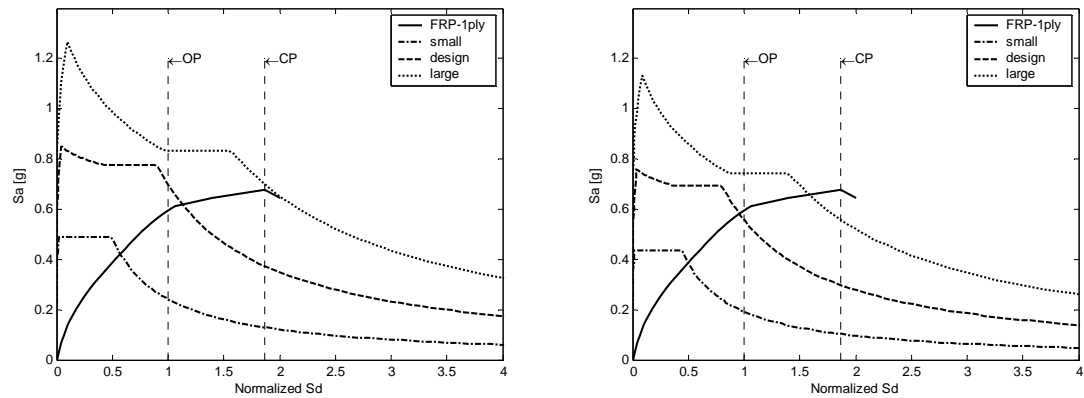(b) Capacity-demand spectra with damping effect.

Fig. 35. Capacity-demand spectra with 2ply FRP for $a_5 = 0.8$ in the transverse direction.
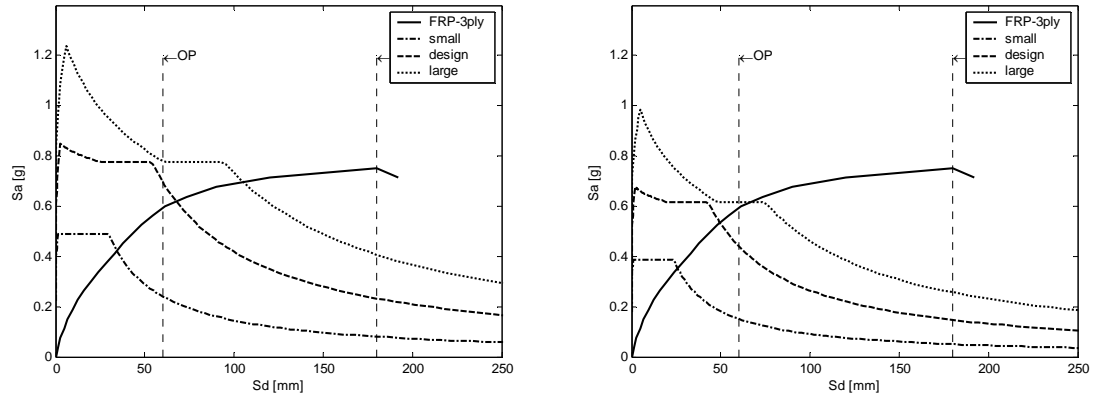
(a) Capacity-demand spectra without damping effect.

(b) Capacity-demand spectra with damping effect.
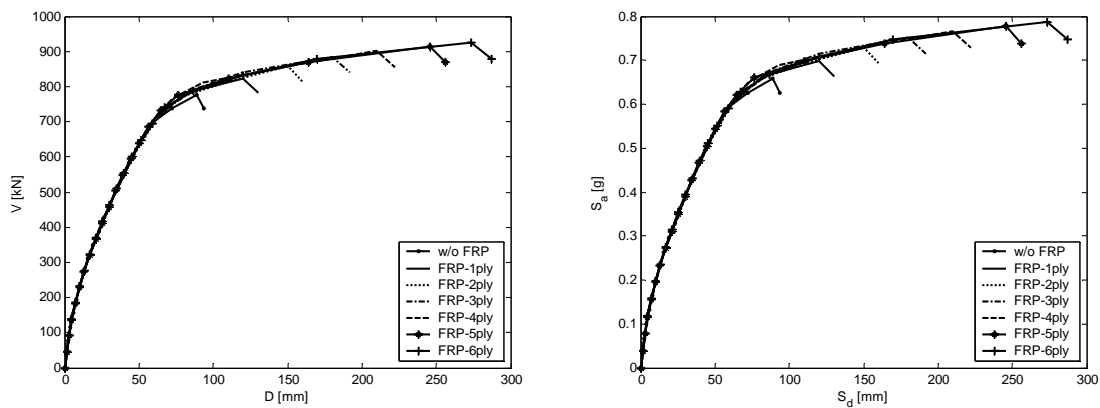
Fig. 36. Capacity-demand spectra with 3ply FRP for $a_5 = 0.8$ in the transverse direction.
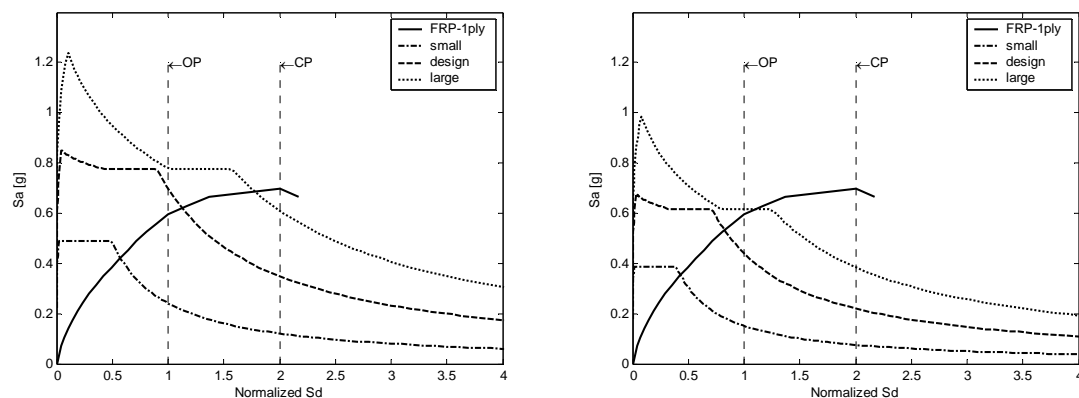
(a) Normalized capacity-demand spectra without damping effect.

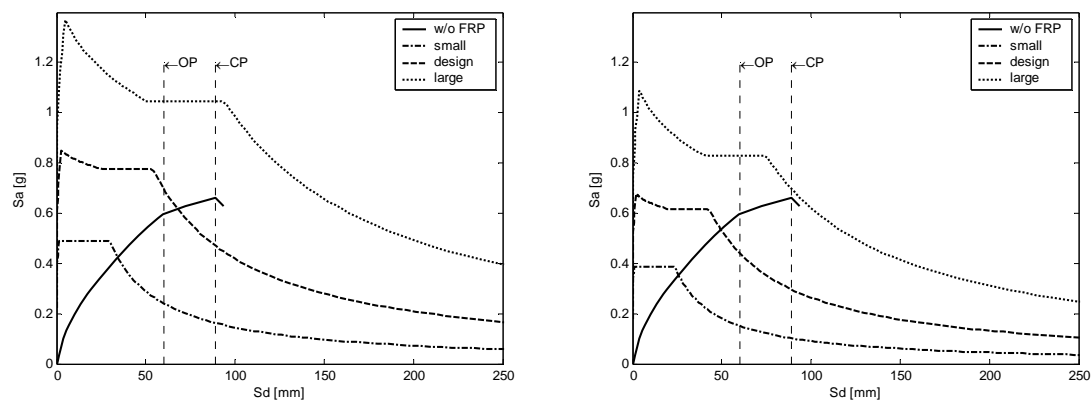(b) Normalized capacity-demand spectra with damping effect.

Fig. 37. Normalized capacity-demand spectra with 1ply FRP for $a_5 = 0.8$ in the transverse direction. Note that both capacity and demand spectra are normalized with respect to OP, which is defined as displacement at yield point.
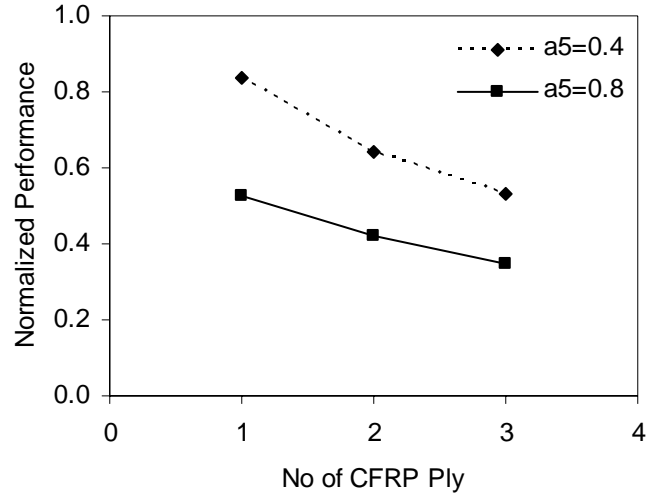
Fig. 38. Normalized performance (demand versus capacity ratio) in the transverse direction at CP level for a 40% (a_5=0.4) and 80% (a_5=0.8) coverage of CFRP ply around the bridge column for the proposed DES methodology that takes into account both damping and strengthening components.

3. CONCLUSIONS

In this study, the responses of a simply supported beam and a plate-strip with different configurations of constrained VE layers were investigated. First, the equation of bending vibration of the beam was formulated and the responses were obtained in the form of acceleration ratio based on steady state analysis. The responses were also obtained for different thicknesses of VE layer as well as different thicknesses of beam.

Then, a new damping-enhanced strengthening (DES) strategy was introduced to enable engineers to retrofit a bridge structure for its normalized performances against multiple objectives under different levels of earthquake hazards. One significant step in achieving this goal was to develop a finite element modeling technique for the implementation of this strategy in practical application.

Specifically, discrete springs were introduced to model the effects of distributed VE damping layers on the response of columns and the structural system at large. The discrete spring model was validated against the analytical solution. The validated model was then applied to investigate the effect of VE layers on the out-of-plane and in-plane motions of the three-column bent from a three-span steel-girder bridge.

The DES methodology was then applied to Old St. Francis River Bridge columns to investigate dual performance objectives. The dual performance levels were considered as OP and CP levels since they are considered to be the minimum design standard in the context of performance-based seismic design. This was done by retrofitting the bridge columns with CFRP along with VE layer for different percentage coverage of the bridge columns.

The DES methodology consists of two components, viz. damping and strengthening component. The damping component was obtained based on steady state analysis and the strengthening component was obtained by performing nonlinear pushover analysis. The dual performance of the bridge column was then evaluated in both longitudinal and transverse directions based on demand versus capacity ratios. Based on the results of this study, the following conclusions can be made:

- VE layer with both-end anchorage case is more effective than that of the other configurations.

- VE layer with smaller thickness is more effective than that of the larger thickness.

- With the same VE layer configuration as well as the same VE layer thickness, the VE layer is more effective when the fundamental frequency of the beam is less and it is less effective when the fundamental frequency goes higher.

- It was observed that the 40% coverage of a circular column by one 2.38 mm VE layer can reduce the peak acceleration at the bridge deck by 14% when the column is subjected to a single curvature action. The same percentage coverage at the lower portion of the column can reduce the responses by 11% when the column is subjected to double curvature action.

- In comparison with the retrofit scheme at both ends of the columns, it was observed that retrofitting of one end of the columns with the same 40% VE coverage is more efficient compared to retrofitting at both ends. It was also observed that the VE layer is more effective for a range of 20-80% coverage.

- When the column is retrofitted with 5ply of CFRP along with VE layer with 40% coverage in the longitudinal direction, it does not satisfy the OP level under a small earthquake; however, it satisfies the CP level under a large earthquake. This implies that the column does not meet dual performance objectives for 40% coverage in the longitudinal direction.

- When the column is retrofitted with 3ply of CFRP along with VE layer with 100% coverage in the longitudinal direction, it satisfies the OP level under a small earthquake and it also satisfies the CP level under a large earthquake. This implies that the column meets dual performance objectives for 100% coverage in the longitudinal direction.

- When the column is retrofitted with 1ply of CFRP along with VE layer with 40% coverage in the transverse direction, it satisfies the OP level under a small earthquake and it also satisfies the CP level under a large earthquake. This implies that the column meets dual performance objectives for 40% coverage in the transverse direction.

- In order to meet dual performance objectives in the both longitudinal and transverse directions, the column is required to be retrofitted with 3ply of CFRP along with VE layer with full coverage. In that case, the damping component ensures the operational level under a small earthquake and the strengthening component ensures the safety level under a large earthquake in the both directions.

REFERENCES

Aiken, I. D., Nims, D. K., Whittaker, A. S., and Kelly, J. M. (1993). "Testing of passive energy dissipation systems." *Earthquake Spectra*, 9(3), 335-370.

Aprile, A., Inaudi, J. A., and Kelly, J. M. (1997). "Evolutionary model of viscoelastic dampers for structural applications." *Journal of Engineering Mechanics*, ASCE, 123(6), 551-560.

ATC/MCEER Joint Venture (2008). *Recommended LRFD Guidelines for the Seismic Design of Highway Bridges*, Applied Technology Council, Redwood City, CA.

Austin, E. M. (1998). "Influences of higher order modeling techniques on the analysis of layered viscoelastic damping treatments." Ph.D. dissertation, Virginia Polytechnic Institute and State University, Blacksburg, VA.

Bentz, E. C. (2000). "Sectional analysis of reinforced concrete." Ph.D. Dissertation, Department of Civil Engineering, University of Toronto, Toronto, Canada.

Bergman, D. M., and Hanson, R. D. (1993). "Viscoelastic mechanical damping devices tested at real earthquake displacements." *Earthquake Spectra*, 9(3), 389-418.

Chang, K. C., Soong, T. T., Oh, S. T., and Lai, M. L. (1992). "Effect of ambient temperature on viscoelastically damped structures." *ASCE Journal Structural Engineering*, 118(7), 1955-1973.

Chang, K. C., Soong, T. T., Oh, S. T., and Lai, M. L. (1995). "Seismic behavior of steel frame with added viscoelastic dampers." *ASCE Journal of Structural Engineering*, 121(10), 1418-1426.

Chang, K. C., Chen, S. J., and Lai, M. L. (1996). "Inelastic behavior of steel frames with added viscoelastic dampers." *ASCE Journal of Structural Engineering*, 122(10), 1178-1186.

Chen, G., Thebeau, P., and Mu, H., (2002). "Seismic vulnerability of highway bridges along a designated emergency vehicle access routes near the New Madrid seismic zone." *7th National Conference on Earthquake Engineering* (CD-ROM), Boston, MA.

Chen, G., Wang, W. and Huang, X. (2006). "Optimal design of RC column seismic retrofitting for multiple performance objectives with an integrated damping and strengthening methodology." *8th National Conference on Earthquake Engineering* (CD-ROM), San Francisco, CA.

Chen, G. and Karim, K. R. (2006). "Damping-enhanced seismic strengthening of RC columns for multiple performance objectives." *5th National Seismic Conference of Bridges and Highways*, San Francisco, CA, Paper No B24.

Chopra, A. K. (2001). *Dynamics of structures*, Prentice Hall, New York, NY.

Fajfar, P. (1999). "Capacity spectrum method based on inelastic demand spectra." *Earthquake Engineering and Structural Dynamics*, 28, 979-993.

FEMA-273. (1997), "NEHRP guidelines for the seismic rehabilitation of buildings." *Building Seismic Safety Council*, Washington, DC.

FHWA (2005). "Seismic retrofitting manual for highway bridges." *Federal Highway Administration*, Publication No. FHWA-RD-94-052.

Foutch, D. A., Wood, S.L., and Beady, P. A. (1993). "Seismic retrofit for nonductile reinforced concrete frames using viscoelastic dampers." *Proceedings of Applied Technology Council ATC-17-1 Seminar on Seismic Isolation, Passive Energy Dissipation and Active Control*, 2, 605-616.

Gehling, R. N. (1987). "Large space structure damping treatment performance: analytic and test results." *Role of Damping in Vibration and Noise Control*, ASME, New York, NY, 93-100.

Hammami, L., Zghal, B., Fakhfakh, T., and Haddar, M. (2005). "Characterization of modal damping of sandwich plates." *Journal of Vibration and Accoustics*, 127, 431-440.

Hanson, R. D., and Soong, T. T. (2001). "Seismic design with supplemental energy dissipation devices." *EERI Monograph*, Oakland, CA.

Hao, M., and Rao, M. D. (2005). "Vibration and damping analysis of a sandwich beam containing a viscoelastic layer." *Journal of Composite Materials*, 39(18), 16211643.

Huang, X. (2005). "An integrated VE damping and FRP strengthening system for performance-based seismic retrofit of RC columns." Ph.D. dissertation, University of Missouri-Rolla, Rolla, MO.

Inman, D. J. (2001). *Engineering vibration*, Prentice Hall, Upper Saddle River, NJ.

International Code Council (2006). *International Building Code*, International Code Council, Inc., Whittier, CA.

Kasai, K., Munshi, J. A., Lai, M. L., and Maison, B. F. (1993). "Viscoelastic damper's hysteretic modal theory, experiment, and application." *Proceedings of Applied Technology Council ATC-17-1 Seminar on Seismic Isolation, Passive Energy Dissipation and Active Control*, 2, 521-532.

Kerwin, E. M. Jr. (1959). "Damping of flexural waves by a constrained viscoelastic layer." *J. Accoust. Soc. Am.*, 31(7), 952-962.

Lin, W. H., and Chopra, A. K. (2003). "Earthquake response of elastic single-degree-of-freedom systems with nonlinear viscoelastic dampers." *ASCE Journal of Engineering Mechanics*, 129(6), 597-606.

Liu, H., Tai, N., and Chen, C. (2000). "Compression strength of concrete columns reinforced by non-adhesive filament wound hybrid composites." *Composites - Part A: App. Sci. & Manufacturing*, 31(3), 221-233.

Lu, B. (2007). "Application of displacement-based design method to blast-resistant reinforced concrete structures." Ph.D. dissertation, University of Missouri-Rolla, Rolla, MO.

Mander, J. B., Priestley, M. J. N., and Park, R. (1988). "Theoretical stress-strain model for confined concrete." *ASCE Journal of Structural Engineering*, 114(8), 1804-1826.

Matsuda, T., Sato, H., Fujiwara, H., and Higashihara, N. (1990). "Effect of carbon fiber reinforcement as a strengthening measure for reinforced concrete bridge piers." *Proc. 1st U.S.-Japan Workshop on Seismic Retrofit of Bridges*.

Mead, D. J. (1962). "The double skin damping configuration." Report No. AASU, University of Southampton, UK.

MCEER (2005). "Seismic retrofitting manual for highway structures: part 1 – bridges." Working Draft, Prepared by the Multidisciplinary Center for Earthquake Engineering Research (MCEER) for Federal Highway Administration.

Mirmiran, A., and Shahawy, M. (1997). "Behavior of concrete columns confined by fiber composites." ASCE *J. Struct. Engrg.*, 123(5), 583–590.

Morgenthaler, D. R. (1987). "Design and analysis of passive damped large space structures." *Role of Damping in Vibration and Noise Control*, ASME, New York, NY, 1-8.

Pantelides, C.P., Gergely, J., Reaveley, L. D., and Volnyy, V. A. (1999). "Retrofit of RC bridge pier with CFRP advanced composites." ASCE *J. Struct. Engrg.*, 125(10), 1094-1099.

Priestley, M. J. N., and Seible, F. (1991). "Seismic assessment and retrofit of bridges." *Struct. Sys. Res. Proj., Rep. No. SSRP-91/103,* University of California at San Diego, San Diego, CA.

Priestley, M. J. N., Seible, F., and Calvi, G. M. (1996). *Sesimic design and retrofit of bridges*, John Wiley & Sons, New York, NY.

RESPONSE-2000 (2009). "Sectional analysis software for reinforced concrete." <http://www.ecf.utoronto.ca/~bentz/home.shtml>.

Ross, D., Ungar, E. E., and Kerwin, E. W. (1959). "Damping of plate flexural vibrations by means of viscoelastic laminar." *Structural Damping* (ed, Ruzicka, E.J.), ASME.

SAP2000. "Integrated software for structural analysis & design." *Computers & Structures, Inc*., Berkeley, CA.

Saadatmanesh, H., Ehsani, M. R., and Li, M. W. (1994). "Strength and ductility of concrete columns externally reinforced with fiber composite straps." *ACI Struct. J.*, 434.

Seible, F., Hegemier, G. A., and Innamorato, D. (1995). "Developments in bridge column jacketing using advance composites." *Proc. Nat. Seismic Conf. on Bridges and Hwy.*, Federal Highway Administration and California Department of Transportation.

Shen, K. L., and Soong, T. T. (1995). "Modeling of viscoelastic dampers for structural applications." *ASCE Journal of Engineering Mechanics*, 121(6), 694-701.

Silva, P. F., Erecson, N. J., and Chen, G. (2007). "Seismic retrofit of bridge joints in central U.S. with carbon fiber-reinforced polymer composites." *ACI Structural Journal*, 104(2), 207-217.

Soong, T. T., and Dargush, G. F. (1997). *Passive energy dissipation system in structural engineering*, John Wiley & Sons, New York, NY.

Soong, T. T., and Spencer, B. F. (2002). "Supplemental energy dissipation: state-of-the-art and state-of-the-practice." *Engineering Structures*, 24, 243-259.

Viti, S., Reinhorn, A. M., and Whittaker, A. S. (2002). "Retrofit of structures: strength reduction with damping enhancement." *KEERC-MCEER Joint Seminar on Retrofit Strategies for Critical Facilites*, Buffalo, NY.

Wang, G. (2001). "Analyses of sandwich beams and plates with viscoelastic cores." Ph.D. dissertation, University of Maryland, College Park, MD.

Xiao, Y., and Ma, R. (1997). "Seismic retrofit of RC circular columns using prefabricated composite jacketing." ASCE *J. Struct. Engrg.*, 123(10), 1357-1364.

Xiao, Y., Wu, H., and Martin, G. R. (1999). "Prefabricated composite jacketing of RC columns for enhanced shear strength." ASCE *J. Struct. Engrg.*, 125(3), 255-264.

Zhang, R. H., Soong, T. T., and Mahmoodi, P. (1989). "Seismic response of steel frame structures with added viscoelastic dampers." *Earthquake Engineering and Structural Dynamics*, 18, 389-396.

Zhang, R. H., and Soong, T. T. (1992). "Seismic design of viscoelastic dampers for structural applications." *ASCE Journal of Structural Engineering*, 118(5), 1375-1392.

VITA

Kazi Rezaul Karim was born on June 1, 1973 in Gopalgonj, Bangladesh. He received his secondary and higher secondary education in Mirzapur Cadet College, Tangail, Bangladesh. After graduation from high school, he attended Indian Institute of Technology, Bombay, India.

During his four years as an undergraduate student at Indian Institute of Technology, Bombay, India, Mr. Karim gained valuable experience both in and out of the classroom. He worked as an engineering intern in Bangladesh Consultants Ltd, Dhaka, Bangladesh for one summer. After fulfilling the requirements, Mr. Karim received his Bachelor of Technology degree in Civil Engineering in July 1996.

Immediately following graduation, Mr. Karim began working for Bangladesh Consultants Ltd, Dhaka, Bangladesh as a Design Engineer. He then enrolled at Missouri University of Science and Technology to pursue his Master of Science in Civil Engineering. His graduate studies focused on development of damping-enhanced strengthening strategy for performance-based seismic design and retrofit of highway bridges. He was fortunate enough to receive a Graduate Research Assistantship from the Department of Civil Engineering. After fulfilling the requirements, Mr. Karim received his MS in Civil Engineering in May 2009.

Mr. Karim joined at Kirkpatrick Engineering, Oklahoma City, in October 2007 and is working as a Structural Engineer.